The Thesis Committee for Rattanaporn Fong-Ngern
Certifies that this is the approved version of the following thesis :

Sequence Stratigraphy, Sandstone Architecture, and Depositional Systems of the Lower Miocene Succession in the Carancahua Bay Area, Texas Gulf Coast

APPROVED BY
SUPERVISING COMMITTEE:

Co-Supervisor: _____
William L. Fisher

Co-Supervisor: _____
William A. Ambrose

_____
Ronald J. Steel

Sequence Stratigraphy, Sandstone Architecture, and Depositional Systems of the Lower Miocene Succession in the Carancahua Bay Area, Texas Gulf Coast

by

Rattanaporn Fong-Ngern, B.S.

Thesis

Presented to the Faculty of the Graduate School of

The University of Texas at Austin

in Partial Fulfillment

of the Requirements

for the Degree of

Master of Science in Geological Sciences

The University of Texas at Austin

August, 2011

Dedication

To Mom and Sister.

Acknowledgements

To make this thesis possible I owe gratitude to a number of people.

Words may not be enough but I would like to express my immense gratitude to Dr. William Fisher, my advisor and co-supervisor, who has guided me through difficult periods of academics and life. Dr. Fisher's words, 'You may knock on my door anytime you want, I'm your advisor' always make me feel warm and comfortable. Without his inspiration and efforts to teach, I would not have finished my degree. I also wish to thank Mr. William Ambrose (Bill), my co-supervisor, who has been very supportive both academically and emotionally. The time Bill contributed and the encouragement he gave me motivated me to be productive, and his great amusing stories soothed me when I was stressful. I am also very grateful to Dr. Ron Steel, my committee member, who always took the time to discuss the research with me despite his busy schedule. He gave me invaluable advice and ideas; without him I would have been lost.

I would like to thank Brigham Exploration Company for the seismic associated well log data and the STARR group of the Bureau of Economic Geology (BEG) for providing me a workstation and software. I appreciate support from BEG research staff especially Dr. Osareni C. Ogiesoba (Chris) who devoted a lot of time to helping me. I am also very thankful to Dallas Dunlap, Thomas Hess and Effie Jaret for their technical support.

I am grateful to the Royal Thai Government for financial support and the Jackson School of Geosciences for an excellent education. I deeply appreciate Patricia Bobeck, a thesis writing workshop instructor, who encouraged me and kindly helped me edit my thesis drafts.

I wish to thank all of my undergraduate teachers at Chiang Mai University, for providing good geological background, especially Dr. Sarawute Chantraprasert, who was my undergraduate advisor and research supervisor. His wisdom and inspiration guided me here.

And last but most important, I am deeply indebted to my mother and sister, Suree and Prapaiphat Fongngern, whose love, support, and sacrifice are the source of the energy I have used to accomplish this goal. It is a great pleasure to thank all of my Thai friends and my University of Texas friends: Saya Ahmed, Diego Valentin, Enrica Quartini, Renas Mohammed, Sarika Ramnarine, Rocio Bernal, Javier Sanchez, Anmar Dávila, Lin Chang, and Henry Campos. Their friendship, advice, and support have enriched my life in the USA.

August 5, 2011

Abstract

Sequence Stratigraphy, Sandstone Architecture, and Depositional Systems of the Lower Miocene Succession in the Carancahua Bay Area, Texas Gulf Coast

Rattanaporn Fong-Ngern, MSGeoSci
The University of Texas at Austin, 2011

Co-Supervisor: William L. Fisher
Co-Supervisor: William A. Ambrose

This study defines depositional environments and constructs the sequence stratigraphic framework of the lower Miocene Oakville Formation and the basal part of the middle Miocene Lagarto Formation in the Carancahua Bay area. The Early Miocene of the northwestern Gulf of Mexico represents a tectonically stable period with a high sediment influx.

The analysis is based on a data set composed of 45 well logs and 200 mile^2 area 3D seismic volume. The study interval was divided into five depositional sequences 1-5 that encompass 0.6-2.5 My. LST, TST, and HST systems tracts were recognized by stacking patterns and bounding surfaces. Sequence thickness increases from sequence 1

to 3 and displays reverse thickness trends from sequence 3 to 5, implying changes in accommodation space relative to sediment supply, beginning with high rates of accommodation and evolving into low accommodation rates relative. Besides type-1 depositional sequence which forms during relative sea-level fall below the shoreline break, regressive units of T-R sequence model were also defined and delineated. The interval contains four regressive units, R-Unit1-4. The R-Unit net sandstone maps exhibit the same characteristic of a dip-oriented source of delta-plain origin and a delta-front depocenter basinward.

Integration of well log patterns, sandstone dispersal trends from net sandstone maps and seismic stratal slices led to interpretation of depositional environments in each sequence. LST deposits are represented mainly by incised-valley fill facies. TSTs are composed predominantly of retrogradational barrier/tidal-inlet facies, whereas other TSTs contain lagoonal and reworked deltaic systems. HST1 is composed mainly of fluvial-dominated deltaic systems, whereas deltaic systems in other HSTs exhibit wave-influenced deltaic and strandplain depositional systems. The integrated methodology reveals depositional facies variations in contrast to previous work that interpreted these deposits as shorezone systems.

During LSTs coarse-grained sediments bypassed shelf through incised valley systems to a downdip depocenter. More sandy sediments were stored on shelf as deltaic and strandplain deposits during HSTs. In contrast to the others, destructive process occurred in TSTs and reworked sandy sediments, for example from delta fronts to barrier bar and lagoonal facies. Submarine fans form by sediments transported through incised-valley systems and delta fronts are commonly good reservoirs. Hence, presence of such depositional facies in the study area might be genetically linked to exploration targets.

Table of Contents

List of Tables

List of Figures

Chapter 1: Introduction

1.1 Research objectives

The objectives of this research are to define depositional environments and recognize and correlate significant stratigraphic surfaces, such as lowstand unconformities, transgressive erosional surfaces, and maximum flooding surfaces that bound systems tracts. These depositional environments and surfaces are the main components to construct a sequence-stratigraphic framework of the Miocene-Anahuac succession in the Carancahua/Matagorda Bay area, the Gulf of Mexico. Another goal of the research is to document the sandstone-body geometry and reconstruct the paleogeography and depositional history. Well logs are used as a primary data set for fine-scale analysis and the 3-D survey is for validating log-based correlations and preparing strata slice illustrations.

1.2 Significance of this research

The Miocene represents a period of high sediment influx, and additionally contains some of the most prolific petroleum fields of the Gulf of Mexico. Although significant research has been done on the Miocene succession, most of it is at a regional scale, encompassing the northwestern Gulf of Mexico. Consequently, a detailed understanding of the depositional environments and a robust sequence stratigraphic interpretation based on consistently applied criteria may help promote efficiency in future petroleum exploration and production.

1.3 LOCATION OF THE STUDY AREA AND DATA SET

The study area is a transition zone between the onshore and offshore Gulf of Mexico in Matagorda/Carancahua Bay. It covers approximately 200 square miles (518 square kilometers) of the E-W striking Caramata 3-D survey in Jackson and Matagorda counties (Fig. 1.1). The Miocene section is at the top of the succession in the area and overlies the Oligocene Frio Formation. The seismic data has a frequency domain in a range of 30 to 45 Hz and vertical resolution of approximately 53 to 70 ft (16 to 21 m).

There are 45 well logs distributed throughout the study area (Fig. 1.2). Common well names are shown in Table 1.1 in the appendix. Spacing between wells ranges from 695 to 5400 ft (212 to 1646 m). Most of the well logs have spontaneous potential (SP), gamma ray, and resistivity log curves available from the bottom of the section to the true vertical depth of 1312 to 1968 ft (400 to 600 m). Well tie with the 3D seismic volume is illustrated in Figure 1.3. Most of sandstones exhibited by well logs correspond with high negative amplitude (red) events; however some do not correlate well with seismic events, perhaps because well logs have higher vertical resolutions than seismic volume and there is noise in sonic log used to tie wells with the seismic volume.

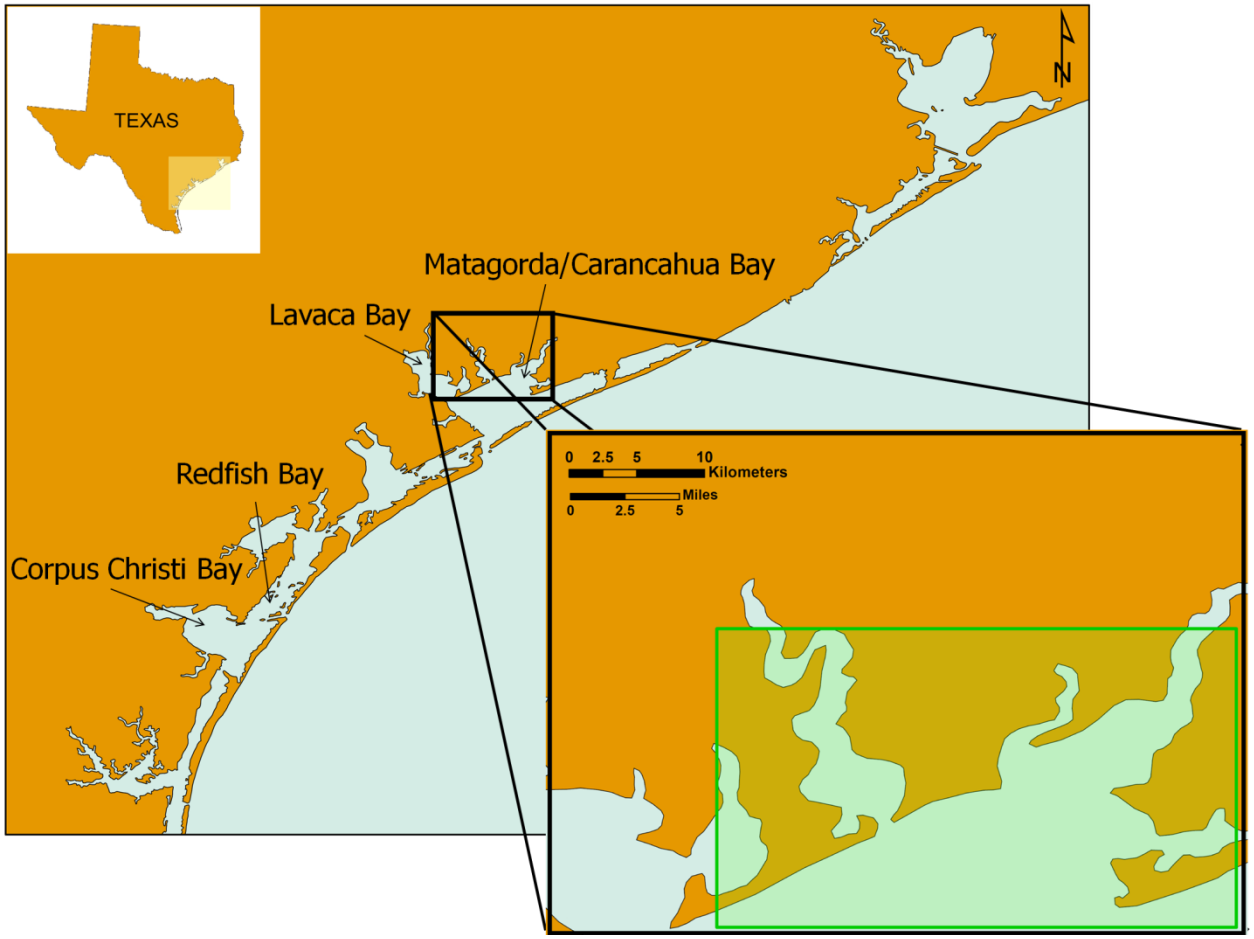

Figure: 1.1 Study area located in Matagorda/Carancahua Bay along the Texas coastline. The black box is the outline of the Caramata survey and the green rectangle represents the outline of 3D seismic volume used in this research.

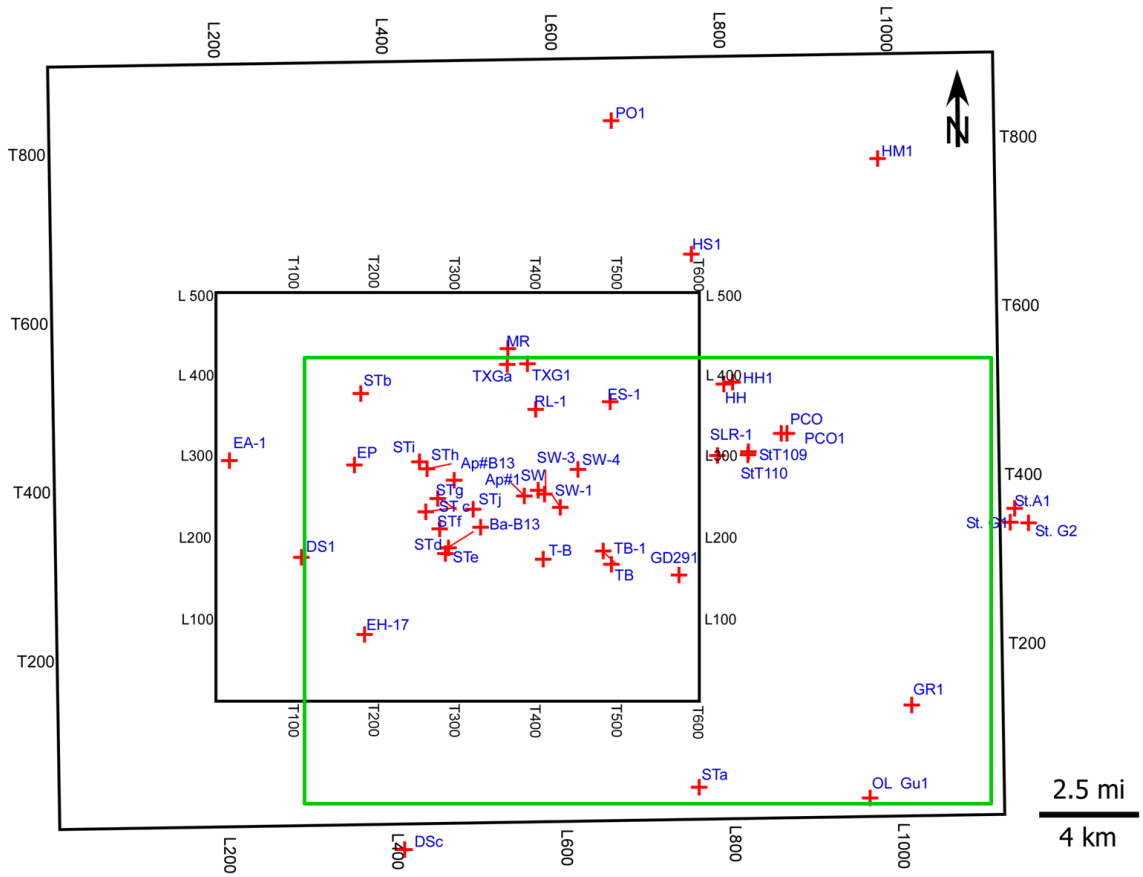

Figure: 1.2 Base map with location of 45 well logs. The bigger and smaller boxes are Caramata and Carancahua surveys respectively. Caramata survey is shown in Figure 1.1. The 3D seismic volume used in this study is in the green rectangle covering approximately 200 mi^2 area.

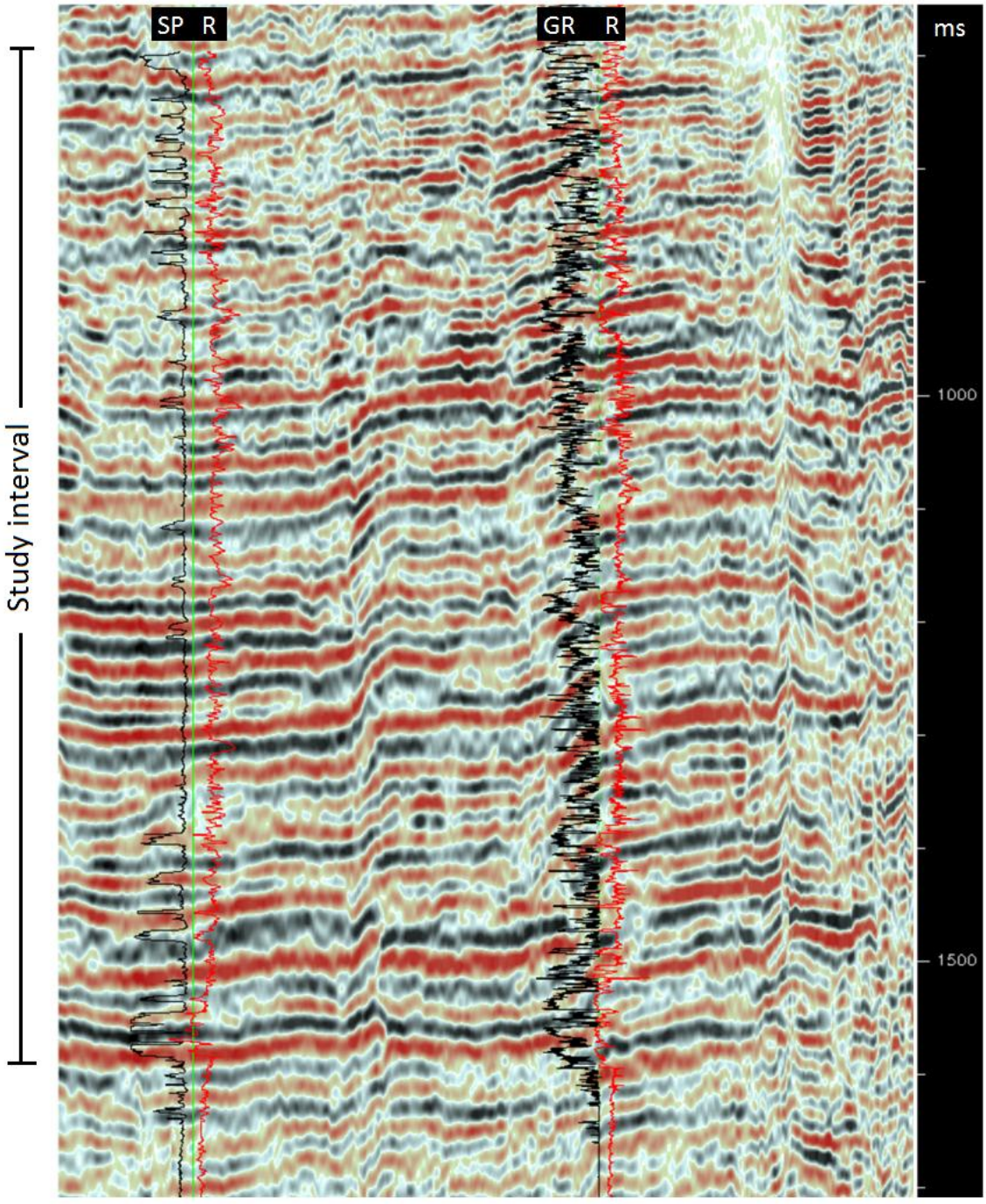

Figure: 1.3 Seismic line with well tie. Most of sandstones exhibited in the well logs correspond with high negative amplitude (red) events.

1.4 PREVIOUS WORK

The locations of previous studies of the lower Miocene strata in the northwestern Gulf of Mexico are shown in Figure 1.4. Ye et al. (1995) interpreted what they believed to be high-frequency glacioeustatic cycles of the Lower Miocene in central Texas to have been deposited in "a barrier/strandplain-shelf-slope apron" environment (Galloway et al., 1986). Ye et al. (1995) divided the succession into three maximum flooding surface-bounded 'sequence cycles' (SC): SC1, SC2, and SC3. They stated that these sequence cycles are comparable to third-order sequences of Exxon (Vail et al., 1991). They explain that each sequence cycle contains parasequence set cycles (PSSC) which are probably at fourth-order sequence scale (Fig 1.5). They suggested that the dominant factor controlling the cycle formation was glacioeustatic sea level change. Without mentioning how, they also interpreted depositional environments of the deposits as fluvial and associated facies, bayhead deltas, shorezone or inner shelf sandstones, shelf/slope sandstones and shelf/slope mudstones. Comparing the cycles to those in western Louisiana area, they found that high frequency cyclicity was better developed in central Texas because the wider paleo-shelf allowed progradation to occur even during sea level rise.

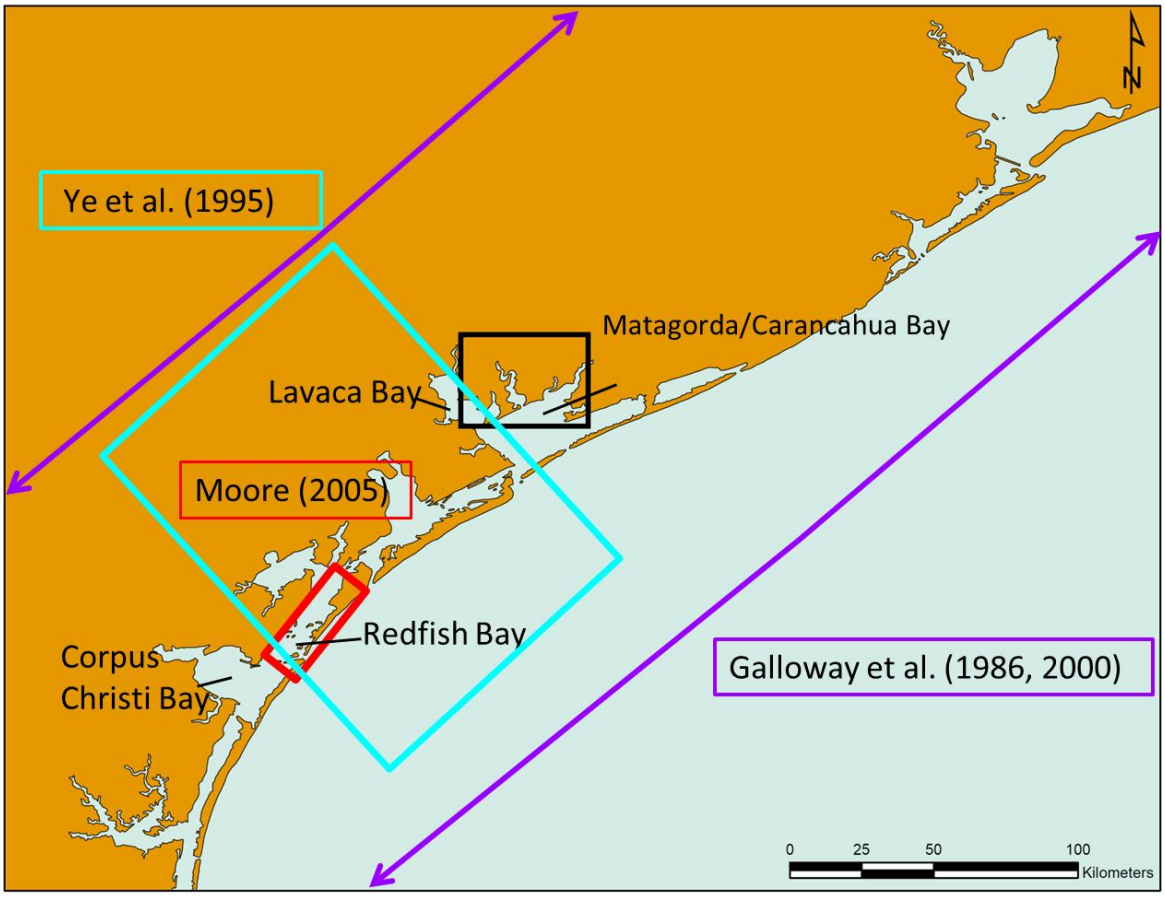

Figure 1.4 Base map displaying the areas of previous studies of lower Miocene succession. Galloway's work will be mentioned in the next chapter.

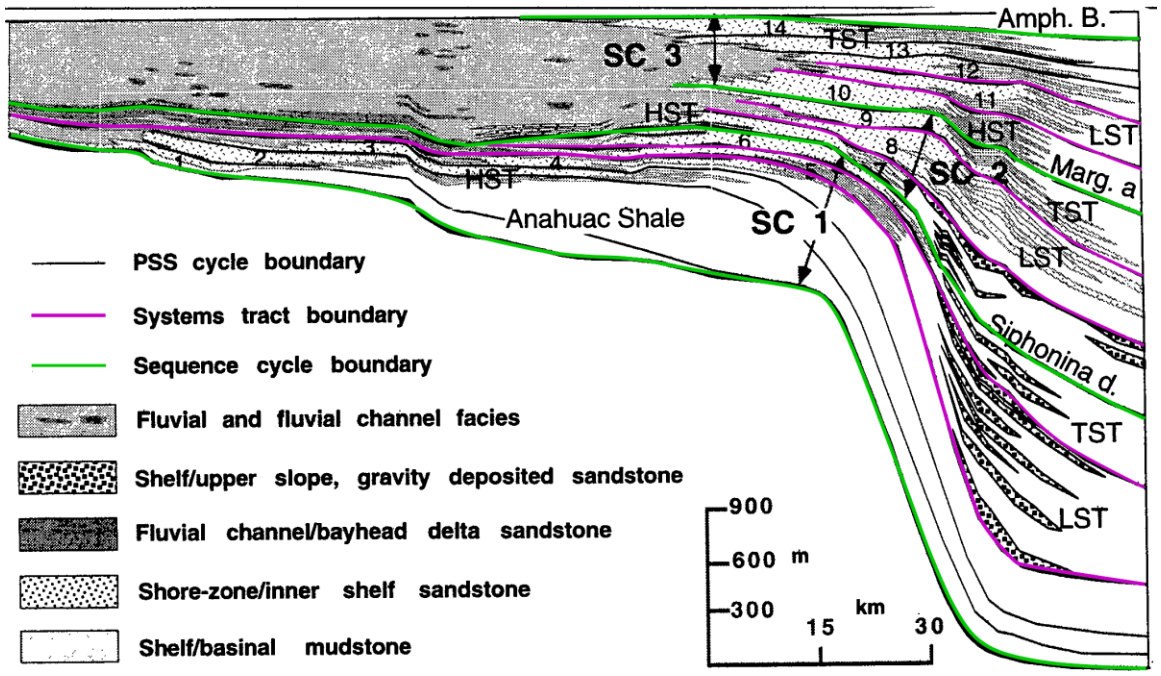

Figure 1.5 The lower Miocene dip transect of central Texas area showing sequence stratigraphic framework, three sequence cycles (SC) and fourteen parasequence set cycles PSSC) defined by Ye at al. (1995).

Moore (2005) studied the sequence stratigraphic framework of the Lower Miocene section of the Red Fish Bay area, Texas Gulf Coast. From a 3D seismic volume and associated wire-line logs, he integrated methodologies of well-log characteristics, structural mapping, isopach mapping and stratal slice analysis to define system tracts and construct sequence stratigraphy of the Upper Oligocene-Lower Miocene succession. He concluded that the Lower Miocene succession consists of four unconformity bounded third-order sequences, sequence I, II, III and IV. The two lower sequences contain a lowstand system tract (LST), a transgressive system tract (TST) and a highstand system tract (HST), but a LST is absent in the upper two sequences. The LSTs were interpreted as incised valley deposits to which he paid special attention to. The incised valley

deposits of sequence I are more sandstone-rich than those of sequence II; the latter are more interbedded. Moore suggested that sediment supply was higher during deposition of Sequence I because of the activity of the Balcones fault system and reworking of Cretaceous strata in central Texas.

Chapter 2: Regional geology and Stratigraphy

2.1 REGIONAL GEOLOGY

The northwestern Gulf of Mexico region is categorized as a divergent to passive margin tectonic setting. The Miocene period is considered to have been relatively tectonically stable period with ongoing thermal subsidence (Galloway, 1989).

As a progradational continental margin, the Cenozoic northwestern Gulf of Mexico was dominated by deltaic and shallow-marine sedimentation on the continental shelf and sliding/slumping and turbidity current dispersal on the slope. Flexural loading of the crust due to depocenter progradation, was the major subsidence mechanisms in the region (Winker, 1982) (Fig. 2.1). However, Galloway (1989) suggests that thermal subsidence of the underlying crust created accommodation space for an 8-14 km thick progradational wedge in the northwestern Gulf of Mexico.

2.2 STRATIGRAPHY

The stratigraphy of the Miocene of the Texas Gulf coast is illustrated in Figure 2.2. The Miocene, which extends from approximately 24 to 5 My, is divided into lower, middle and upper intervals. In terms of lithostratigraphy, the lower to the lower-middle Miocene is correlative with the Fleming Group which contains the Oakville and Lagarto Formations. The upper-middle to upper Miocene is comparable to the Goliad Formation. In this study, the data cover the complete lower Miocene section and the bottom part of middle Miocene.

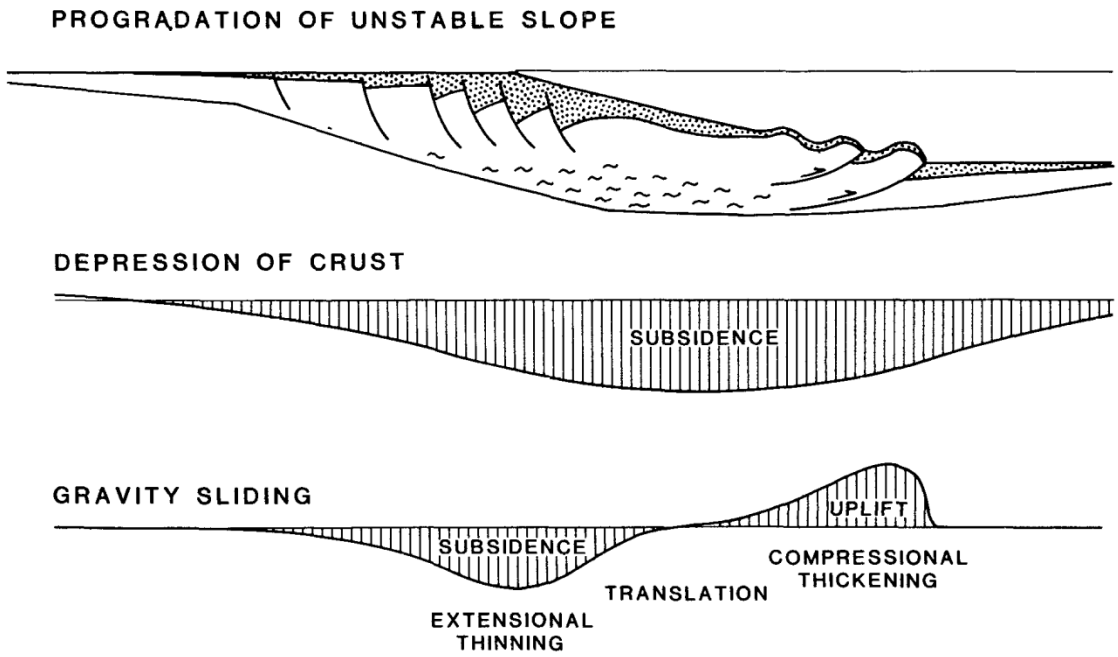

Figure: 2.1 Diagram showing major subsidence mechanisms of the Cenozoic deposits in northwestern Gulf of Mexico margin by Winker (1982).

The Miocene is one of major continental-outbuilding periods of the northern Gulf of Mexico during the Cenozoic; the Oakville Formation prograded farther basinward than the Oligocene paleo-shelf-edge (Galloway et al., 1986). The underlying Oligocene Frio Formation represents the highest sediment influx of the Cenozoic at its lower part (Galloway et al., 2000). The Frio which is one of the important petroleum intervals of the Tertiary in the Gulf of Mexico is a progradational, delta-dominated sedimentary wedge containing thick undercompacted prodelta and slope mud that was partitioned by several major growth faults on the slope (Galloway et al., 1982). The growth faults are believed to have been activated by loading stress from sediment accumulation during periods of third-order relative sea-level fall. Turbidity currents and other gravity flows transported unstable distal delta-front deposits to the continental slope to form basin floor fans and subsequent slope fan complexes. The loading of the lowstand depocenter on muddy slope

later created failure along arcuate surface of growth faults providing accommodation space as intraslope subbasin on their hanging walls (Brown et al., 2004b). In Lavaca Bay area, the lower to upper Frio Formation exhibits a stratigraphic succession of lowstand slope fans, lowstand progradational wedge, and high-frequency transgressive-regressive cycles respectively. Growth faults have influence on controlling sandstone body geometry of the lowstand slope fans and lowstand progradational wedge (Ambrose et al., 2010).

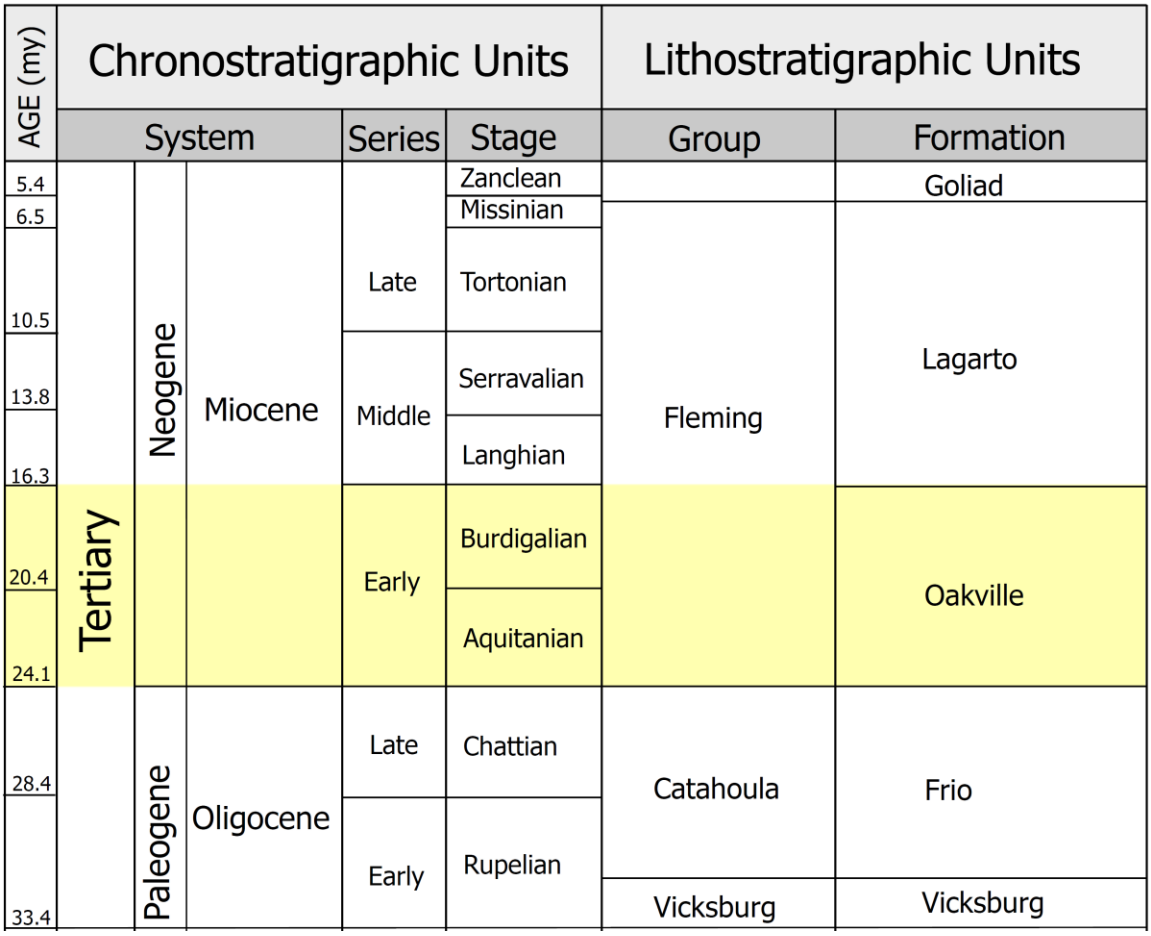

Figure: 2.2 Chronostratigraphic chart of the Oligocene to Miocene systems. The highlighted time is the current study interval (modified from a Wheeler Chart of Northwest Margin of the Gulf of Mexico Basin (Brown and Loucks, 2009)).

2.3 STRUCTURAL FRAMEWORK

Lower Miocene structures occurring along the coastal plain and continental shelf of the northwestern Gulf margin are classified into two groups by Galloway et al. (1986). The first group is reactivated structures that were triggered by loading of a prograding sedimentary wedge and stress produced by subsidence and loading within the Cenozoic continental platform. Examples of structures reactivated by sediment loading are the Frio and Vicksburg fault zones located landward of the Frio paleo-margin. Stress from crustal subsidence and loading-reactivated growth-fault zones consequently, "have generated low-relief rollover anticlines or local dip reversals within lower Miocene deposits" (Galloway et al., 1986). The second group is syndepositional structure, typically growth faults within the progradational wedge and their associated downdip compressional structures that include shale ridges. Such structures are created by gravity deformation caused by a rapid-sedimentation load. This type of structure zone is located further basinward of the study area.

During the middle-upper Miocene, the main mechanism that created structures is gravity driven deformation. Growth faults found on the mud-rich continental slope resulted from rapid progradation. Antithetic faults that terminate into the main down-to-the-basin faults formed some major strata offsets and small-scale grabens. Similar to the lower Miocene structures, reactivated faults are caused by rapid progradation of middle and upper Miocene sedimentary wedges over the underlying lower Miocene deposits (Morton et al., 1988).

Diegel et al. (1995) studied the tectono-stratigraphic framework of the northern Gulf of Mexico and categorized the area of interest as an "Oligocene-Miocene detachment province" which is genetically related to salt welds. The province is

characterized by listric down-to-basin growth faults and thick deltaic sediments deposited basinward of the Paleocene-Eocene Wilcox fault system.

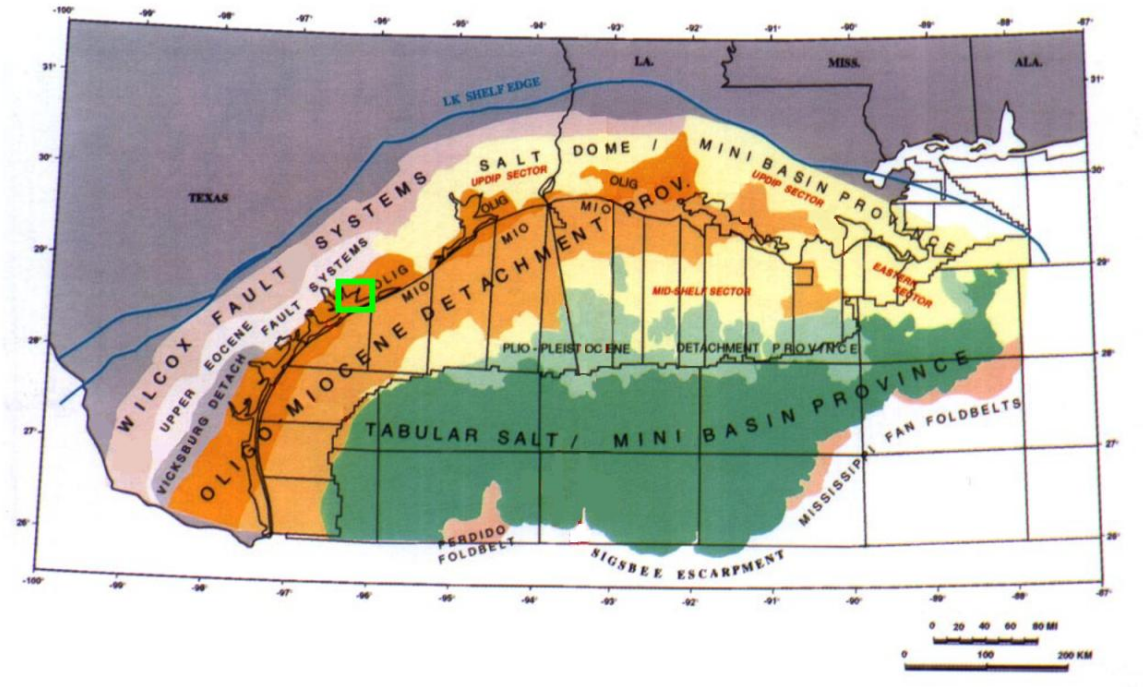

Figure: 2.3 Tectono-stratigraphic provinces of the northern Gulf of Mexico Basin interpreted by Diegel et al. (1995). The study area is categorized as the Oligocene – Miocene Detachment Province.

2.4.1 Structural interpretation

In this study, major faults and two reference horizons were interpreted in Geoprobe® using both amplitude and semblance volumes. Most of the observed faults have high-angle dips and some of them penetrate the Anahauc and upper Frio Formations. Three groups of faults can be classified according to their orientations (Fig 2.4, 2.5 and Table 2.1). First group forms the major fault zone located to the east (basinward) of the area: Cara 102, Cara 103, Cara 104, Cara 105, Cara 106 Cara 107, and

Cara 110. This fault zone is characterized by the coupling of synthetic and antithetic faults forming small grabens. The faults strike NE-SW, subparallel to the paleoshoreline. The strike-similar faults are usually closely spaced and at some point they merge with the others, or are terminated against a nearby fault.

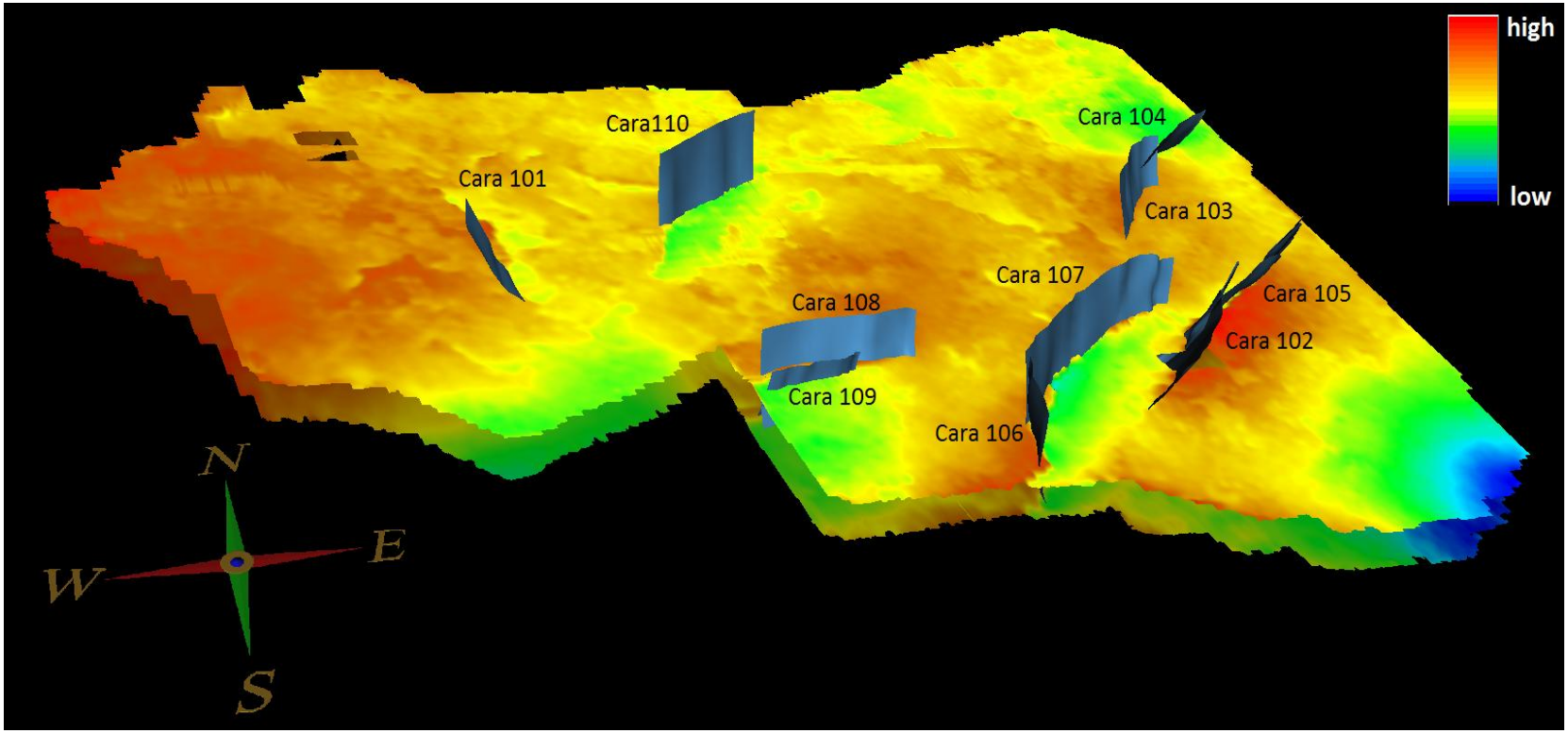

Figure: 2.4 Major faults interpreted in the study area with two reference horizons. Three groups of faults were defined by their orientations. This view is looking to the northeast direction.

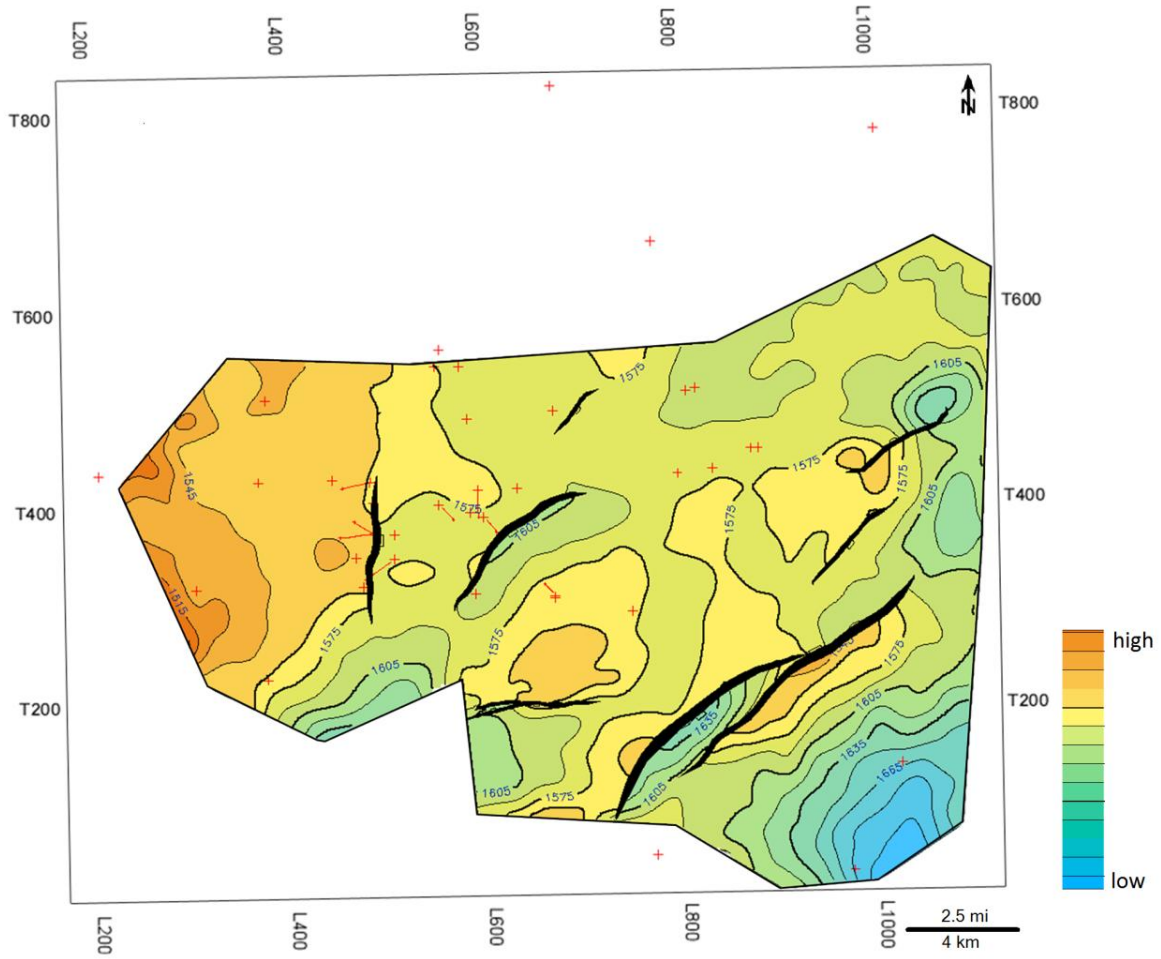

Figure: 2.5 A structural map of the study area shows fault trace on the lowermost interpreted horizon, Horizon A (Fig 4.6 and 4.13) which is a major sequence boundary between Late Oligocene and Early Miocene. A unit of contour lines is in two-way travel time (ms).

The second group of fault has a high angle and strikes E-W, Cara 108 and Cara 109. The major trend of these faults is almost perpendicular to the paleoshoreline. The third group of fault is NNW-SSE to N-S trending listric fault, Cara 101.

There are small rollover anticlines observed against some of these faults especially the large ones, for examples Cara 107, Cara 102 and Cara 108. Also, there is no drastic thickness change of the lower Miocene successionacross these faults consequently, they are interpreted as sediment loading-reactivated faults, some of them are contemporaneous structures with small growth rate and the others may have been generated after the time of early Miocene deposition.

Group	Name	Fault throw (ft)
Group 1	Cara 102	145
	Cara 103	74
	Cara 104	90
	Cara 106	280
	Cara 107	292
	Cara 105	195
Group 2	Cara 110	209
	Cara 108	214
	Cara 109	367
Group 3	Cara 101	97

Table 2.1 Group of faults and their approximately throw values.

2.3 DEPOSITIONAL HISTORY

The Miocene section of Matagorda Bay is situated between Houston and the Rio Grande embayment (Fig. 2.6). The section is approximately 40 mi (64 km) landward of the Lower Miocene shelf margin (Fig. 2.7). The lower Miocene deposits followed a long-term transgression during Late Oligocene as reflected by the Anahuac shale and its upper limit is bounded by the *Amphistegina B* shale. The Oakville Formation in the study area

was dominated by interdeltaic-shorezone depositional environments called the Oakville shorezone (or the Matagorda barrier-strandplain system) (Fig. 2.8), which typically consists of strike-elongate sand bodies bounded landward by lagoonal mudstone and basinward by transitional-outer shelf mudstone (Galloway et al., 1986). “The Oakville shorezone contains the greatest sand volume of any early Miocene coastal depositional system” (Galloway et al., 2000).

The shorezone system was replaced by the wave-dominated South Brazos delta system (or the Corsair delta of Galloway et al., 2000) in the middle Miocene. The progradational delta wedge produced a 50-to-200 ft (15 to 60 m) thickness of sandstone and the thickest sand bodies occur at the location of fault zones. This deltaic system built out the shelf margin 25 miles (50 kilometers) farther than the lower Miocene wedge (Morton et al., 1988). Although the delta system continued to build until the upper Miocene, a sandy strandplain was the prominent depositional environment since most of the depocenter/sediment supply shifted to the Mississippi embayment (Galloway et al., 2000).

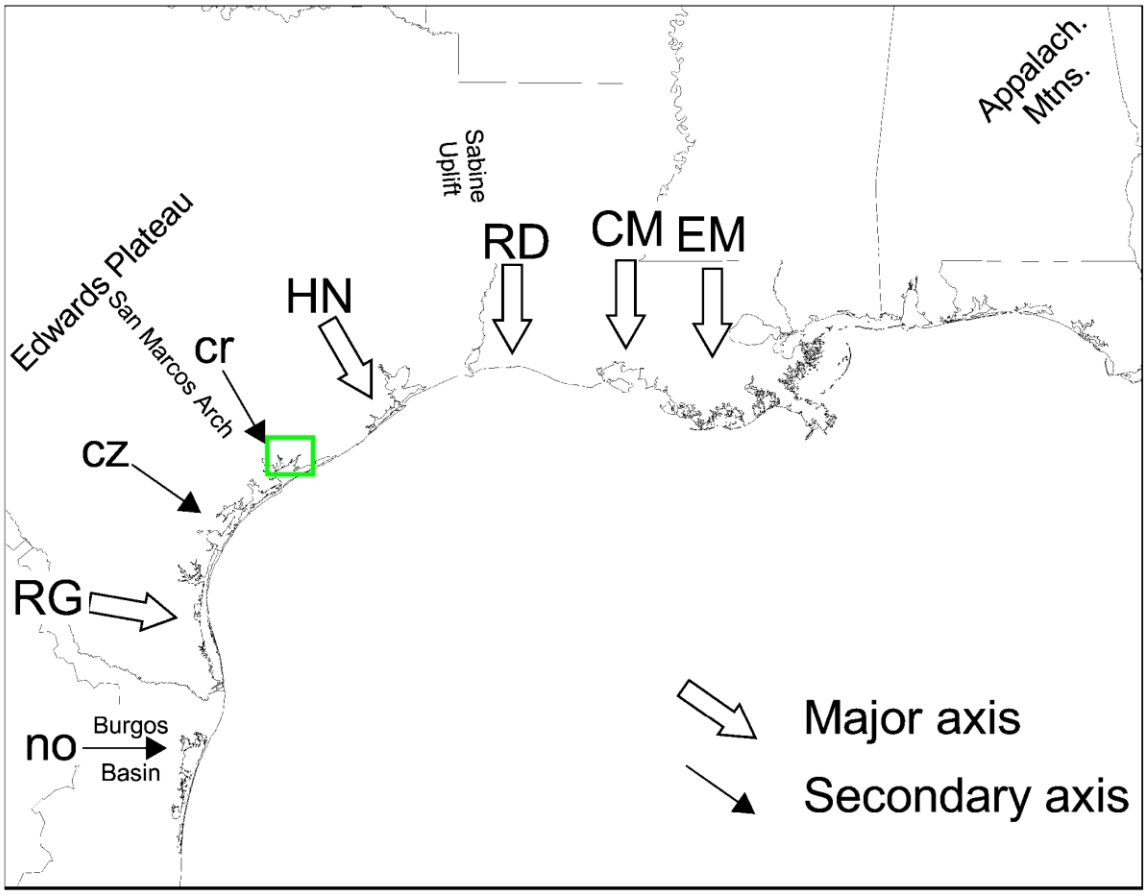

Figure: 2.6 Sediment dispersal systems/ axis of sediment supply for large deltas during Cenozoic of the central and northern Gulf of Mexico. The study area, in the green box, corresponds to the Corsair delta system (modified from Galloway et al., 2000).

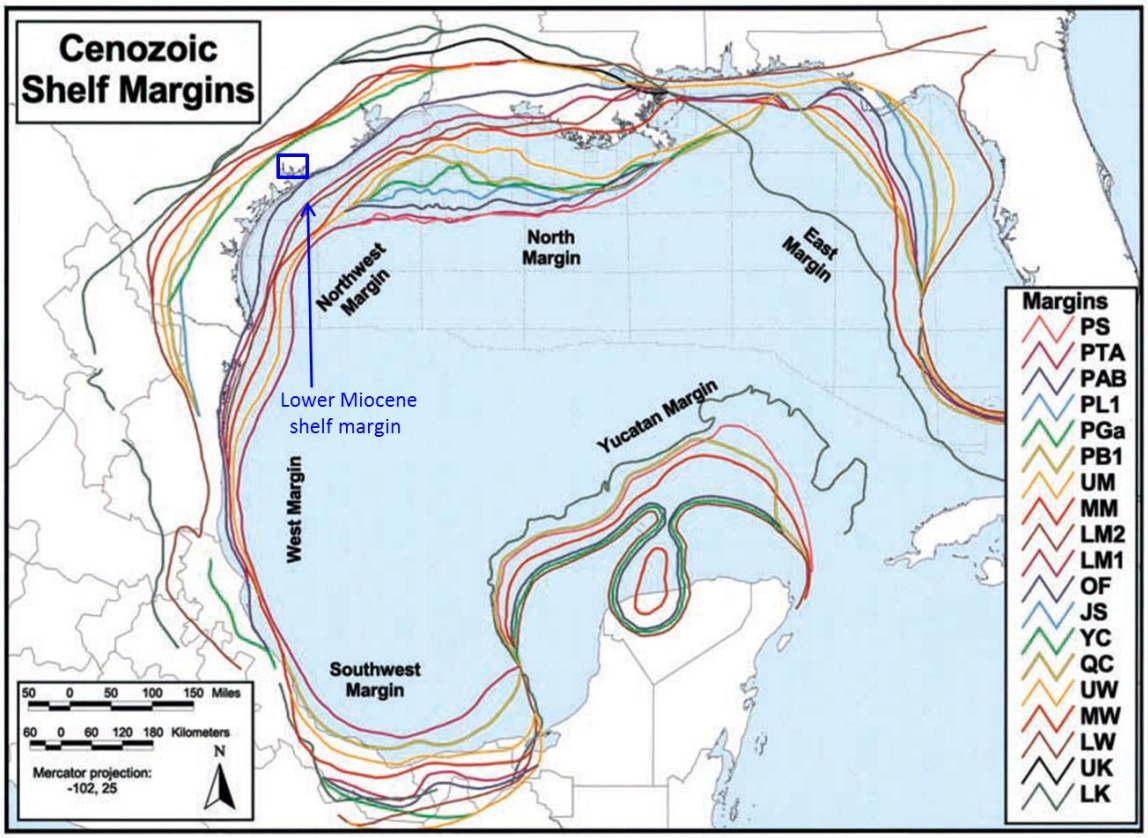

Figure: 2.7 Map of the Gulf of Mexico illustrating relative positions of shelf margin through time. The study area in the blue box is approximately 40 mi away from the Lower Miocene shelf margin (modified from Galloway et al., 2000).

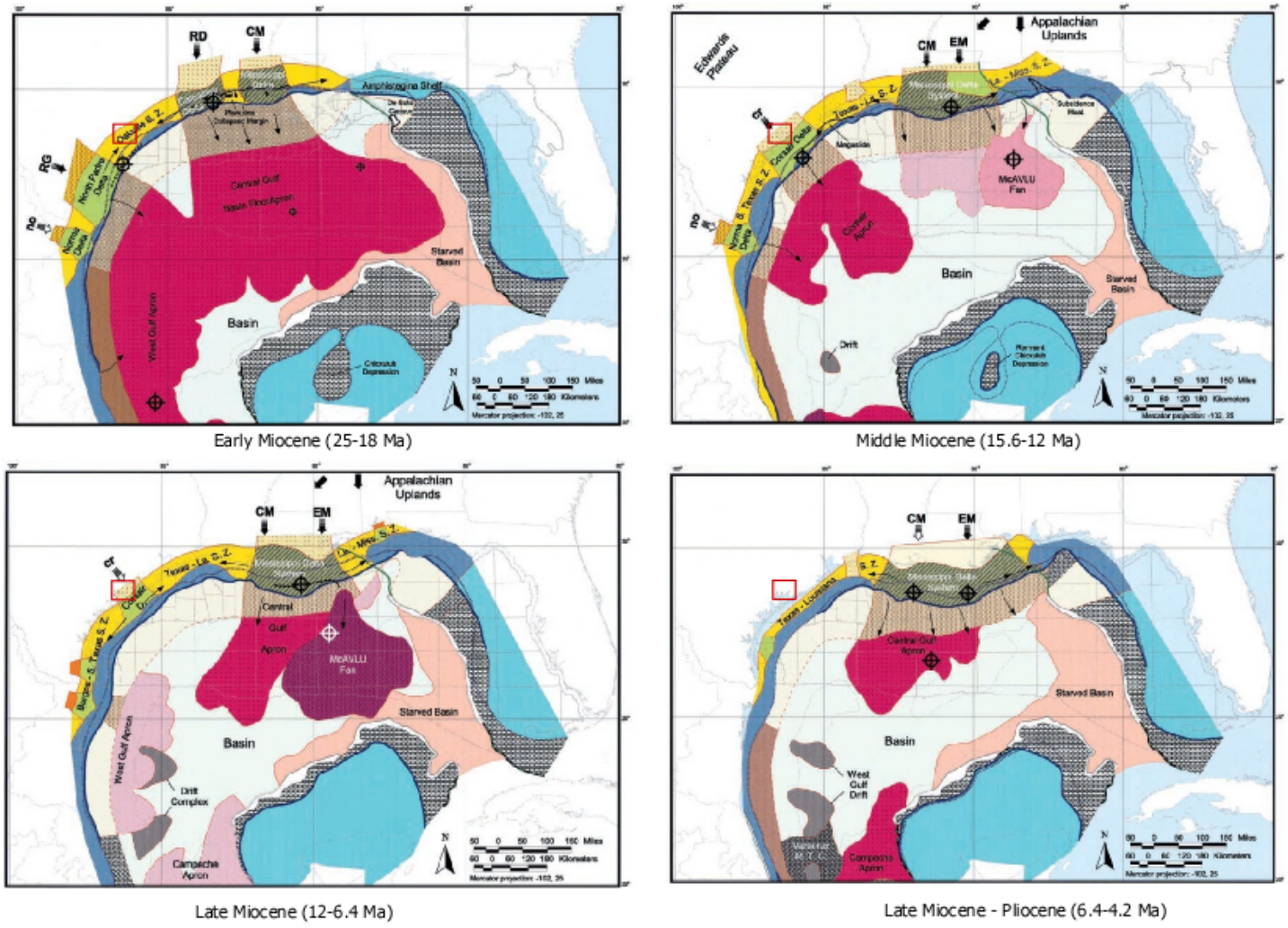

Figure: 2.8 Depositional history of the study area during the Miocene (modified from Galloway et al., 2000).

Chapter 3: Depositional Environments

In order to define systems tracts and build up the stratigraphic framework, it is crucial to primarily recognize depositional environments. In this chapter five depositional environments will be discussed with reference to the three main systems tracts: lowstand-transgressive, transgressive and regressive systems tracts.

In this study area, a lowstand-trasgressive tract is usually dominated by an incised valley system. During the late lowstand or transgressive segments of any cycle, facies within the incised valley consist predominately of bayhead delta and nearshore-shelf deposits. In the regressive segment of cyclse, strandplain/shorezone and progradational delta facies are dominant.

3.1 WELL LOG INTERPRETATION

Wire-line logs offer a good resolution of depositional environments. Gamma ray (GR), spontaneous potential (SP) and resistivity (R) log curves are used in this research. GR logs indicate presence and volume of clay or shale in rocks by detecting energy emitted from thorium (Th), uranium (U) and potassium (K), common radioactive minerals in clay. SP logs measure electrical potential generated by ion exchange of two porous media or permeable rocks. Main factors controlling the ion exchange are temperature, salt concentration in drilling mud and pores, and pore connectivity. Since shale is normally impermeable, the SP log commonly displays null or near-zero values. R logs measure resistivity of the formation from which porosity, degree of cementation, water saturation and resistivity of connate water can be inferred. Porosity and electrical resistivity are variables from which hydrocarbon saturation can be calculated. (Torres-Verdin, 2010)

Only one of gamma ray or SP logs is used with resistivity log for recognizing depositional environment. Nevertheless, I observed that SP logs display a flat or featureless curve across some sandy interval thus; the depositional environment and systems tracts might be misinterpreted by using only SP with resistivity logs. The possible reasons for flat SP curve across a sandy interval are that first, SP value is suppressed by presence of hydrocarbon or deep mud filtrate invasion in the sand. Second, the contrast of salt concentration between two layers of rock is not enough to trigger ion exchange, in other words, the two sands contain similar pore fluids (Torres-Verdin, 2010). Besides detecting sandstones that do not show up in an SP curve, a gamma ray log also shows better detail of stacking patterns (fining upward, aggrading or coarsening upward). Examples of such case are illustrated in Figure 3.1.

3.2 DEPOSITIONAL ENVIRONMENTS IN LOWSTAND SYSTEM TRACTS

3.21 Incised-valleys

3.211 Concept and model

An incised-valley system usually occurs in lowstand systems tracts. It is defined as "a fluvially eroded, elongate topographic low that is characteristically larger than a single channel, and is marked by an abrupt seaward shift of depositional facies across a regionally mappable sequence boundary at its base. The fill typically begins to accumulate during the next base-level rise, and may contain deposits of the following highstand and subsequent sea-level cycles" (Zaitlin et al., 1994). Incised valley systems mainly consist of the valleys and their fills. Formation of an incised valley is possibly induced by falling of base level which allows the river to move basinward to the steeper gradient or a change in topographic slope (a knickpoint). In the other case, increase of water discharge to sediment discharge ratio influenced by climate or possibly tectonics

can trigger fluvial erosion as well. Both situations result in the higher transportation capacity of the river compared sediment discharge, and as a result, excess energy leads to erosion of the underlying surface by fluvial processes. Fluvial lag sediments deposit at the river mouth and along the base of the valley, above the erosional incised-valley base, when the sea level reaches its lowest point and starts to rise. As the incised valley is being flooded due to transgression, the fluvial deposition steps back landward and the depositional environment changes to an estuary which is defined by Dalrymple (2006) as 'a transgressive coastal environment at the mouth of a river, that receives sediment from both fluvial and marine sources, and that contains facies influenced by tide, wave and fluvial processes. The estuary is considered to extend from the landward limit of tidal facies at its head to the seaward limit of the coastal facies at its mouth.' The estuarine deposits including fluvial, coastal and marine facies are the main component of the incised-valley fills.

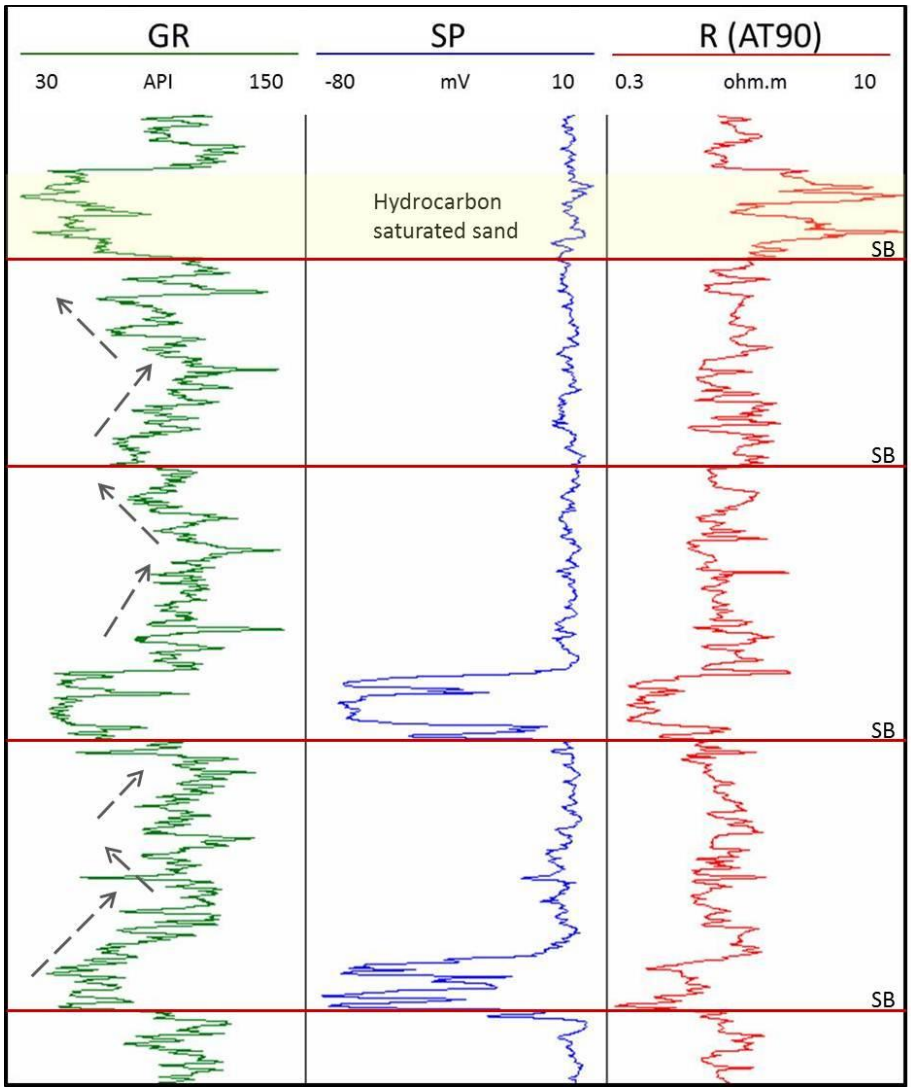

Figure 3.1: An example of three main logging measurements employed in this study: gamma ray (GR), spontaneous potential (SP) and resistivity (R) logs. In the hydrocarbon-saturated sandstone, the SP curve is null whereas the GR log is responsive. In addition, stacking patterns are easily defined from GR log as shown by dash arrows. Consequently, it is suggested that use of the curves altogether can yield more accurate results.

The fundamental characteristics of the incised-valley systems suggested by Zaitlin et al. (1994) are as following (Fig. 3.2):

1) The valley is a negative, erosive paleotopographic feature, the base of which truncates underlying strata, including any regional markers.
2) The base and wall of the incised-valleys represent a sequence boundary recording relative base level fall.
3) The incised-valley fill above the sequence boundary exhibits a basinward shift in facies
4) As a result of filling in response to rising base level, depositional markers within the deposits of the incised-valley fill onlap the valley base and walls.

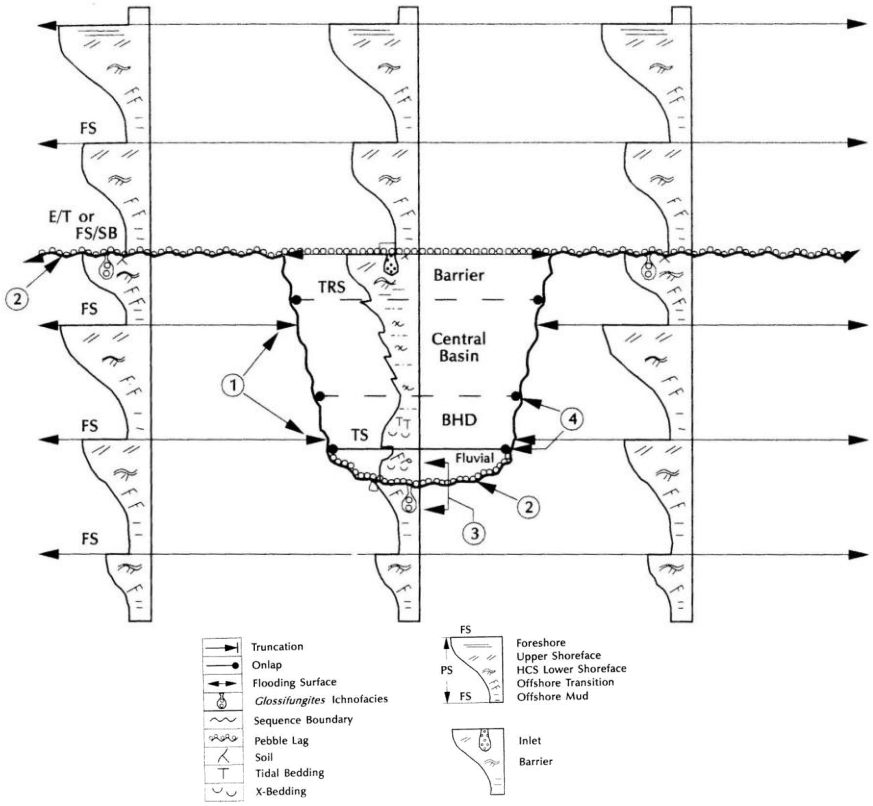

Figure 3.2: A transection of an incised-valley showing its fundamental characteristics. Explanations of each number are in preceding text. (Zaitlin et al., 1994)

One might misinterpret a distributary channel as an incised valley, in fact they are different in size, formation and lithofacies, and for example, a distributary channel width can be hundred to thousand foot wide but an incised valley can be at the scale of few to tens of miles. An incised valley can cut through an entire underlying depositional cycle whereas a distributary channel rarely cuts through its own prodelta. Additionally, most distributary channel fills are encased in mouth-bar mudstone but incised-valley fills are encased in marine mudstone (Van Wagoner et al., 1990).

Zaitlin et al. (1994) classified incised-valley systems by two criteria: their physiography and fills. In terms of physiography, incised-valley systems can be divided into piedmont and coastal types. The piedmont incised valley systems are fed by headwater from a mountain that flows across a significant change in topographic gradient whereas the coastal incised-valley systems are restricted in a flat coastal area. An example of the coastal incised-valley system is the Trinity/Sabine incised valley system, offshore of Galveston Bay of which the oldest incision age is 100 ka (Thomas and Anderson, 1994). According to the presence or absence of high-frequency sequence boundaries within incised-valley fills, an incised-valley are categorized as simple and compound incised-valley fills. The idealized model of a simple incised valley fill is shown in Figure 3.3.

3.212 Incised-valley recognition in well logs

Well log patterns of an incised valley and its fill is illustrated in Figure 3.4. Because the base of incised valleys represents a sequence boundary (Zaitlin et al., 1994), there is an abrupt leftward deflection in well log curves that record erosion and basinward shift in facies. Incised-valley fill processes commence during lowstand of sea level if sediment supply is sufficient and continuous during subsequent transgression.

Consequently, incised-valley fills commonly consist of fluvial, estuarine and marine facies (Boyd et al., 2006). Their well log expression is typically a sharp base and blocky aggradational sand body with the top exhibiting an upward-fining trend that records transgression. Lowstand deposits of interpreted sequence 1 and 2 (Fig 4.17) display characteristic of incised-valley systems which will be explained in detail in the following chapter.

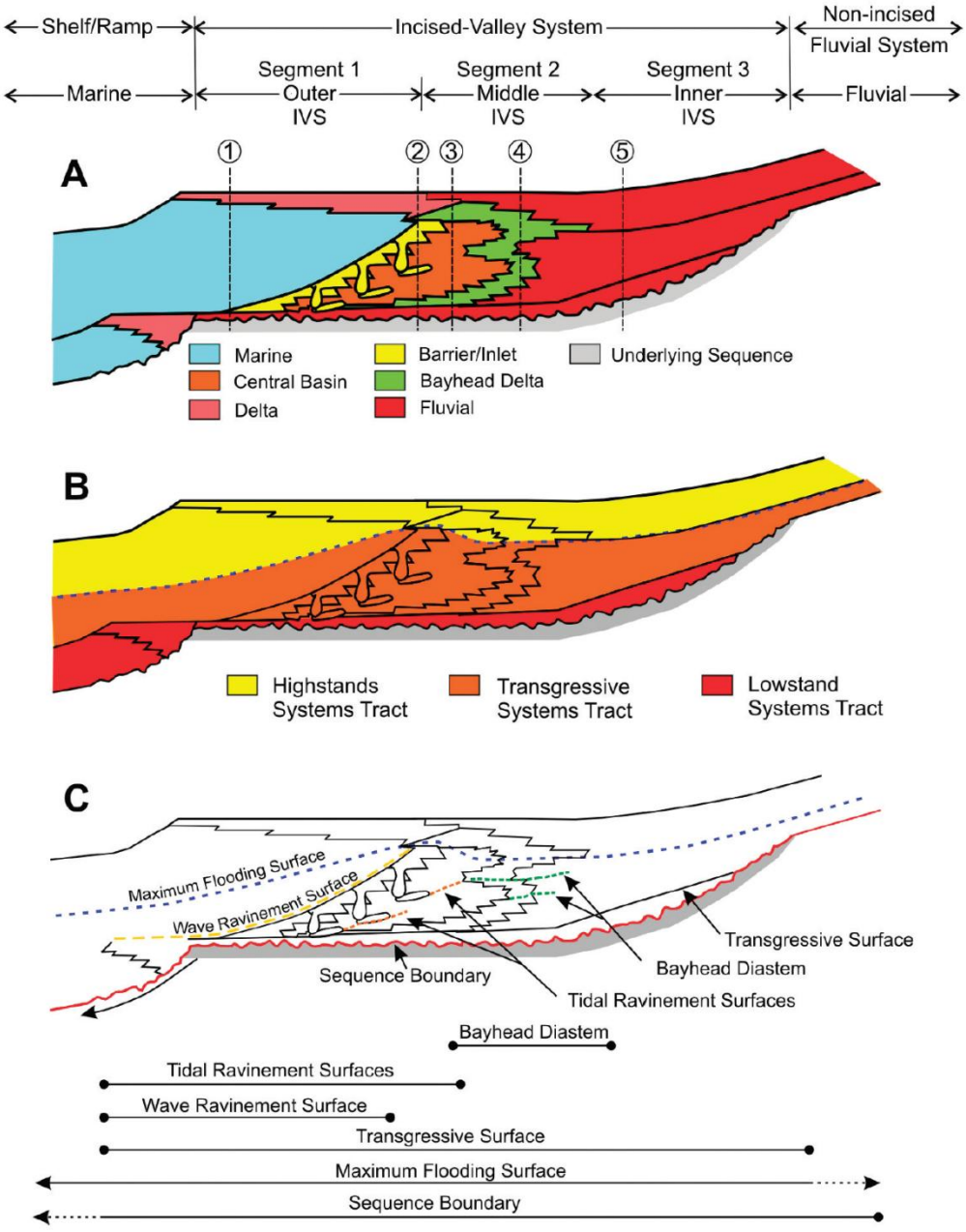

Figure 3.3: A dip section model of a simple incised valley fill in a wave-dominated estuary. A, B and C display depositional environments, systems tracts and stratigraphic surfaces respectively. (Boyd et al., 2006)

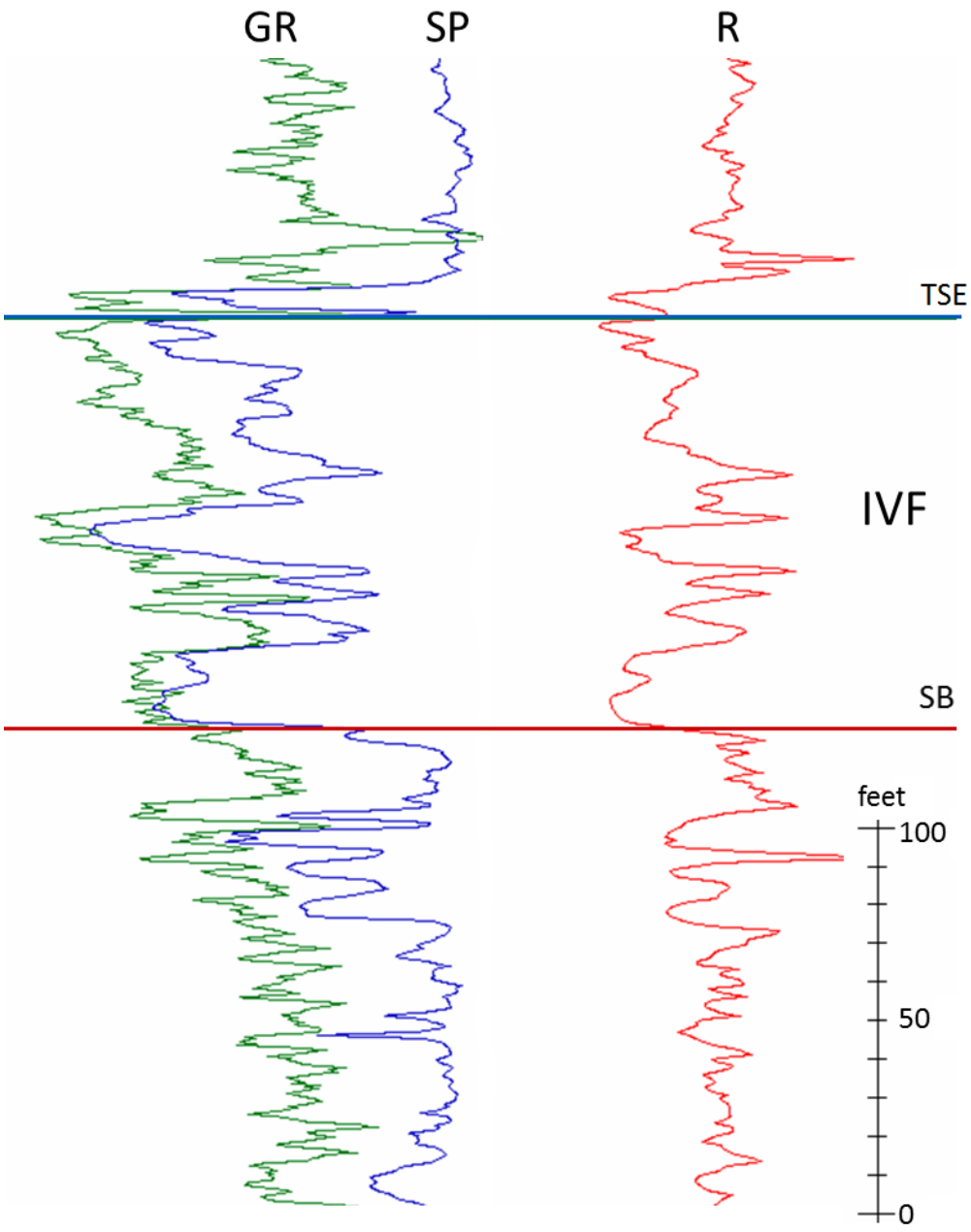

Figure 3.4: Recognition of an incised-valley (IV) in well logs. The typical pattern of the valley is a sharp-based blocky sandstone truncating the underlying progradational highstand deposits. The incised-valley fills are composed of various facies (discussed in Fig 3.7) and can be up to 100-ft (30 m) thick. The top of the incised-valley fills (IVF) is bounded by a flooding surface in turn overlain by a retrogradational upward right deflection stacking pattern.

3.3 DEPOSITIONAL ENVIRONMENT IN TRANSGRESSIVE SYSTEM TRACTS

3.31 Bayhead delta

3.311 Concept and model

During transgression, a shelf-margin or progradational delta retreats back into a drowned incised-valley or estuary and its size decreases .This type of delta is called a bayhead delta (Dalrymple et al., 1992). The delta is one of the system composing incised-valley fills in the middle incised-valley system (Segment 2 in Fig. 3.3). A bayhead delta is the smallest among all shelf deltas it is commonly < 10-m thick and normally fluvial dominated because of being protected from wave and tidal influence in an embayment behind a barrier (Fig. 3.5). The main characteristics of bayhead deltas are summarized by Porębski and Steel (2003) as shown in a Table 3.1.

The Gum Hollow fan delta (McGowen, 1971) is an example of a modern bayhead delta. It started to form around 70 year ago along the north shore of the Nueces Bay, Texas. The delta is partly fed by an artificial drainage system and some natural channels. Its morphology is attributable to climate-controlled depositional events such as rainfall and hurricanes. The subaerial delta plain is composed of longitudinal bar and braided channels.

3.312 Bayhead delta recognition in well logs

In this study, bayhead deltas form the most proximal part of retrogredational incised-valley fills. It occurs above lagoonal deposits or other blocky fluvial deposits. Characteristics of bayhead deltas in well logs are shown in Figure 3.6. The log curves display an upward coarsening succession that is commonly <10 m-thick. The GR log shows serrate curves indicating heterolithic facies which suggests more fluvial than wave

influence. There may also be tidal influence. There are back-stepping or upward fining patterns at finer scale that might record high frequency transgressive events..

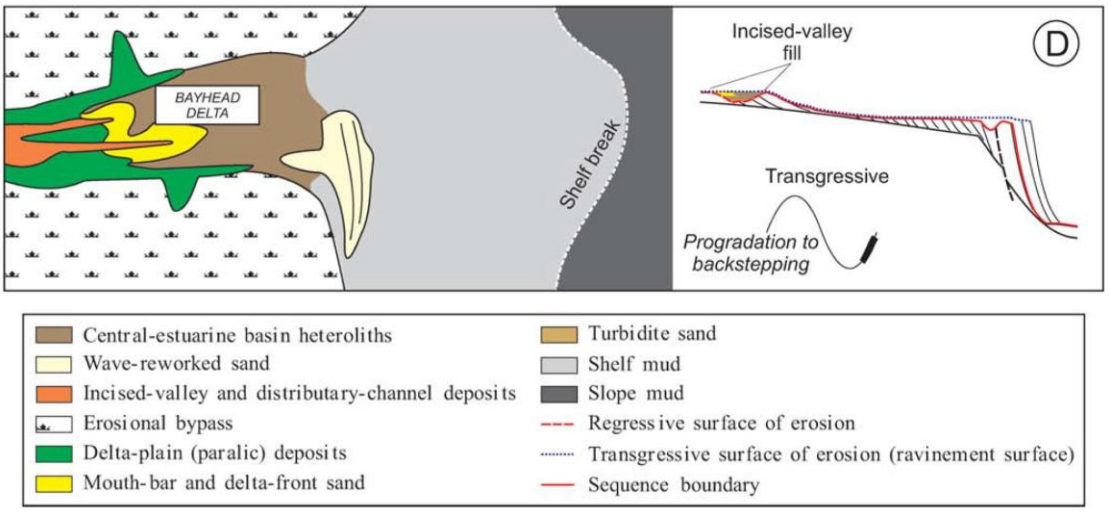

Figure 3.5: Position, environment and associated stratigraphic surface of bayhead deltas in relation to sea level change (Figure 1D in Porębski and Steel, 2006).

	Bayhead deltas	Inner-Shelf Deltas	Mid-Shelf Deltas	Shelf-Margin Deltas
Shape	Confined, funnel-shaped	Birdfoot, lobate to cuspate	Erosional pods common	Lobate to strike-elongate
Clinoform slope	?	Usually < 0.001*	< 0.5°, but can be as much as 8°**	Up to 8°, usually 3–6°
Clinoform height	Several meters	Few tens of meters	Few tens of meters	Several hundreds of meters
Thickening trend	Landwards	Landwards	Seawards, or no distinct trend	Seawards, with maximum near shelf break
Dominant energy flux at delta front	Fluvial; can be tide influenced	Fluvial, wave or tide	Fluvial or wave	Fluvial or wave; tide influence may become important during late lowstand
Delta-top facies	Fluvial distributaries	Delta plain with thick distributary channel sand	Thin to absent delta plain; thick distributary channel sand below incised valley systems; erosional bypass in places	No delta plain; thin fluvial distributaries where delta perches below shelf edge. Erosional bypass common
Delta-slope facies	Heterolithic, ripple-laminated foresets	Varies depending on delta front regime	Sandstone to heterolithic foresets; rare turbidite sands	Sandstone to heterolithic foresets; slumped mouth-bar sand embedded in prodelta shales; common hyperpycnal sand turbidites. Growth faults and diapirs
Updip termination	Intertonguing with paralic deposits	Intertonguing with paralic deposits	Erosional pinchout within mid-shelf shales	Erosional pinchout within outer-shelf or upper slope shales
Downdip termination	Pinchout within central estuarine-basin heteroliths	Pinchout with inner-shelf to mid-shelf shales	Pinchout within outer-shelf shales	Pinchout within slope shales
Clinoform breakpoint trajectory	Landward rising to basinward rising	Basinward rising	Horizontal to basinward falling	Basinward falling, aggraded to landward rising
Systems tract	Transgressive	Highstand	Falling stage	Falling stage to lowstand

Table 3.1: Characteristics of shelf deltas summarized by Porębski and Steel (2003). Bayhead delta detail is highlighted in an orange rectangle.

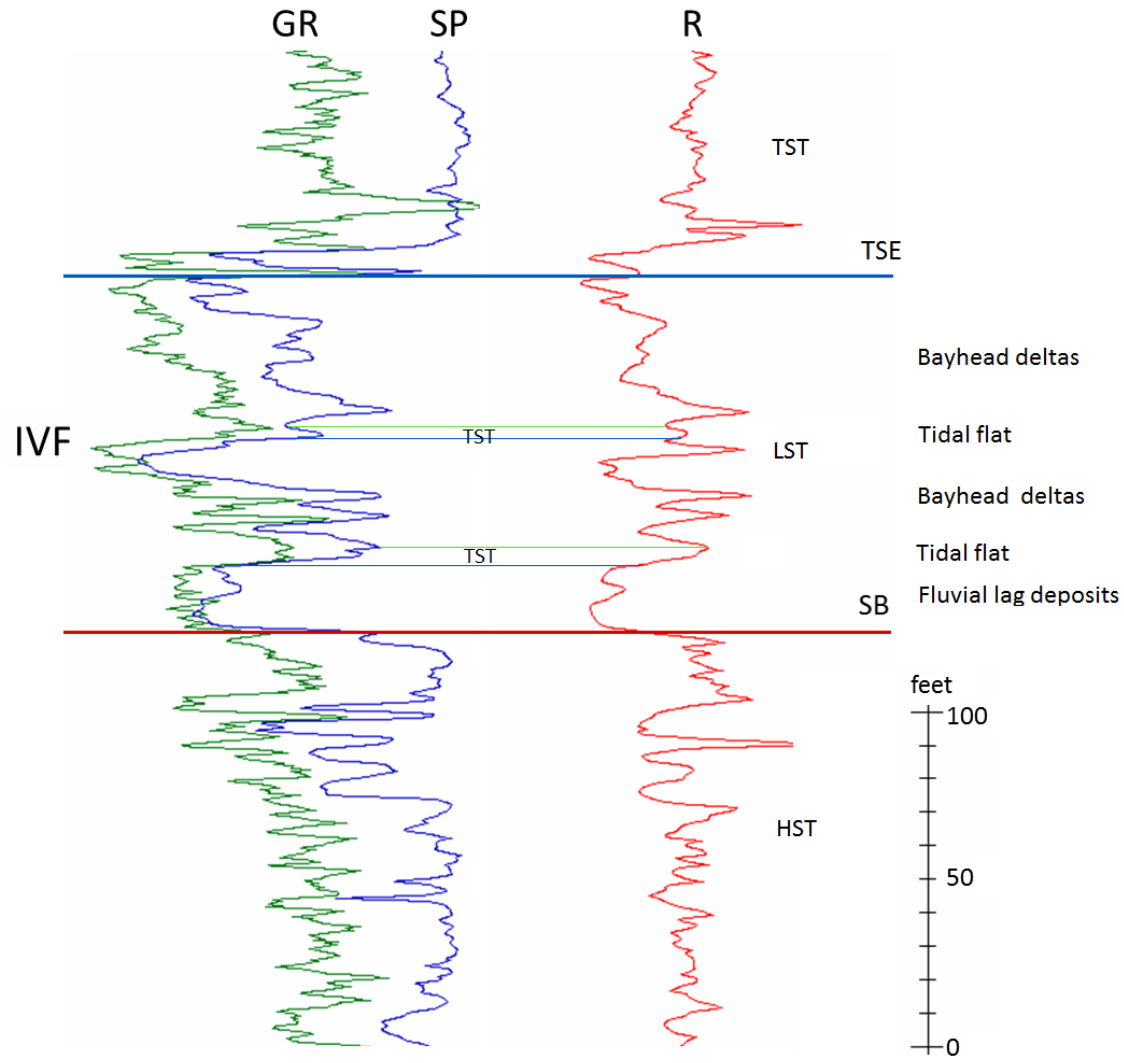

Figure 3.7: Features of bayhead deltas in well logs. They are characterized by a thin upward- coarsening (progradational) succession overlain by flooding surface. There are at least two delta lopes presented in this section. Each is approximately 15 ft (5m) thick.

3.32 Barrier-lagoon system

3.321 Concept and model

Barrier/lagoon environments are typically formed during transgression (Fig.3.7). A barrier island is well developed on a relatively flat continental shelf with high enough sediment supply (usually supply by longshore drift) and low-to-moderate tidal range. Barrier morphology depends mainly on tidal range and shoreline stability. Stubby barrier island can also be found in mesotidal (tidal range 2-4 m) coastlines (Hayes, 1976). They typically do not form in macrotidal regimes (tidal range >4 m). Lagoons are muddy protected environments landward of barrier bars. In some coastal areas, bays and estuaries occur landward of lagoons in embayments. Variation of the lagoonal environment is controlled by climate, tidal range, storm frequency and, sediment supply. Lagoonal deposits are characterized by discrete muddy facies that might grade upward from backbarrier to shoreface or commonly abruptly to shelf facies in a transgressive facies succession. In such stratigraphic succession barrier-lagoon systems might occur above a ravinement surface (Galloway and Hobday, 1983; Cattaneo and Steel, 2002). It should be noted that this transgressive ravinement commonly erodes completely the barrier so that the barrier is partially preserved or preserved only at the transgressive-regressive turnaround position (Cattaneo and Steel, 2002).

One important way of differentiating lagoonal from estuary deposits is the nature of the sedimentary fill. Barrier-lagoon systems contain mainly sediments derived from the marine realm and usually have no fluvial influence whereas estuaries derive much sediment from a river at their landward end (Boyd et al., 2006).

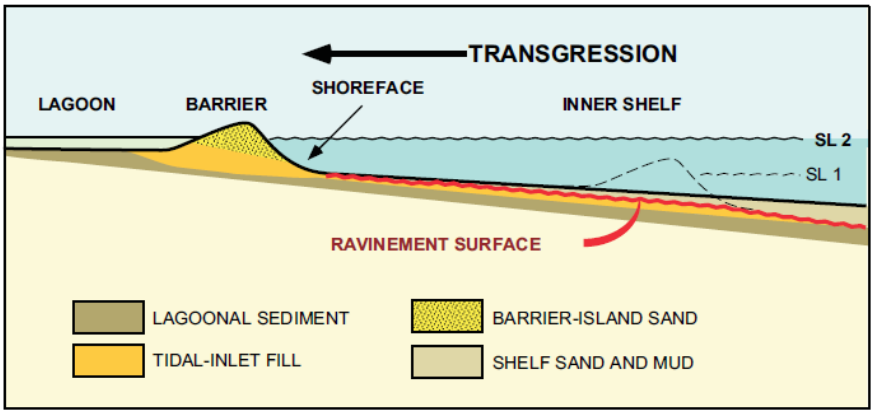

Figure 3.6: A diagram shows formation of barrier bar during transgression. The sand body at the time of sea level 1 (SL 1) is reworked by wave processes. A ravinement surface on underlying deposits is created by wave scouring during barrier back-stepping. (Clifton, 2006)

3.322 Barrier/lagoon recognition in well logs

Figure 3.7 shows how barrier-lagoonal facies appear in well logs. Lagoonal facies (embayment) are recognized by a distinct muddy interval recorded by serrate GR response. The presence of some upward-coarsening intervals implies stepping back of barrier bars or wash-over fans over the muddy lagoonal facies. The lagoonal facies are well illustrated by well logs and a net sandstone map (Fig 4.15) of TST1 deposits. The remnant of barrier bar deposits at top of Fig. 3.7 is very thin (a few meters), and could be termed a transgressive lag deposit, overlies a transgressive ravinement surface.

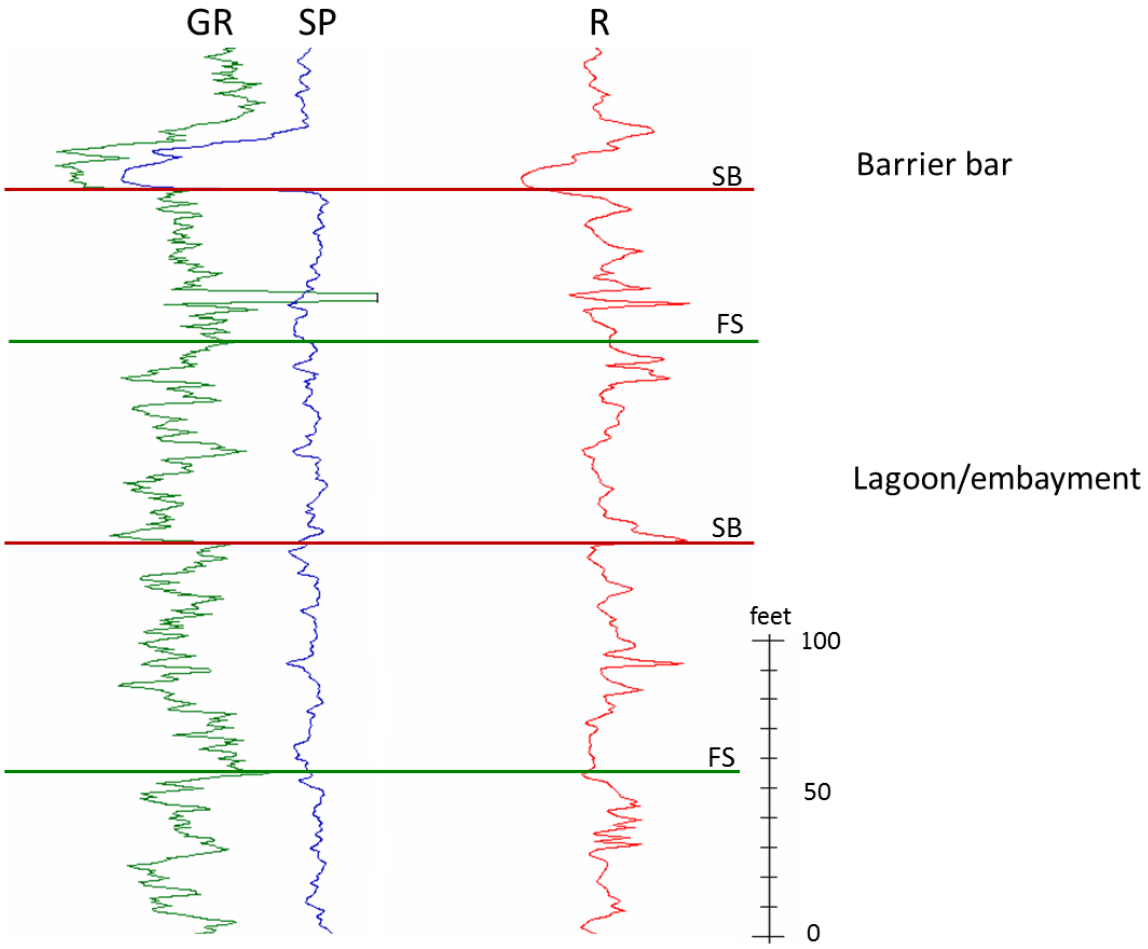

Figure 3.7: Lagoon/embayment is sand-poor facies. In this example it is composed of muddy to silty sediments, capped by barrier-bar deposits. The remnant of a barrier bar is now expressed by a sharp transgressive revinement surface (or SB in high frequency sequence scale) and thin overlying shelf lag, as it is only a couple of meters thick.

3.4 DEPOSITIONAL ENVIRONMENT IN REGRESSIVE SYSTEM TRACTS

3.41 Delta

3.411 Concept and model

A delta forms at the seaward end of a river where it delivers substantial sediment to a basin. One of the main characteristics of a delta is its progradational nature (protrusional at the coast) because of being fed by a fluvial system. Deltas are commonly built around or on a margin of basins and are commonly major basin filling processes. Galloway (1975) classified deltas by the main processes controlling their geometry and facies distribution and according to his tripartite chart, three types of delta are divided as fluvial-, wave- and tide dominated deltas (Galloway and Hobday, 1983). Additionally, delta morphology and facies distribution depend on density contrast of inflowing water and water in the basin, sediment discharge, water depth, accommodation space, and geometry of the receiving basin (Bhattacharya, 2006).

A delta system is composed of three main environments: a subaerial delta plain (topset), a delta front (foreset), and a prodelta (bottom set). The distributary channel is a typical building block in the delta plain setting and there are also other associated nonmarine to brackish facies such as floodplain and levee, crevasse splays, marshes and interdistributary bays. A delta front has a seaward dipping (few degrees) character sometimes called a clinoform, usually with a height of less than 100 m. Delta fronts contain, on average, coarser sediments than delta plains and are predominantly channel-mouth bars, shoreface (lateral to mouth bars) and tidal flat facies. A prodelta occurs seaward of the delta front and is where muddy sediment deposits fall out of suspension at a slightly deeper water level. A prodelta contains mud, silt and organic matter such as plant debris or fossils derived from river flooding and storms. Progradation of delta

systems produce a typically upward-coarsening succession from prodelta to delta front in which thickness can range from meters to a hundred meters (Bhattacharya, 2006).

3.412 Delta recognition in well logs

Deltas are usually recognized by upward-coarsening grain size patterns. The log facies succession of a delta system is displayed in Figure 3.8. Each main delta unit is approximately 30-m thick and bounded at the top by flooding surfaces. A single package of delta (6-13m thick in Fig. 3.8) is called a parasequence (Van Wagoner, 1990). The blocky or fining upward interval that overlies the upward-coarsening delta front is interpreted as a distributary channel. Deltas are depositional component of most HSTs mapped in this study, as discussed later in chapter 4.

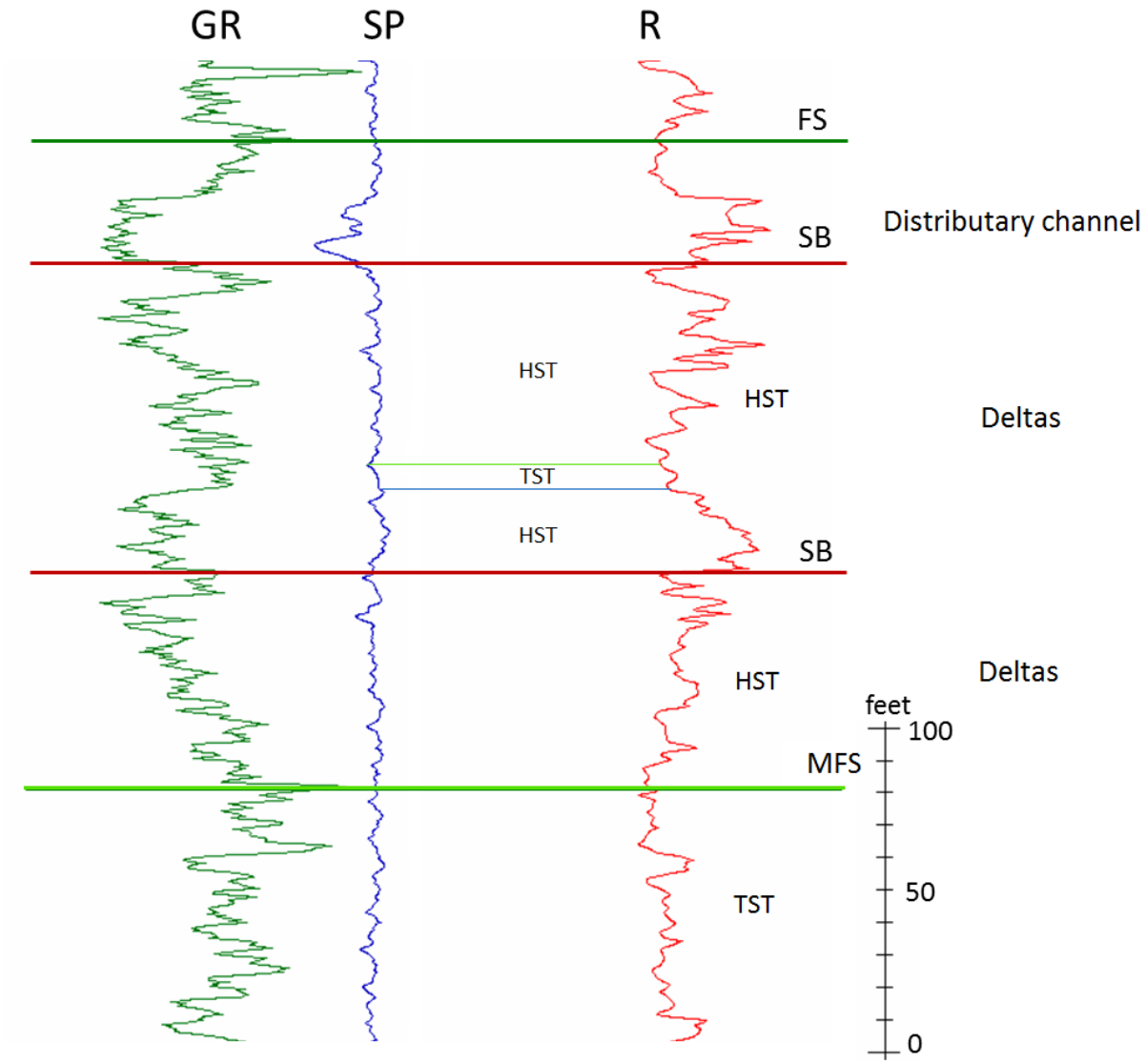

Figure 3.8: Well log patterns of a deltaic environment.

3.42 Shorezone

3.421 Concept and model

The shorezone (shoreface and foreshore) is a transition zone between wave base to the landward limit of wave processes (Fig 3.9 and 3.10). Shorezone and delta systems share similar environmental component such as beach, barrier, lagoon, estuary and tidal

channel but the delta system is distinguished by its river-fed, (or in this case, progradational) nature while shorezone systems derive sediments along strike by longshore currents. Most shorezone sediments are from along-strike reworked delta lobes, and channel-mouth deposits (Galloway and Hobday, 1983).

Complete stratigraphic succession from bottom to top of the shorezone environments is muddy shelf, shoreface, foreshore, and non-marine or lagoonal facies (Figs. 3.9 and 3.10). The shoreface is a stable part of the prograding shoreline of which the upper part has the highest wave energy, featuring subaqueous dune deposits as products of longshore and rip currents. Waves transport sediments by two main processes: at sea they create water movement and at the shoreline they produce longshore and rip currents. Shoreline facies characteristics and distribution depend largely on the energy regime. The shoreline profile of high-energy, storm-dominated shoreline (i.e. the modern California coast) differs from the one with lower energy (i.e. southeastern coast of Spain). Studies of the Pleistocene Texas Gulf Coast point out that the successions are in a fair-weather dominated, low-energy, barred setting with fine-grained deposits. Additionally, in the passive margin setting where rivers flow on a relatively flat coastal plain, shorelines usually contain finer-grained sands than those in tectonically active settings (Clifton, 2006).

As mentioned above that shorezone systems are composed of various depositional environments, however in a regressive condition the most common environment is strandplain environment. Strandplains, composed of beach ridges or shoreface facies, are accretional, strike parallel sandy coastal facies which have width in a range of 6-25 miles (10-40 kilometers) and can be from three to tens of ft (1- 4 m) high. However, the deposits are generally < 30 ft (10 m). A strandplain normally represents sandy deposits, if it is muddy then the term ‘chenier’ is used (Galloway and Hobday, 1983).

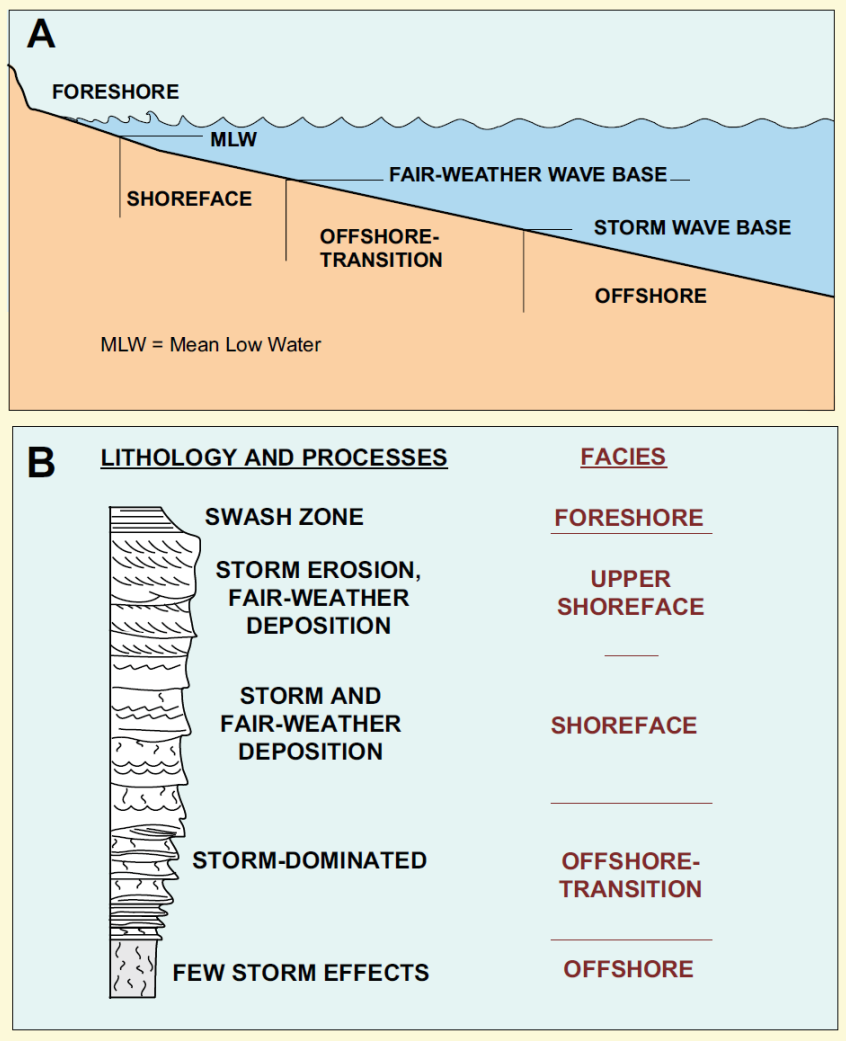

Figure 3.9: Shorezone facies model of Reading and Collinson (1996) (Clifton, 2006). A is the profile from beach to offshore showing wave bases. B is the facies succession with upward-shoaling trend.

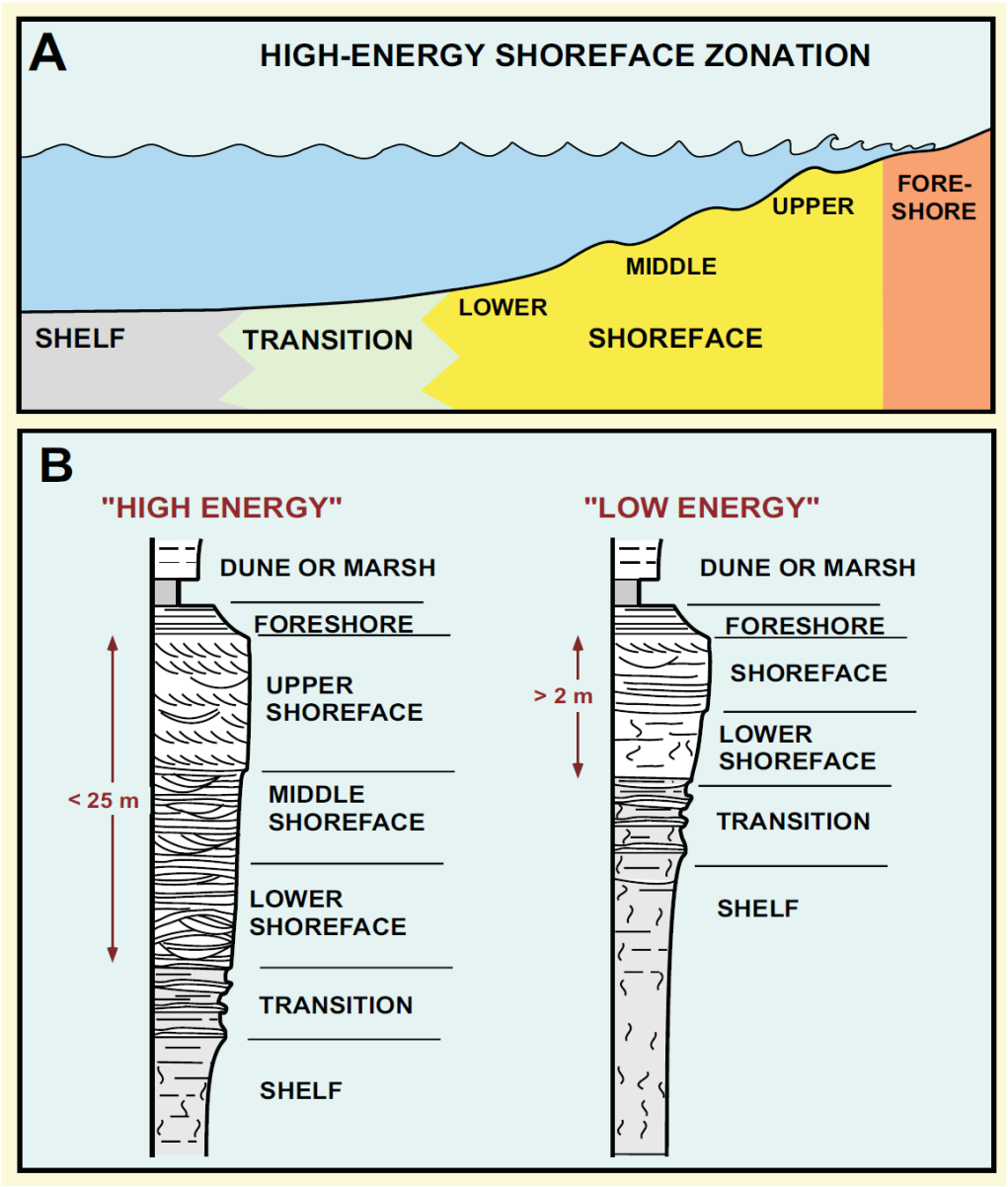

Figure 3.10: Shorezone facies model of Galloway and Hobday (1996) cited in Clifton (2006). A is a high-energy shorezone profile including the transition zone between shelf and shoreface. B is comparison of high- and low-energy shorezone facies successions. Both show upward-shoaling trend.

3.422 Strandplain/shorezone/ recognition in well logs

Strandplains have progradational to aggradational facies successions. The deposits are usually clean sandstones owing to wave reworking processes. Strandplains can have a transitional or sharp-erosional base. Sharp-based strandplain deposits are caused by sea-level fall or forced regression for example, the Cardium Formation of Alberta of which the hummocky cross-stratified sandstone (HCS) was removed by wave erosion during sea level fall (Plint, 1988, Fig 3.11). However, Posamentier et al. (1992) suggest that sharp-based shoreface deposits are more likely to occur at their proximal position only. The well log in Figure 3.12 is an example of sharp-based strandplain deposits that overly muddy shelf facies. The section above the sequence boundary displays upward coarsening trend which could represent a progressive facies change from lower to upper shoreface where sands are coarser and/or cleaner. There was a break of minor transgression before deposition of the upper strandplain which displays aggradational stacking pattern. Strandplain/shore zone environment was interpreted as a depositional environment during highstand condition of sequence 4 discussed in the next chapter.

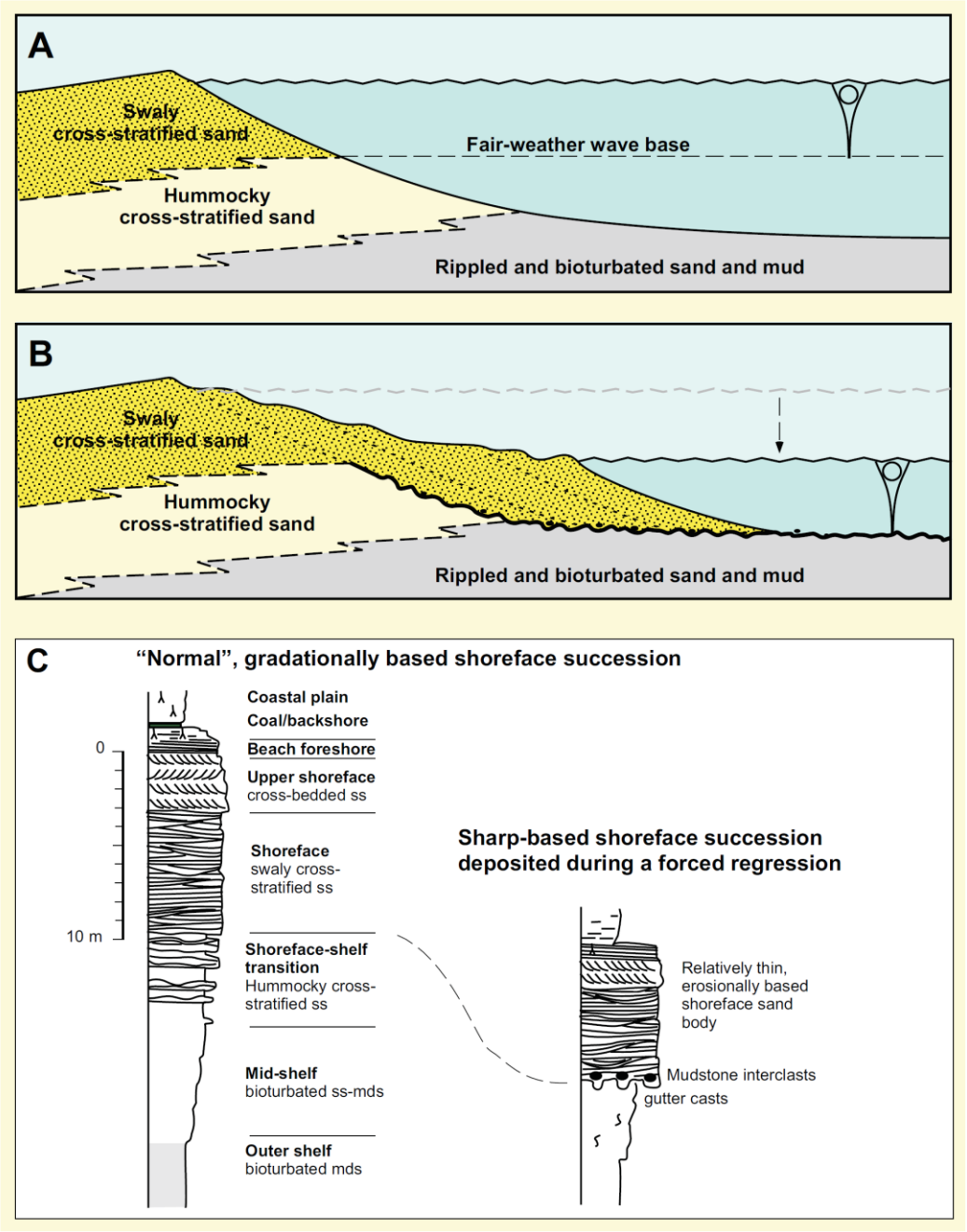

Figure 3.11: The shoreline forced regression model of Plint (1988) shows shoreface as the swaly cross-stratified-sand. During sea level fall, waves create erosional surface and shoreface system migrates basinward (A and B), consequently shoreface deposits show sharp base (C).

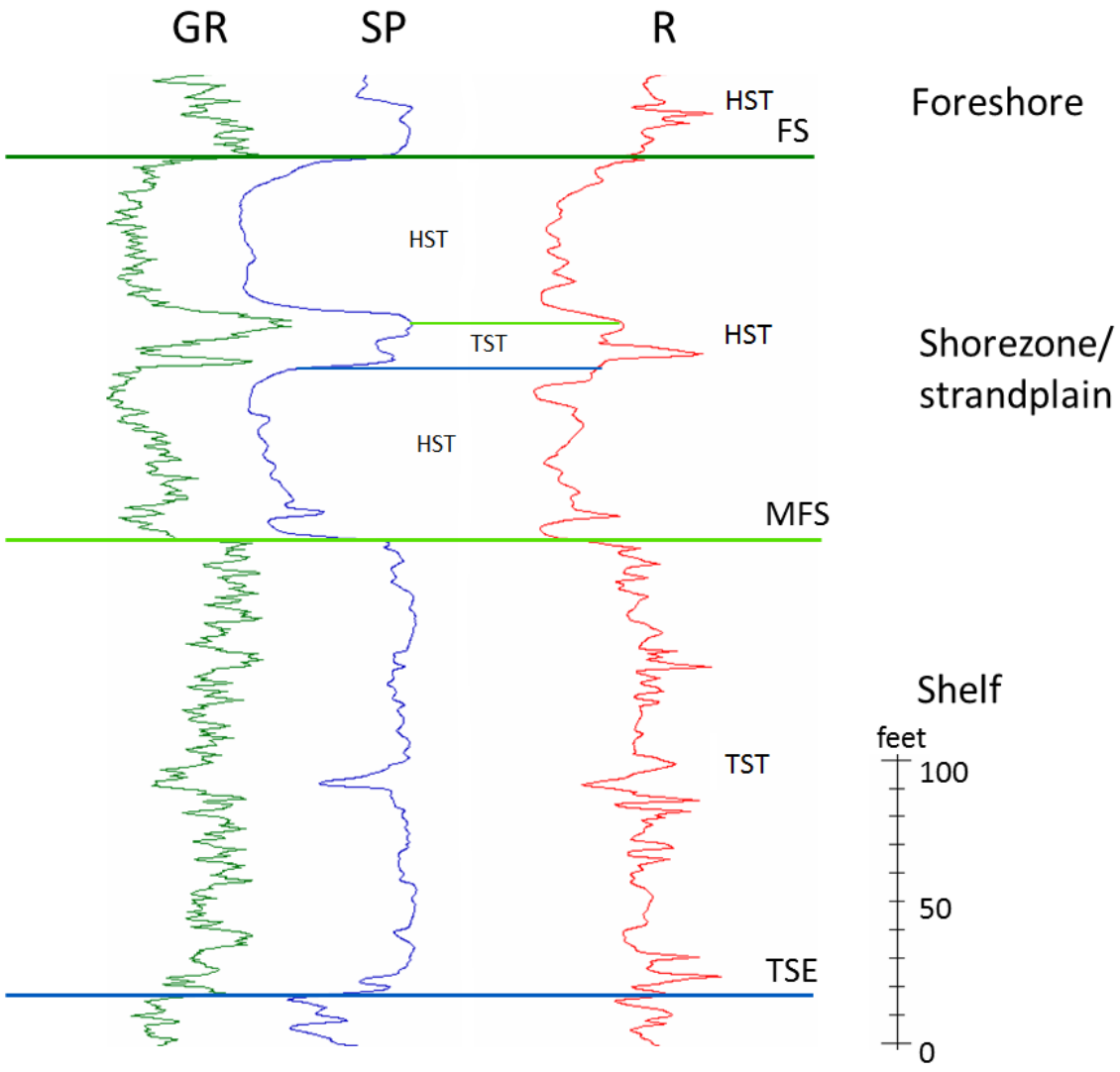

Figure 3.12: Example of strandplain/ shorezone pattern in well logs. It is composed of sandy deposits which have sharp base and progradational to aggradational stacking patterns.

Chapter 4: Sequence Stratigraphy and Depositional Systems

4.1 Sequence Stratigraphic concepts and Methodology

Sequence Stratigraphy is 'the study of genetically related facies within a framework of chronostratigraphic significant surfaces' (Van Wagoner et al., 1990). It is different from other stratigraphic principles because sequence stratigraphy is 'a genetic, process-based approach' (Catuneanu et al., 2010). Sequences are fundamentally composed of, from larger to smaller scales, parasequence sets or systems tracts (Brown and Fisher, 1977) and parasequences. Sequence and systems tracts formation are normally a response to allocyclic changes created by unsteady rates of the external driving controls whereas parasequences are mainly a response to autogenic changes despite steady rates of the external drivers (Muto and Steel, 1998; Muto et al., 2007).

There are three main types of sequence stratigraphic models defined in the literature; depositional sequences (Mitchum et al., 1977), genetic stratigraphic sequences (Galloway, 1989) and transgressive-regressive (T-R) sequences (Johnson and Murphy, 1984; Embry and Johannessen, 1992). Mitchum et al. (1977) introduced depositional sequences as 'stratigraphic units composed of a relatively conformable succession of genetically related strata and bounded at its top and base by unconformities or their correlative conformities'. Later, the definition of sequence was redefined by some authors such as 'a stratigraphic unit bound by specific type of unconformity and its correlative surface' (Embry, 2009) and 'a succession of strata deposited during a full cycle of change in accommodation or sediment supply' (Catuneanu et al., 2009).

4.11 Type-I depositional sequence

This study defines third- and fourth-order type-I depositional sequences following the type-I depositional sequence in a basin with a shelf-break model of Van Wagoner et

al. (1990) (Fig. 4.1). The type-I sequence forms during relative sea level fall (when rate of eustatic fall outpaces rate of subsidence) below the depositional shoreline break. Each sequence is bound by a sequence boundary, which is a subaerial erosional surface. The Type-I sequence consists of three systems tracts; lowstand (LST), transgressive (TST) and highstand systems (HST) tracts. Systems tracts are recognized by stratal stacking patterns (Fig. 4.2), their positions within the sequence, and by bounding surfaces. Lowstand systems tracts (LST) are characterized by sharp-based sandstone bodies directly overlying sequence boundaries. The sharp bases represent basinward shift in facies and erosion of underlying highstand facies. From the sharp base, lowstand deposits commonly exhibit progradational to aggradational stacking patterns up to a turnaround point marking the onset of retrogradation, in turn overlain by a transgressive surface of erosion (TSE). A transgressive systems tract (TST) is a unit between a TSE and a maximum flooding surface (MFS). It is composed of retrogradational parasequence set, and exhibits an upward-fining pattern below the MFS. A highstand systems tract (HST) overlies the MFS and is bounded above by the next sequence boundary. At the early stage, HSTs normally display aggradational stacking patterns and grade upward into progradational patterns (Van Wagoner et al., 1990). Stratigraphic surface and systems tract recognition patterns in well logs used in this study are illustrated in Figure 4.3.

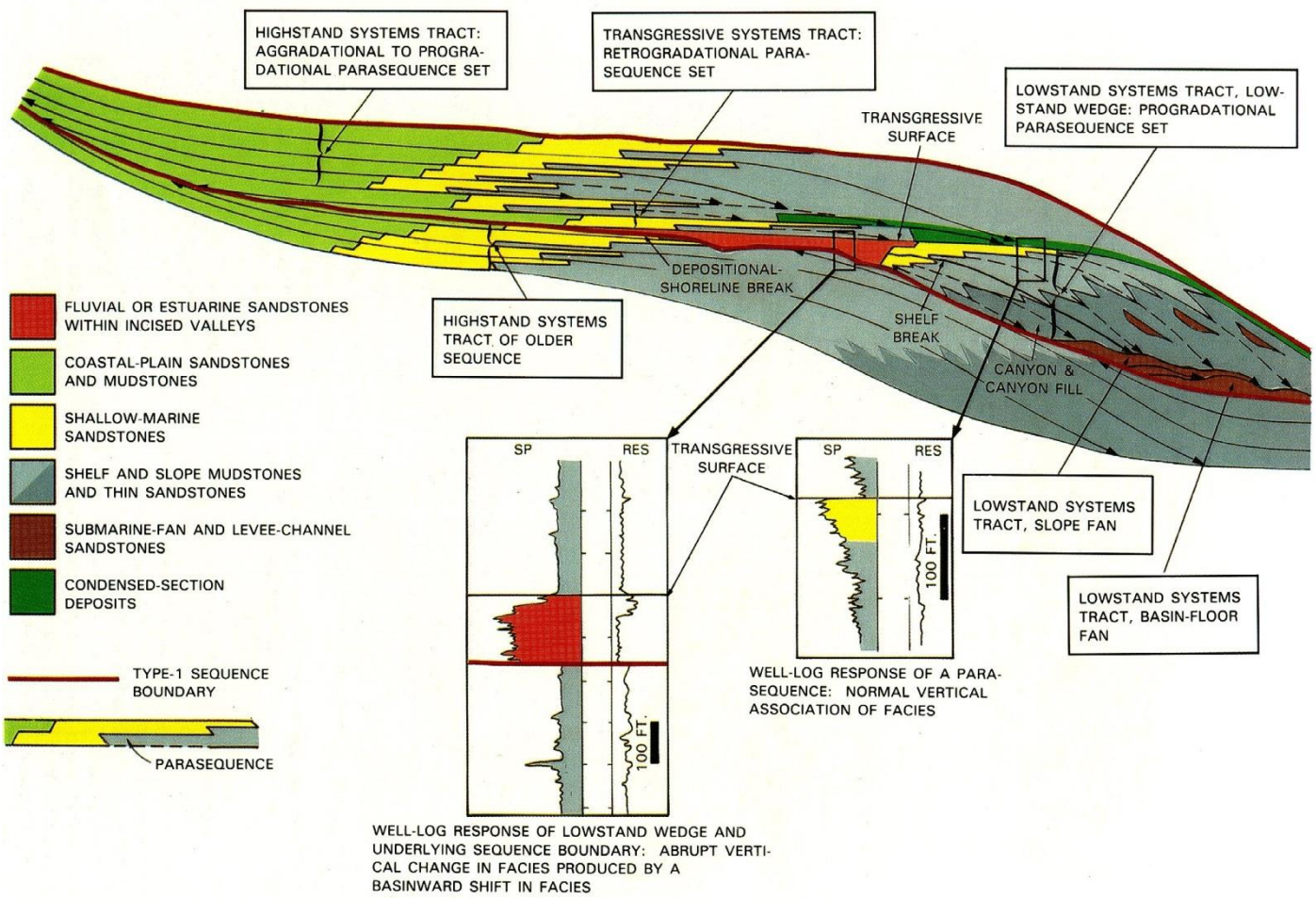

Figure: 4.1 Type-I depositional sequence idealized model of the continental platform with a shelf-break (Van Wagoner, 1990).

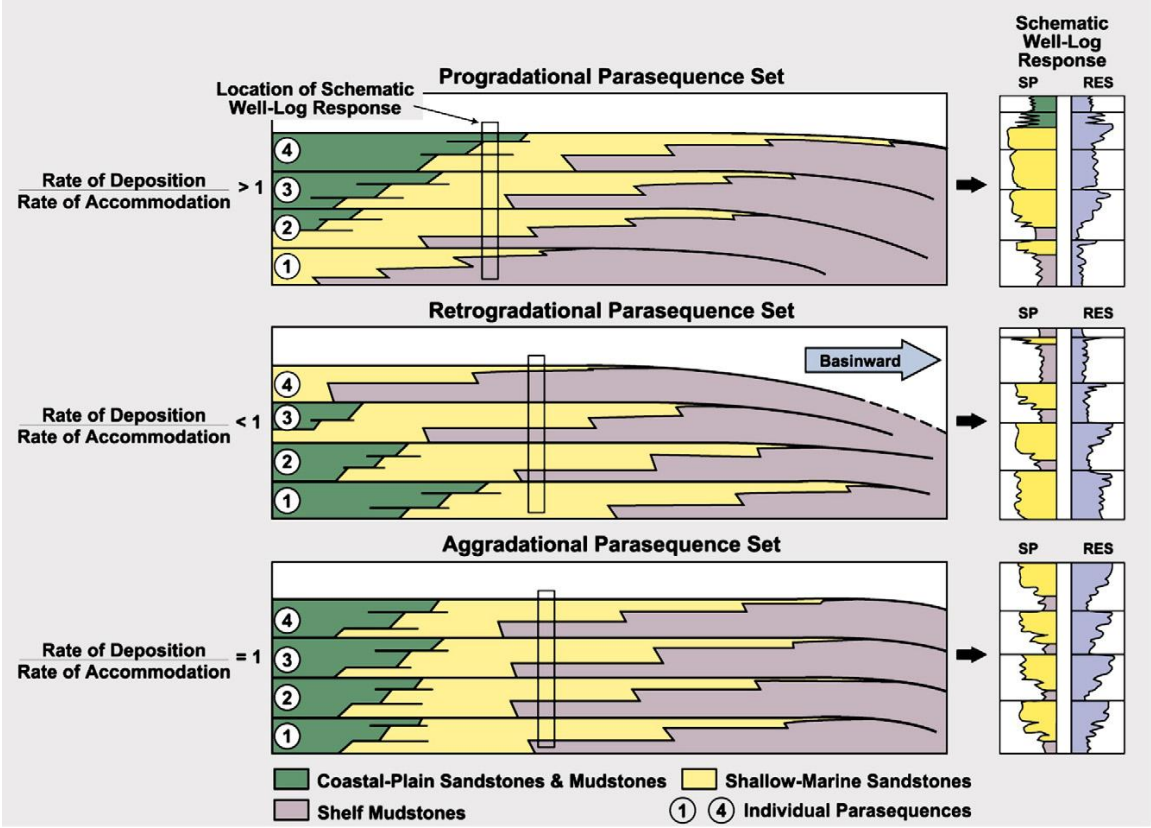

Figure: 4.2 Parasequence vertical stacking patterns and progradational, aggradational and retrogradational parasequence sets, the result of interplay between depositional and accommodation rates. Stacking patterns are key to recognizing systems tracts. A LST contains progradational to aggradational parasequence sets. A TST typically exhibits retrogradational stacking patterns whereas a HST displays aggradational to progradational stacking pattern. The characteristic of stacking patterns in well logs is shown in Figure 3.3 (modified from Van Wagoner, 1990).

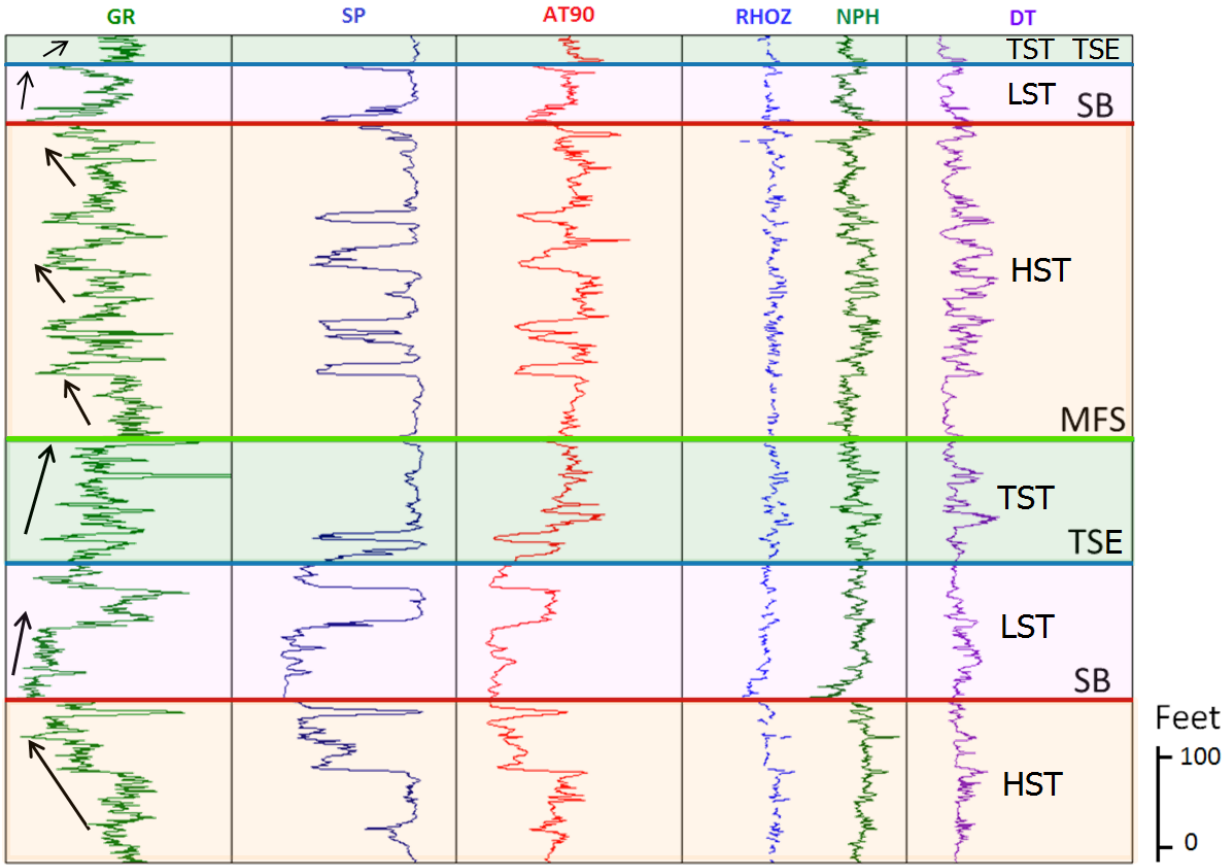

Figure: 4.3 Stratigraphic surface and systems tract recognition patterns. In this study three log curves are used that include gamma ray (GR), spontaneous (SP) and resistivity (R). The other curves are density (RHOZ), neutron density (NPH) and sonic (DT), used to assure accurate correlations between wells. According to Van Wagoner (1990), a sequence boundary (SB) occurs typically below a sharp-based sandstone with a blocky or upward-fining GR or SP response, which truncates progradational highstand deposits. Similarly, resistivity curves may also feature an abrupt rightward or leftward deflection, depending on type of fluid contained in rock pore (water or hydrocarbon). The TSE occurs typically at a turnaround point on GR or SP curves, recording an upward-fining vertical profile marking the onset of marine transgression. Where the LST is absent, the TSE is defined at the top of upward-coarsening deposits. The MFS occurs typically at the greatest rightward GR deflection and the most positive SP position, whereas the R curve shows the lowest value (leftward deflection). These log responses correspond to the finest or muddiest lithologies.

4.12 Transgressive-regressive (T-R) sequence

According to Johnson and Murphy (1984) a T-R sequence is composed of a transgressive systems tract (TST) and a regressive systems tract (RST). A TST is bounded by maximum regressive surfaces (MRS) or transgressive surface (TS) of Van Wagoner (1990) at its base and maximum flooding surface (MFS) at its top. A RST overlies TST and is bounded at the top by a MRS of the next cycle. In 1992, Embry and Johannessen revised the definition of a sequence as a unit bounded by a composite sequence boundary including the subaerial unconformity and marine portion of the maximum regressive surface. This type of sequence group is composed of two genetic units, which are the forced and normal regressive units together in a regressive systems tract. This is a pragmatic approach for a marine setting where the transgressive and regressive events are well preserved.

4.13 Well log correlation

I use the S^5 benchmark chart of Carancahua Bay area (Fig. 4.4, unpublished chart of Hammes, 2007) as a reference for well log correlation. The S^5 benchmark chart or 'Site-specific sequence-stratigraphic section' benchmark chart is a composite wireline log selected from deepest wells in a subbasin. Stratigraphic sections from individual wells that compose the S^5 benchmark chart are unfaulted and have complete sections. The chart integrates a wide variety of data such as lithology, biostratigraphy, coastal onlap curves, depositional environments, chronostratigraphy, as well as systems tracts, and associated surfaces which are designated by specific colors on well logs (Brown et al., 2005). The charts have been successfully used to correlate stratigraphic sections across the growth faulted subbasins such as the Oligocene Frio Formation in the Corpus Christi area by Brown et al. (2004b) and in and across three Frio subbasins: Corpus Christi, Red Fish and Mustang Island in the South Texas area by Bonnaffé at el. (2008). Additionally, Moore

(2005) successfully applied the same method to the lower Miocene Oakville Formation in the Red Fish bay area.

4.14 Stratal slicing

According to Zeng and Hentz (2004) statal slicing was introduced by Zeng et al. (1998) to visualize seismic geomorphology that can be used to infer sandstone-body geometry and depositional environments. It is applicable to the high-frequency sequences that are typically too thin to be resolved from seismic data. These high-frequency sequences commonly appear as a single seismic event. Examples include Miocene fourth-order sequences in the Gulf of Mexico that range in thickness from 30-100 ft (10-30 m). Stratal slicing is particularly applicable for complex and lenticular sandstone architecture such as that encountered in fluvial, lower coastal plain, and deltaic systems. The procedure is to first generate a stratal slice in a 3D seismic volume, mapping reference horizons assumed to be time-equivalent that are relatively flat and continuous. Examples include marine condensed sections, flooding surfaces, and coal beds. Then the reference horizons are flattened and the resulting stratigraphic section is sliced proportionally between the horizons by using the application called Recon™ as shown in Figure 4.5 (Zeng and Hentz, 2004). The reference horizons on normal 3D seismic volume and on the flattened volume are shown in Figure 4.6.

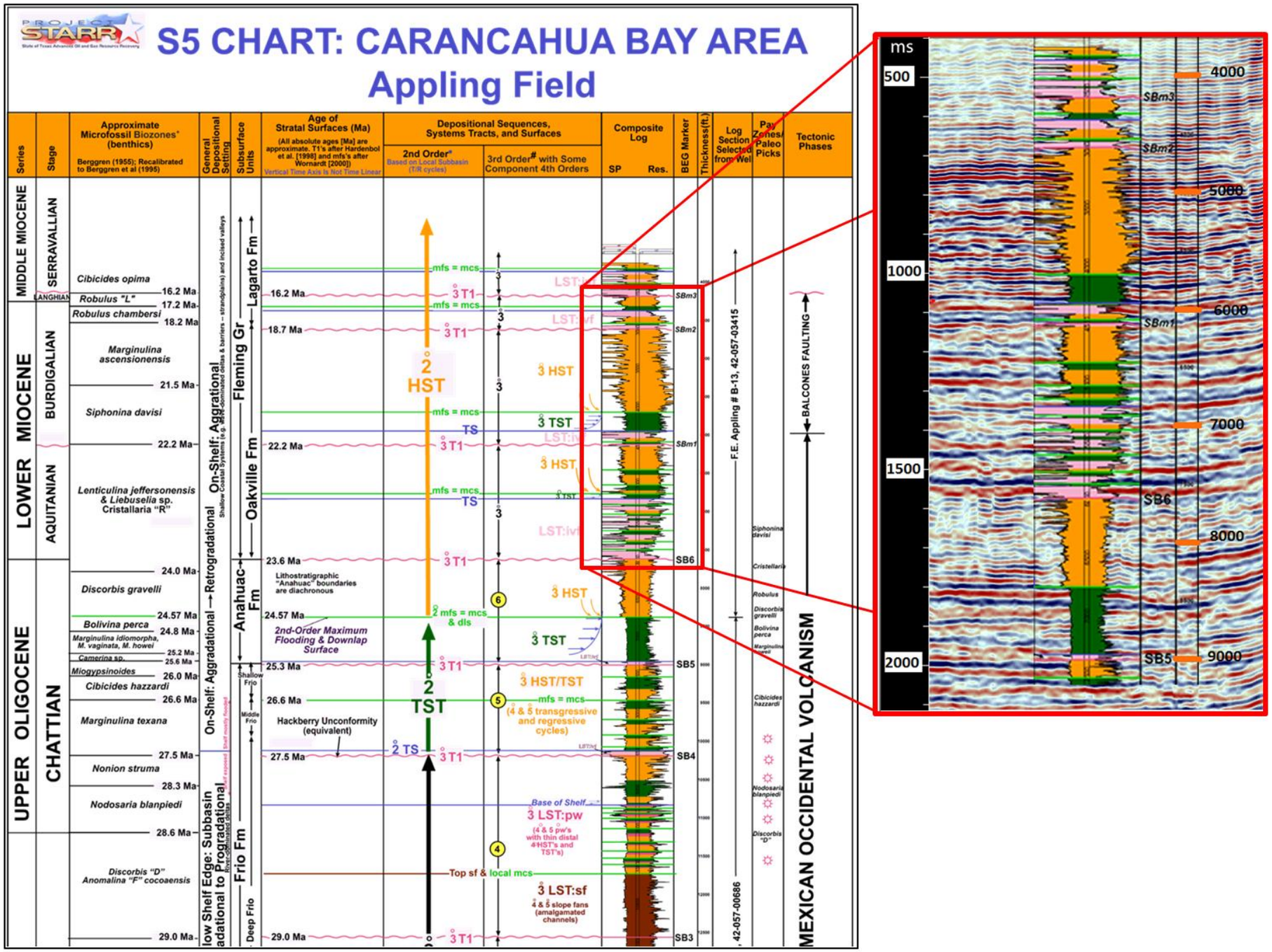

Figure: 4.4 The S^5 benchmark chart of the Carancahua Bay area. The study interval is in the red box, tied to a seismic section the blocky sand bodies correspond to high negative amplitude events.

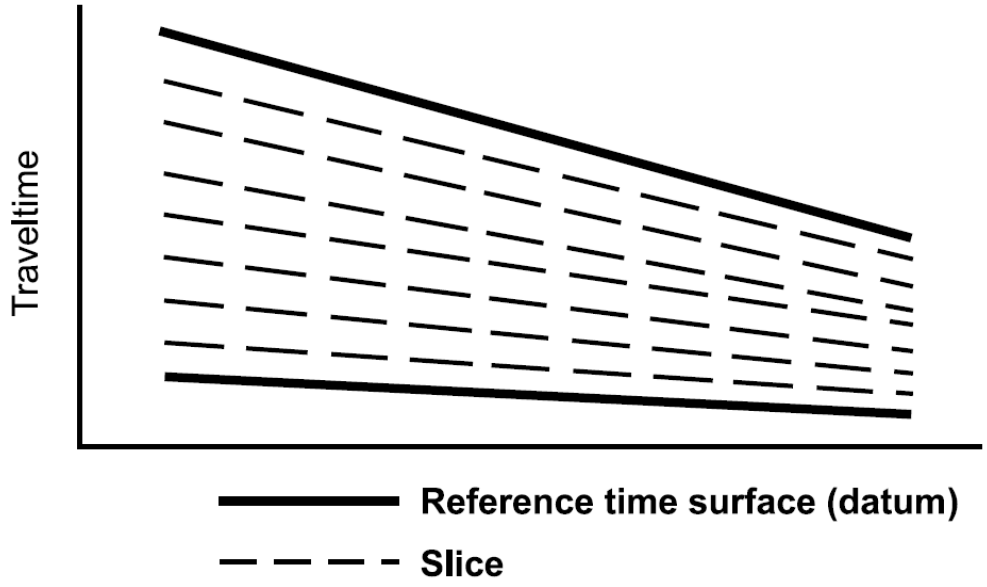

Figure: 4.5 Simplified diagram showing how stratal slices are generated. (from Figure 9c of Zeng and Hentz, 2004)

4.2 SEQUENCE STRATIGRAPHIC ANALYSIS BY AN INTEGRATION OF WELL LOG CORRELATION, NET SAND MAPPING AND STRATAL SLICING

4.21 Type-I depositional sequence

In order to cover most of the study area, five well log correlations were produced (Fig 4.7); two strike and three dip oriented lines (Fig. 4.8-4.12). The correlation including the lower Miocene interval (23.6 – 18.7 Ma) which is the Oakville Formation and the basal part of the middle Miocene Lagarto Formation (18.7-16.2 Ma) contains five sequences, from bottom to the top sequence 1-5, which have an approximate duration of 0.6-2.5 Ma (third-order sequences). Sequence thickness increases upward from sequence 1 to sequence 3 and then shows a reverse trend from sequence 3 to sequence 5. Such trends imply that accommodation space was increasing during formation of sequence 1 to sequence 3 and decreasing afterward. Lower and middle Miocene LSTs show more

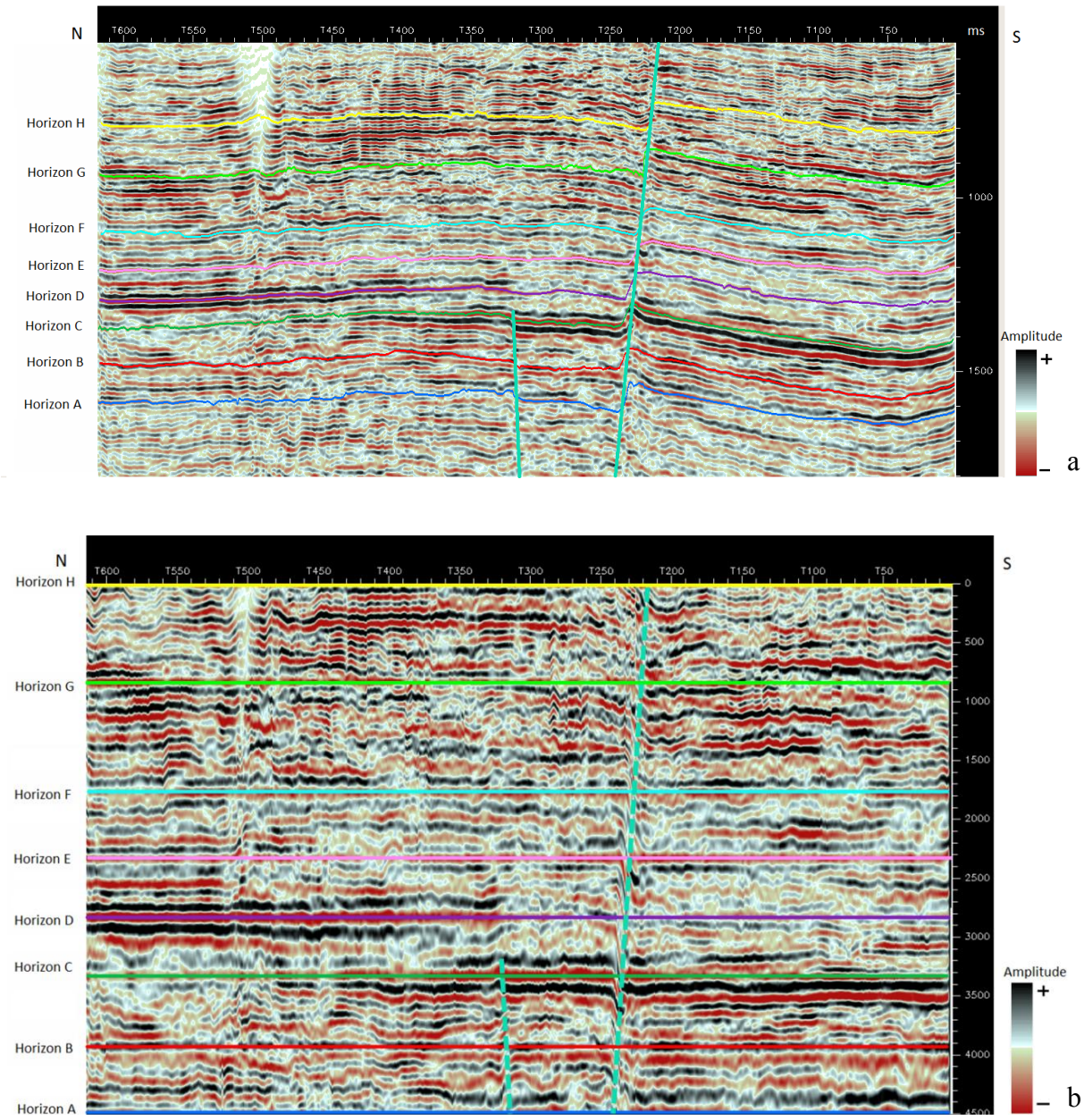

Figure: 4.6 Eight reference horizons on normal 3D seismic volume (a) and flattened volume (b). It is notable that horizon G and H are not well flattened and reflectors above horizon F are discontinuous possibly from seismic processing. Thus analysis of strata slice was focus on the interval between horizons A-F.

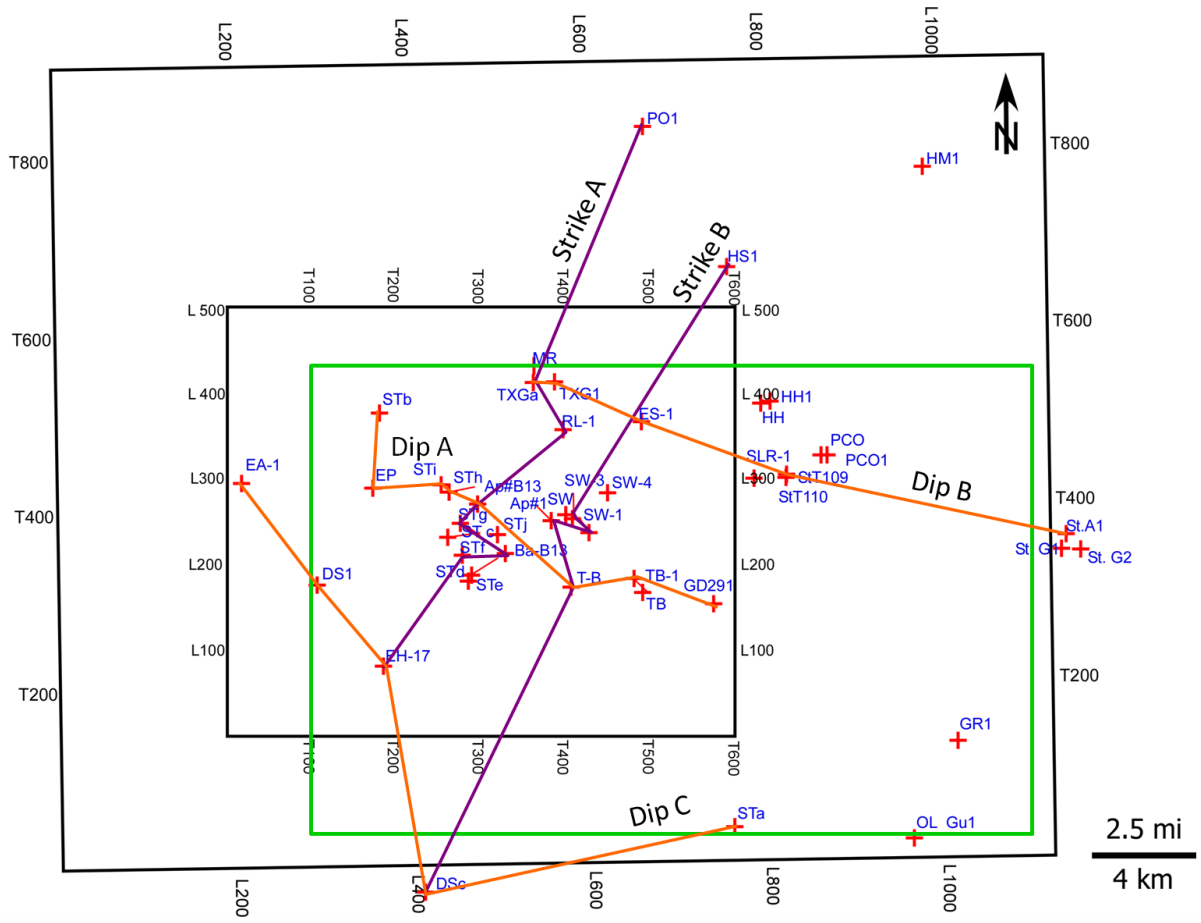

Figure: 4.7 Map view showing location of five well log correlations.

thickness variation along strike sections than dip sections and only sequence 1 is dominated by LST whereas others are dominated by HSTs. Eight stratal slices were selected to support depositional environment interpretation. Their positions on the stratigraphic section are shown in Figure 4.13.

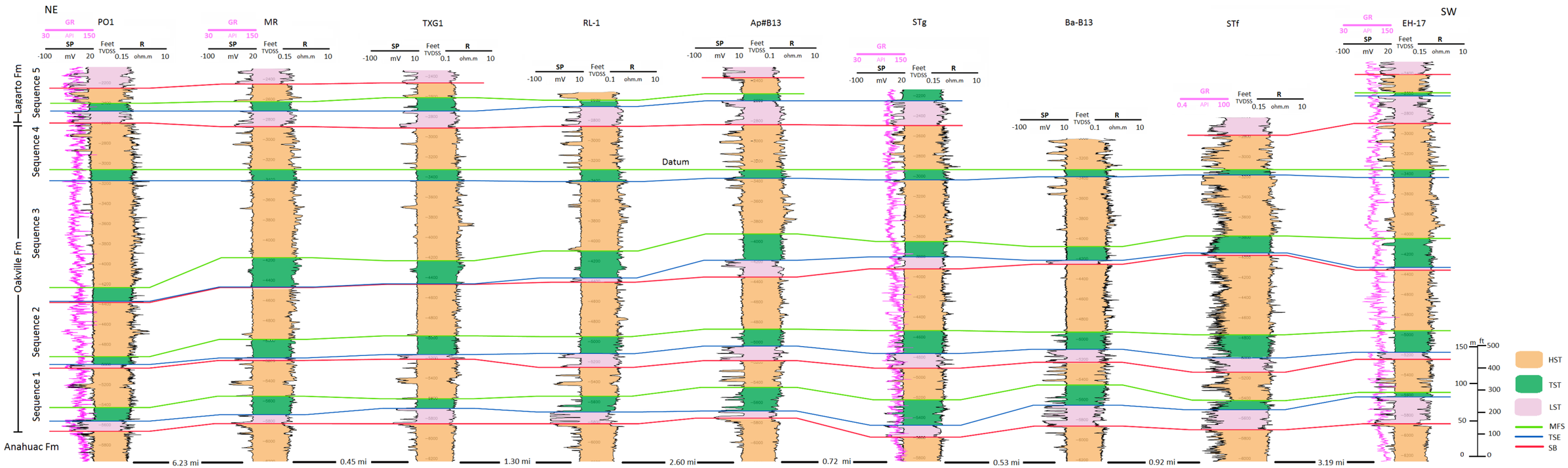

Figure: 4.8 Strike line A showing main well log correlations in this study. Erosional relief associated with LST thicknesses, approximately 50 to 150 ft (15-45 m), is illustrated on this line.

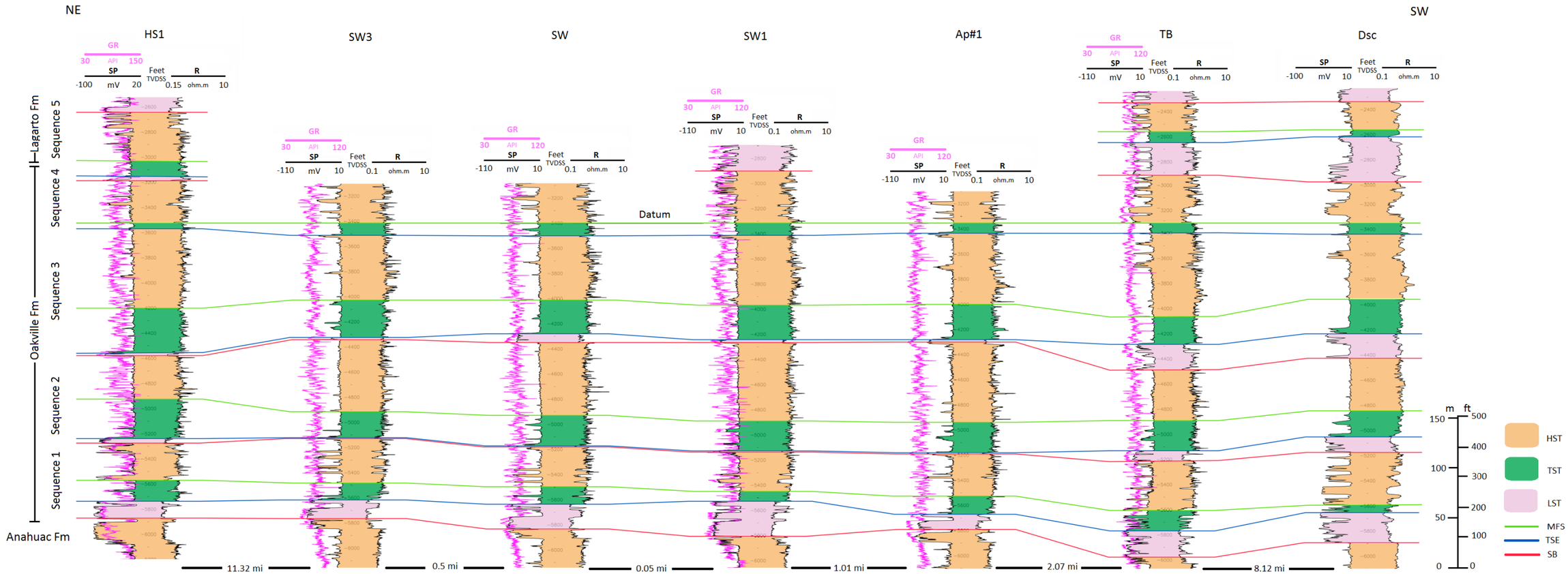

Figure: 4.9 Strike line B is located basinward of the strike A. LST1 is thicker than on Strike A whereas LST2 is present only on the southwest end of the line.

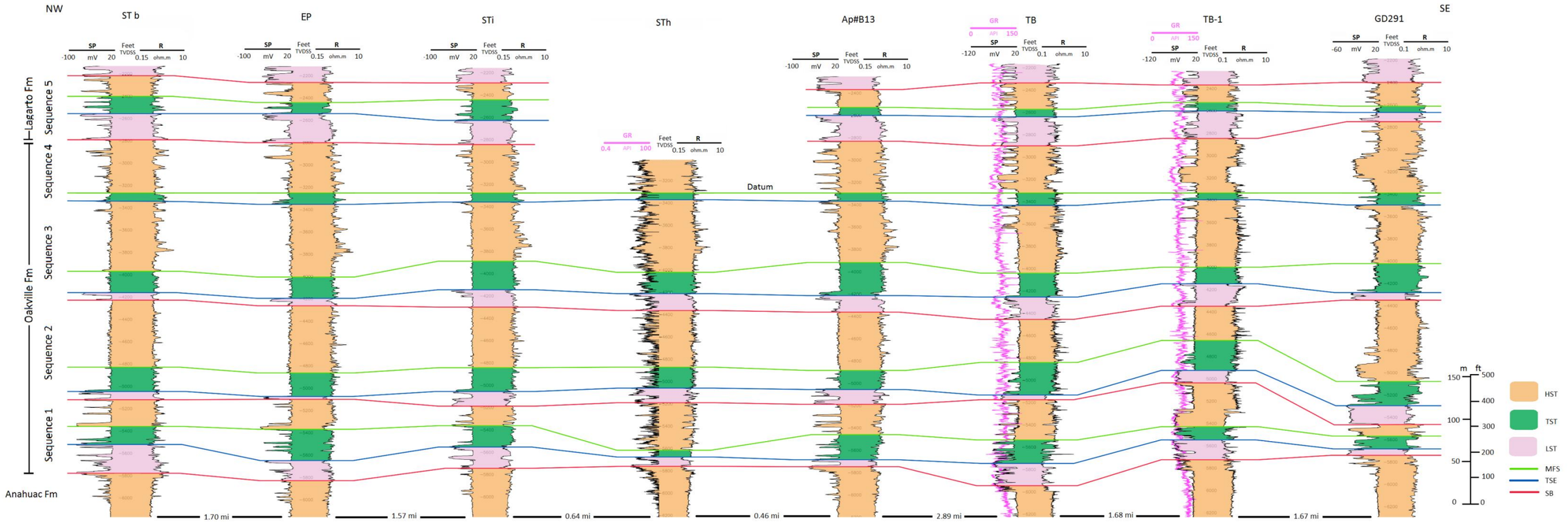

Figure: 4.10 Dip line A is located in the middle, runing from northwestern to southwestern part of the study area. LST1 deposits are relatively thick and heterogeneous to the west and become more massive toward the southeast. LST2 is generally thinner than LST1 but, similarly the deposits become more massive and cleaner toward the southeast end of the line.

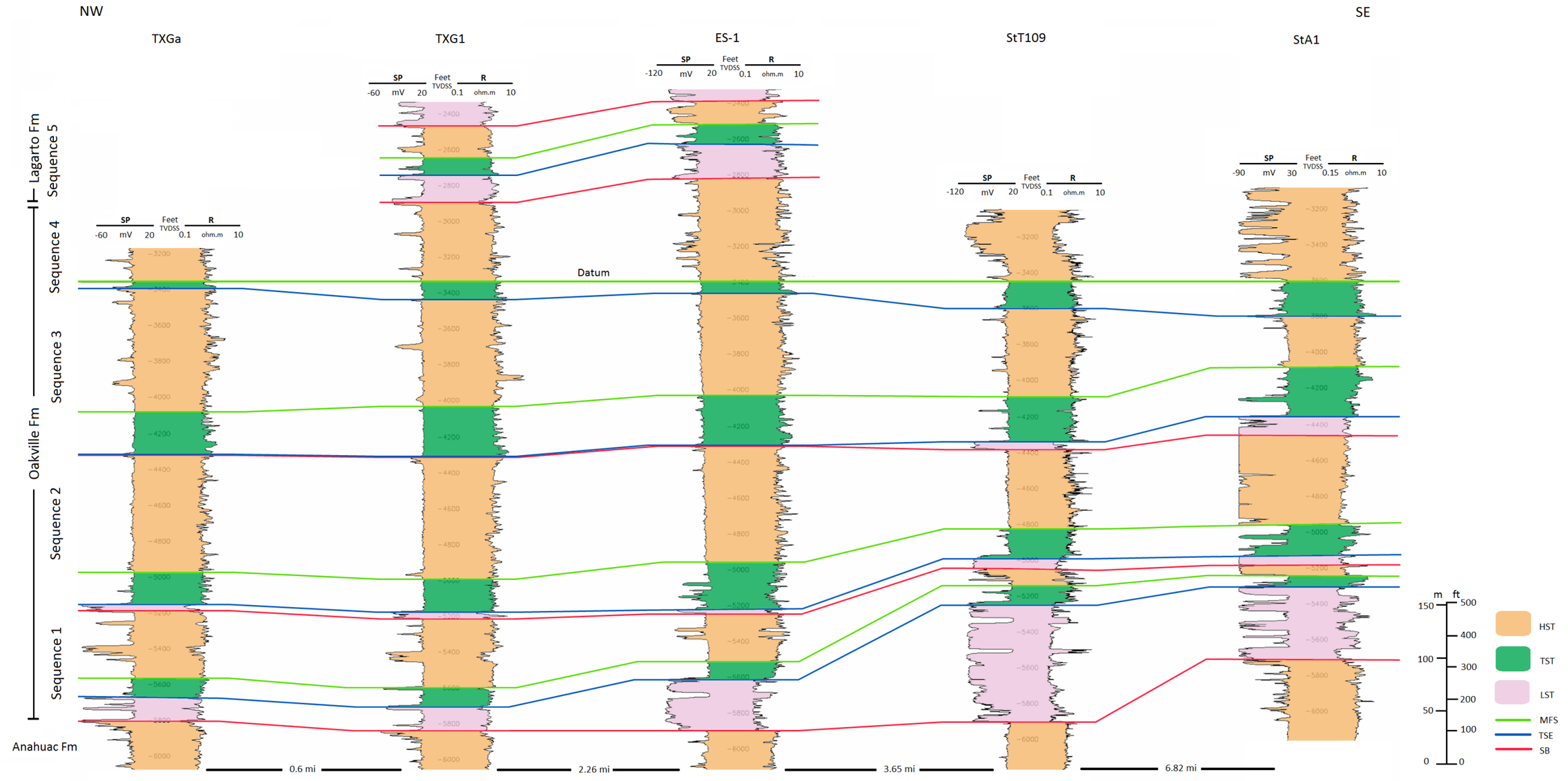

Figure: 4.11 Dip line B is oriented along the north margin of the study area and intersects the thickest sandstone intervals in sequences 1, 2 and 3.

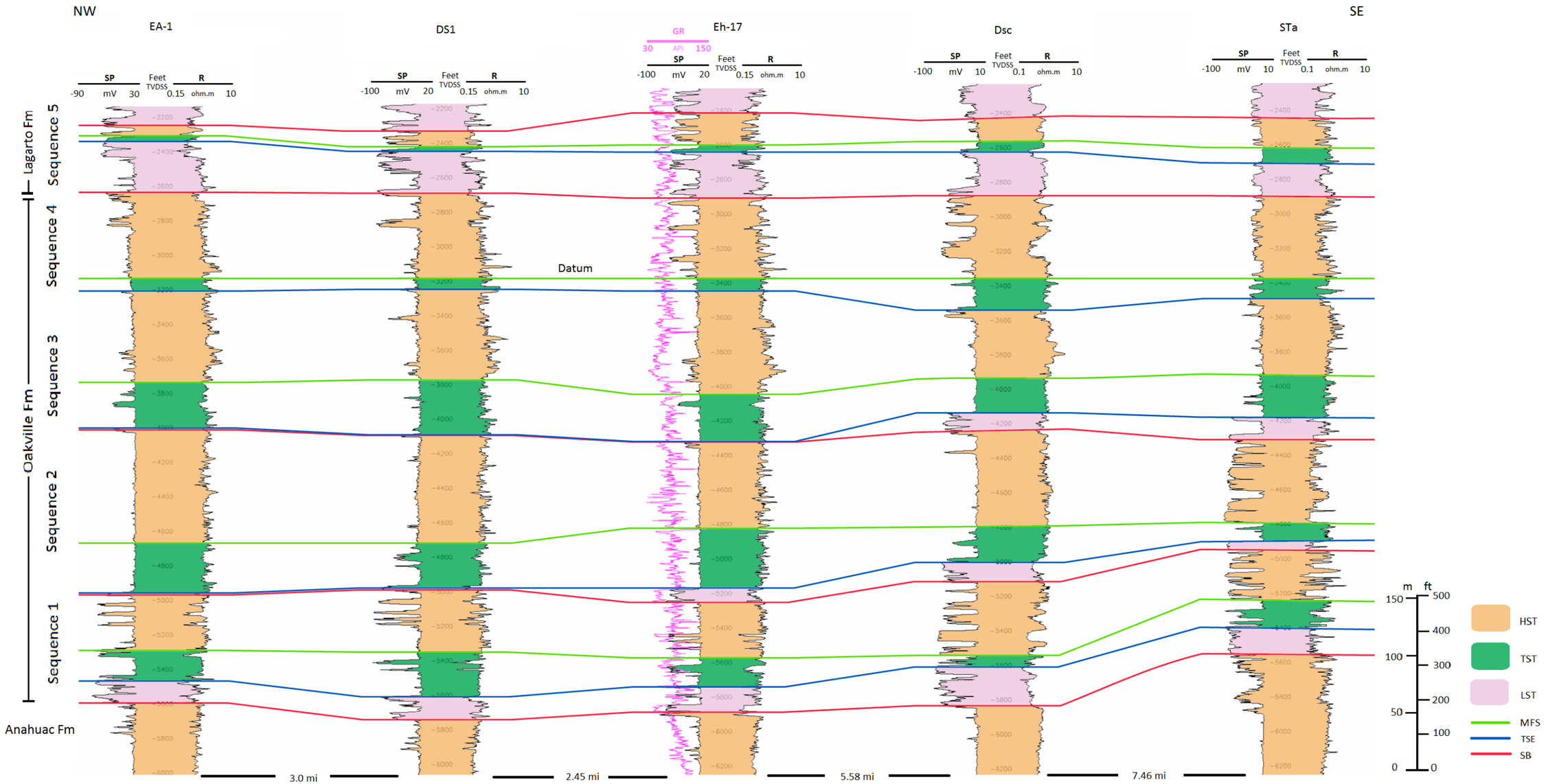

Figure: 4.12 Dip line C runs along the southern margin of the study area. Only LST1 is present and have pretty constant thickness through the line. LST 2 and 3 are intersected just the southeast end of the line.

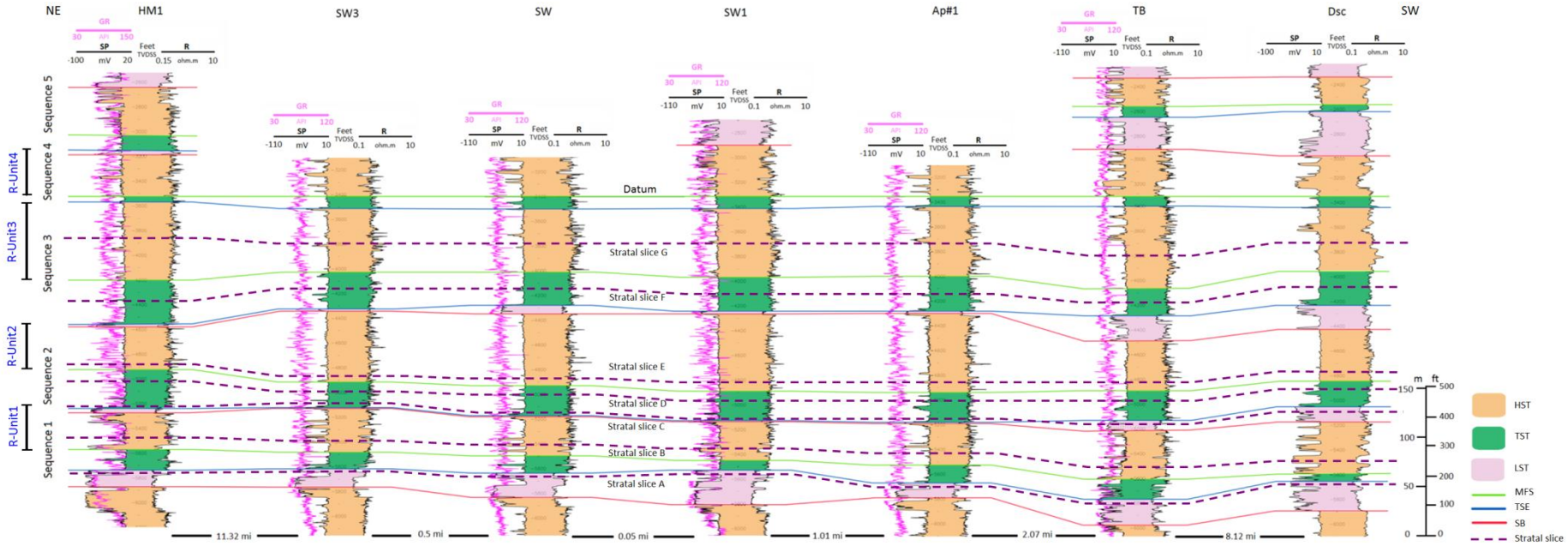

Figure: 4.13 Positions of eight stratal slices on Strike B line displayed by purple dash line. The interval of regressive units which will be mentioned later are also illustrated in this figure.

4.211 Lower Miocene Sequence 1

Sequence 1 is approximately 300 ft (100 m) thick. A LST is the most prominent systems tract in the sequence. The LST is characterized by a thick (up to 100m) undifferentiated sandstone body with a sharp erosional base, inferred to be a major sequence boundary between Oligocene and Miocene strata. Sandstones become less blocky toward the top of the sequence and display a retrogradational trend marking the onset of transgression at a TSE. The LST ranges in thickness from 50 to 300 ft (15 to 100 m) and displays more thickness variability along strike than along dip. Based on the log character and geometry, the LST is interpreted to be an incised valley fill complex which may include basal fluvial deposits as well as marine mudstone and bayhead delta deposits (Fig.3.4). Additional evidence supporting this interpretation is from the LST1 net sandstone map and the stratal slice A in Figures 4.14 and 4.18 respectively. The net sandstone map displays a dip-elongate sandstone dispersal pattern and the stratal slice reveals high amplitude (red) tributary, dip-oriented patterns.

The seismic cross-section of the incised valley shows a seismic reflector that terminates against the valley walls. The sandstones with blocky log responses that overlie the sequence boundary are interpreted to be fluvial deposits possibly overlain by transgressive estuarine facies. Sandy deposits in this system tract are as much as 300 ft thick in along depositional dip (Fig. 4.11).

The TST above the LST is characterized by retrogradational stacking pattern. It is bound at the top by a MFS. Based on GR and SP responses, the TST deposits contain less sandstone than the LST. The TST 1 net sandstone map and well log patterns (Fig. 4.13) of thin sandstone encased in thick muddy interval behind the thick massive sandstones suggest a barrier-lagoon/embayment environment (Fig. 3.7). In dip section C (Fig 4.12),

well logs display subtle upward-coarsening patterns that may indicate higher frequency base-level change or coastal offlap.

The HST above the MFS has aggradational to progradational stacking patterns. HST deposits are not as sandy as the LST deposits. From a upward-coarsening well log patterns (Fig.3.8), the HST1 net sandstone map (Fig 4.15), and a stratal slice B (Fig. 4.19), the depositional system in HST is interpreted to be prograding deltaic system (likely fluvial-dominated according to a heterogeneous lithology from well logs and a symmetrical lobate net standstone geometry) and lower shoreface deposits.

4.212 Lower Miocene Sequence 2

Sequence 2 ranges in thickness from 300–400 ft (100-120 m) (Fig. 4.8, 4.9, 4.10, 4.11, and 4.12). The LST in sequence 2 has similar character to that of LST1 which is a blocky sandstone with a sharp erosional base representing a sequence boundary (Fig.3.4) which 10-80 ft of the underlying strata have been eroded. However it is less sandstone rich, and is only approximately 80 ft (24 m) thick, resembling the Lower Miocene sequence II of Moore (2005). LST deposits in sequence 2 are locally absent. The wireline log patterns and stratal slice C (Fig. 4.20) suggest an incised-valley system. The valley is more likely restricted to the southern and basinward of the study area whereas the northern part appears to consist of interfluves which correspond to high positive amplitude. The valley fill might correspond to the high negative (red) amplitude with dip-elongate patterns in the stratal slice map (Fig. 4.20). Within the possible incised-valley the small sinuous high amplitude feature is also observed, which could be fluvial channels in the incised valley. Zeng and Hentz (2004) state in their study of the Miocene deposits in Tiger Shoal area, offshore Louisiana that incised valleys exhibit strong negative amplitude and sinuous-dip-oriented feature on the strata slices. The valleys are commonly 1.6-30 mi wide. Moreover, the ‘curved amplitude’ features observed along the

valley margins were interpreted to be fluvial meander point bars. The stratal slice map does not display any significant patterns to the west, however, the lower negative amplitude might represent an interfluve area. The other possibility is that the weakly negative amplitude area might be the relict highstand coastal plain deposits which consist of muddier lithology than the lowstand deposits according to Zeng and Hentz (2004).

The TST lies above the LST or the HST1 where the LST2 is absent. The TST2 has an overall retrogradational stacking pattern. A thick interval of muddy facies (50-150 ft or 15-45 m) with interbedded sandstones suggests a lagoon-embayment system and at more basinward location, such as on Dip A section, back-stepping parasequences might suggest a reworked deltaic system. The stratal slice D in Figure 4.21 provides the feature of potential reworked delta lobes supporting this interpretation.

The HST is the thickest systems tract in sequence 2 which ranges in thickness from 150-320 ft (45-98 m) but low sandstone content is inferred from the SP response. The GR curves of landward wells show fining upward- patterns (Fig. 4.8, 4.9 and 4.12) that indicate fluvial channel facies while at the more basinward location, a progradational deltaic system is inferred. The stratal slice E (Fig. 4.22) reveals a prominent sinuous channel feature that is interpreted to be a fluvial channel system.

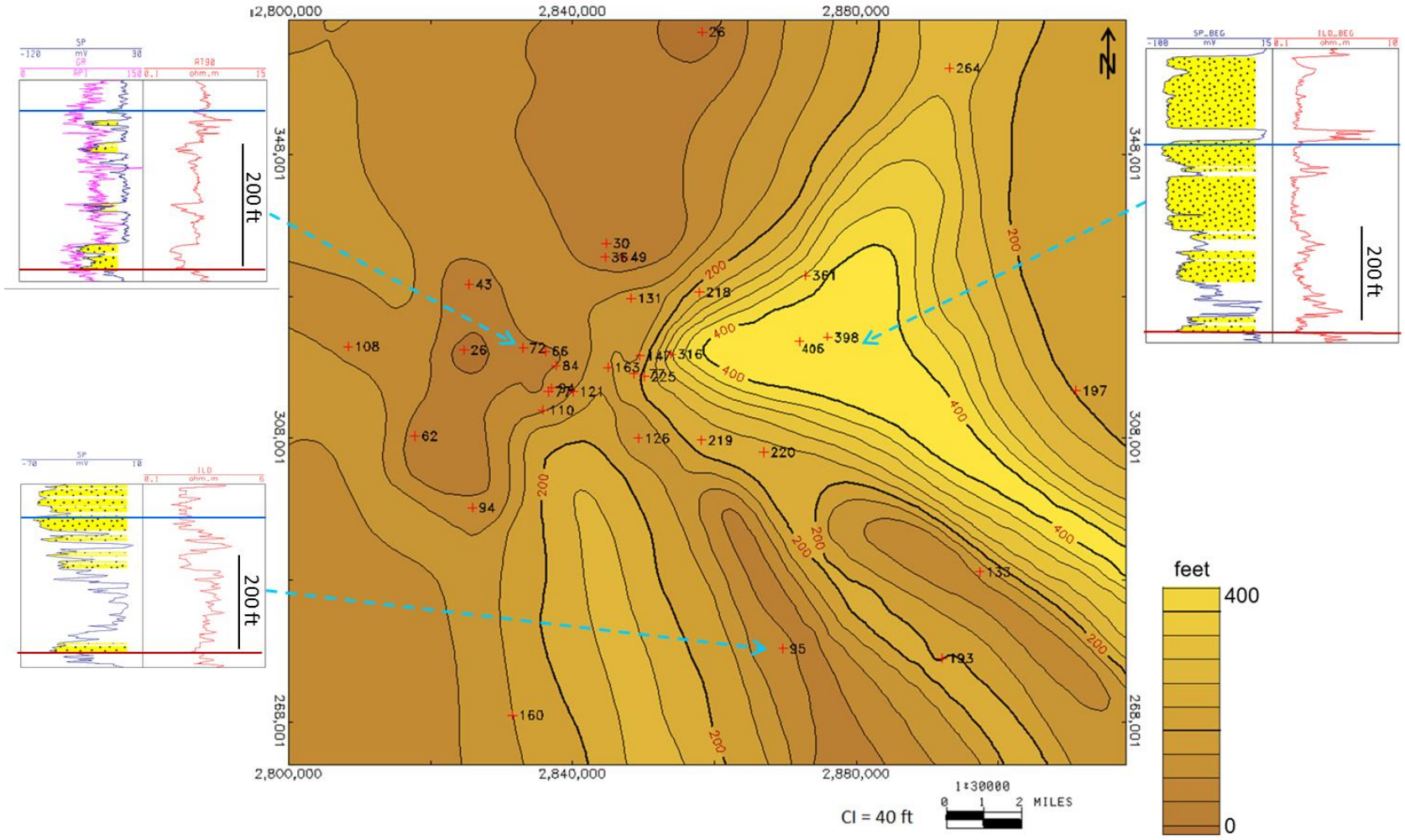

Figure: 4.14 Net sandstone map of LST1 showing dip-oriented sediment dispersal patterns within an incised-valley system.

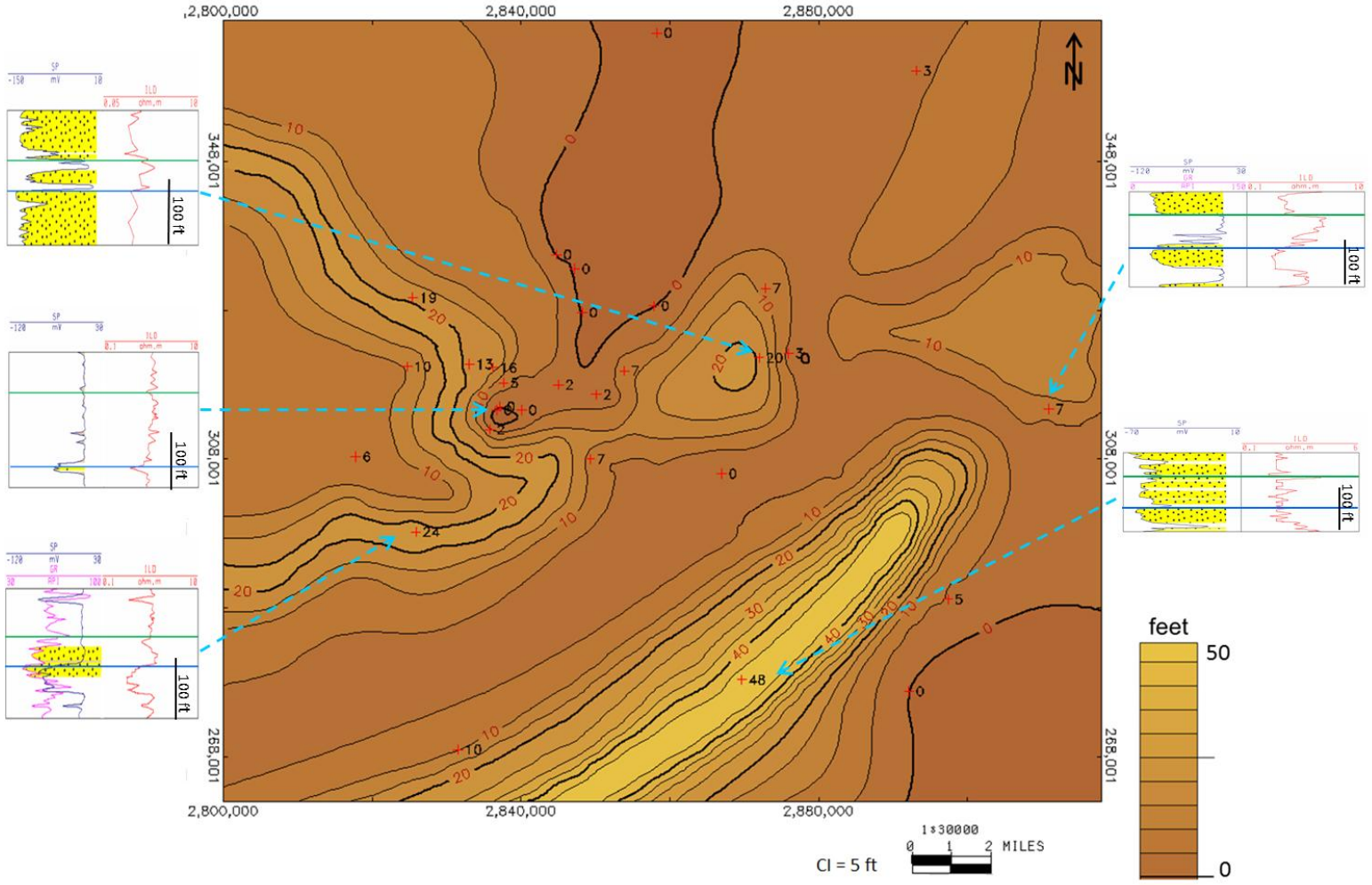

Figure: 4.15 Net sandstone map of TST1. Sediment dispersal and well log patterns suggest barrier bar and tidal inlet facies.

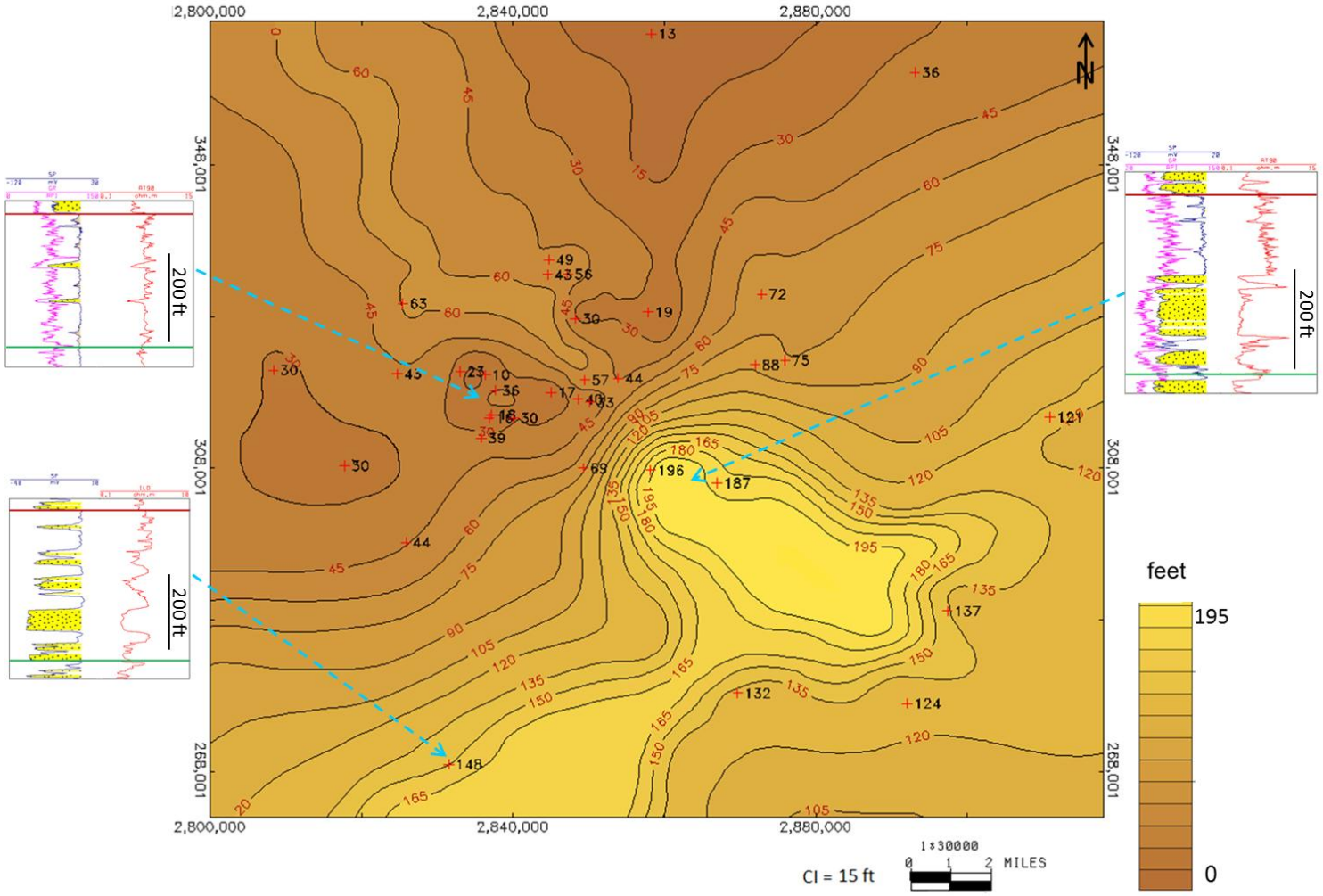

Figure: 4.16 Net sandstone map of the HST1 illustrating a transitional environment from barrier bar and tidal inlet to deltaic systems.

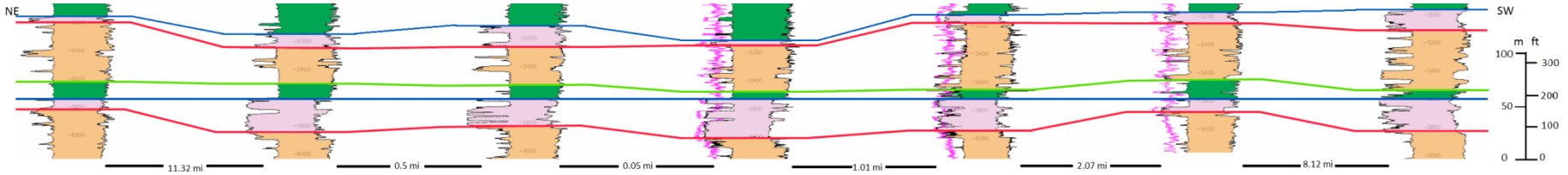

(a)

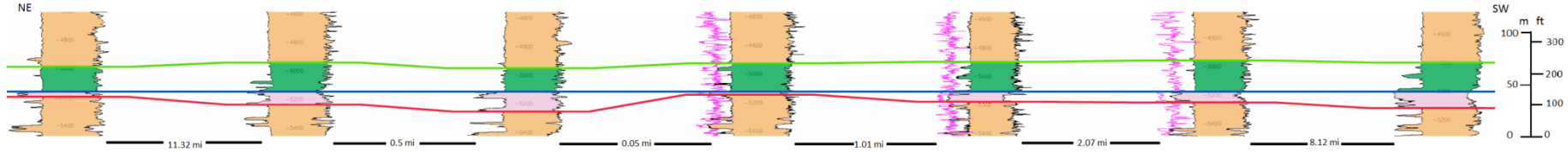

(b)

Figure: 4.17 Sequence 1(a) and sequence 2 (b) from Strike line B illustrating geometry of LST deposits which are interpreted as incised-valley fills. The TSEs were flattened in order to show better geometry of the valley.

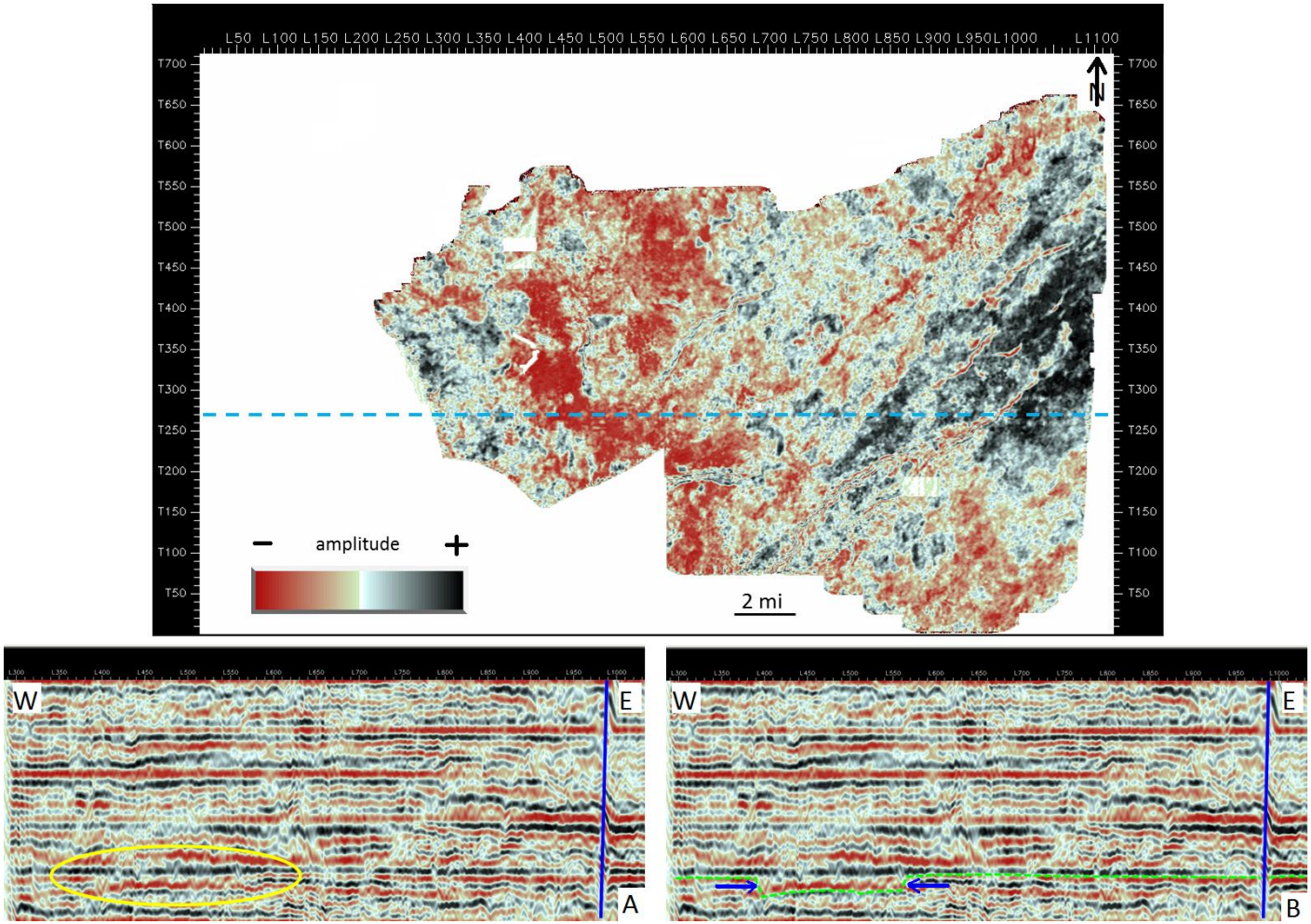

Figure: 4.18 Stratal slice A illustrating the high negative amplitude of dip-oriented patterns. In the seismic cross section, reflectors exhibit onlap on both sides. The event is interpreted to be an incised-valley fill.

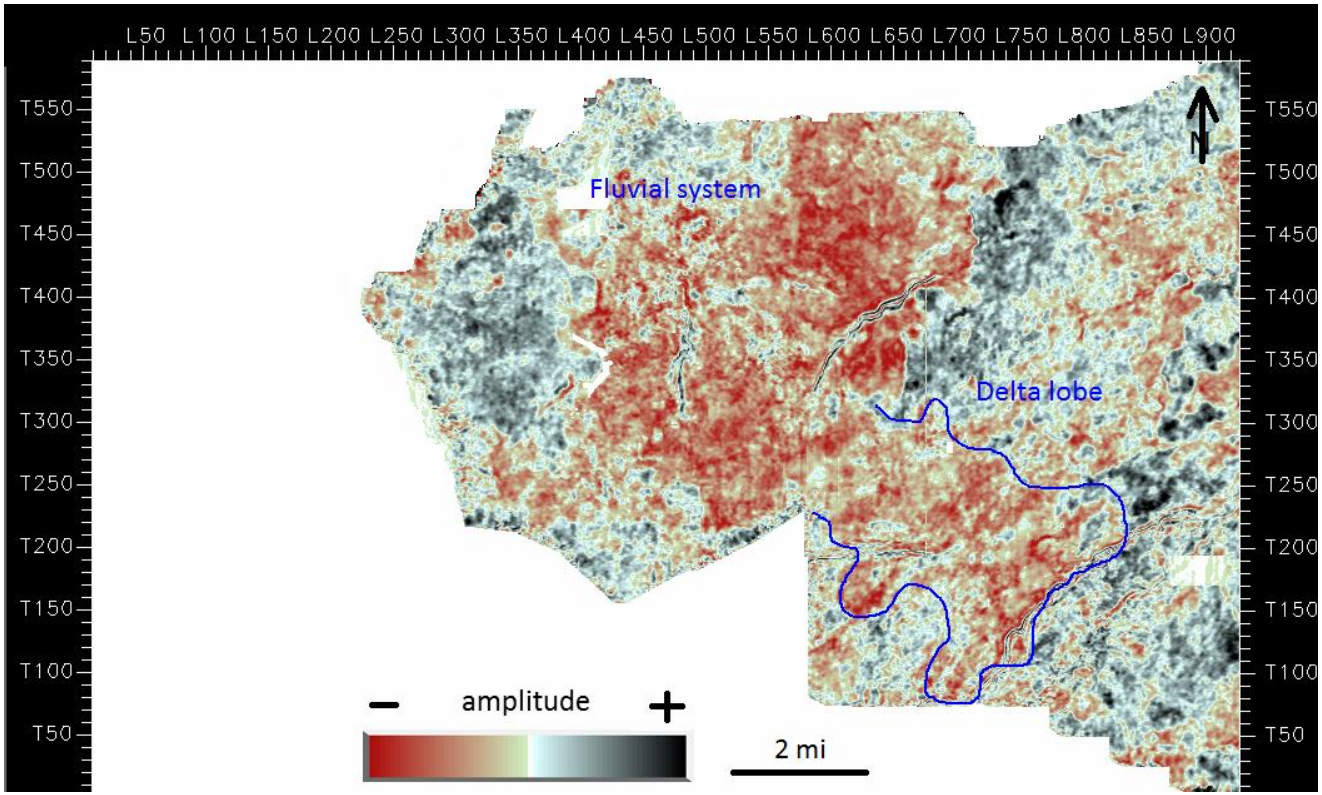

Figure: 4.19 Stratal slice B, through the HST1 deposits, displaying the high amplitude lobate feature interpreted as a deltaic system which is supplied by fluvial system in the northwestern area.

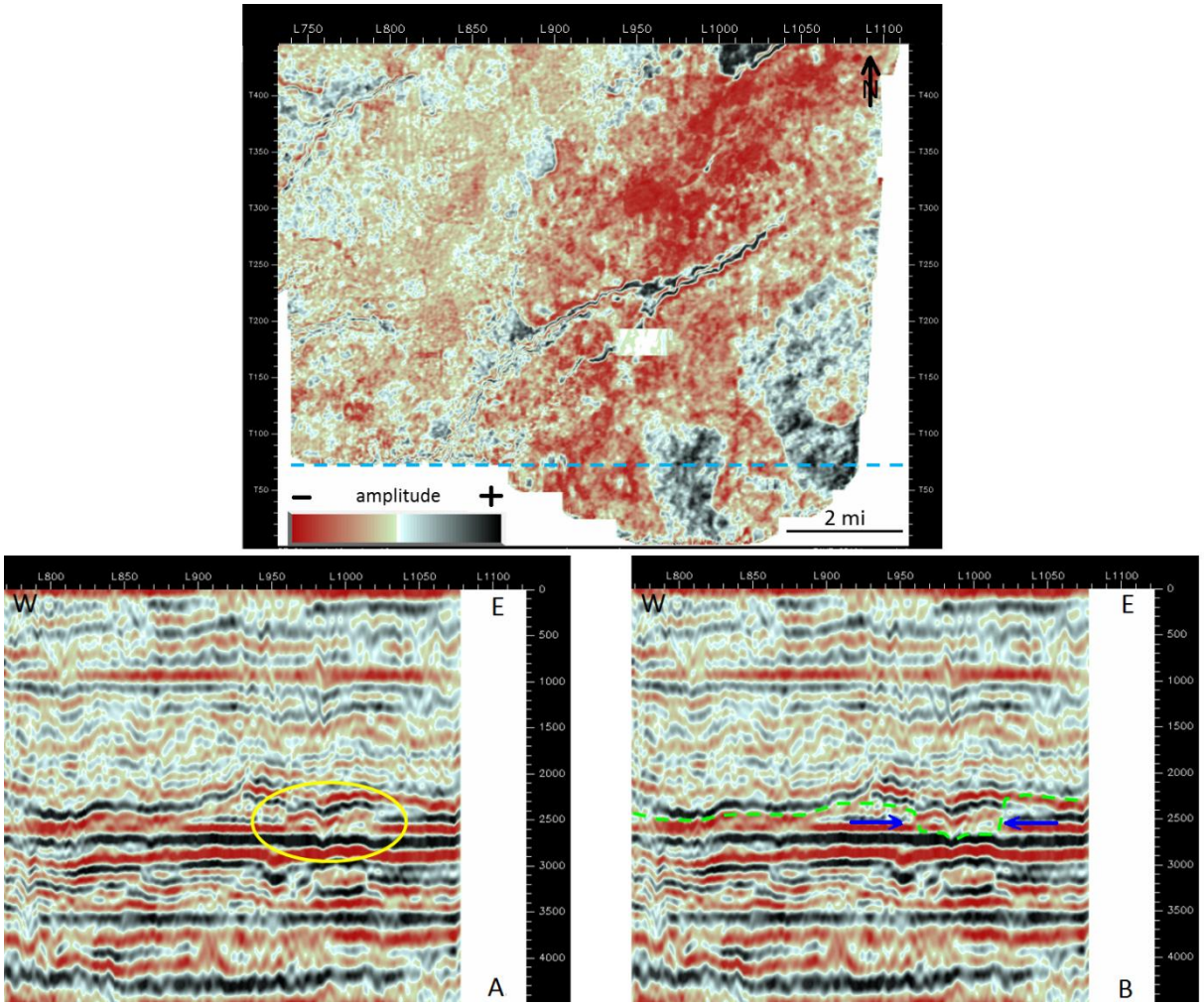

Figure: 4.20 Stratal slice C through the basal part of LST2. The great negative amplitude has a dip-elongate pattern and shows erosional relief with onlapping reflectors in cross section. It is interpreted to be an incised-valley complex with sinuous fluvial channel trends.

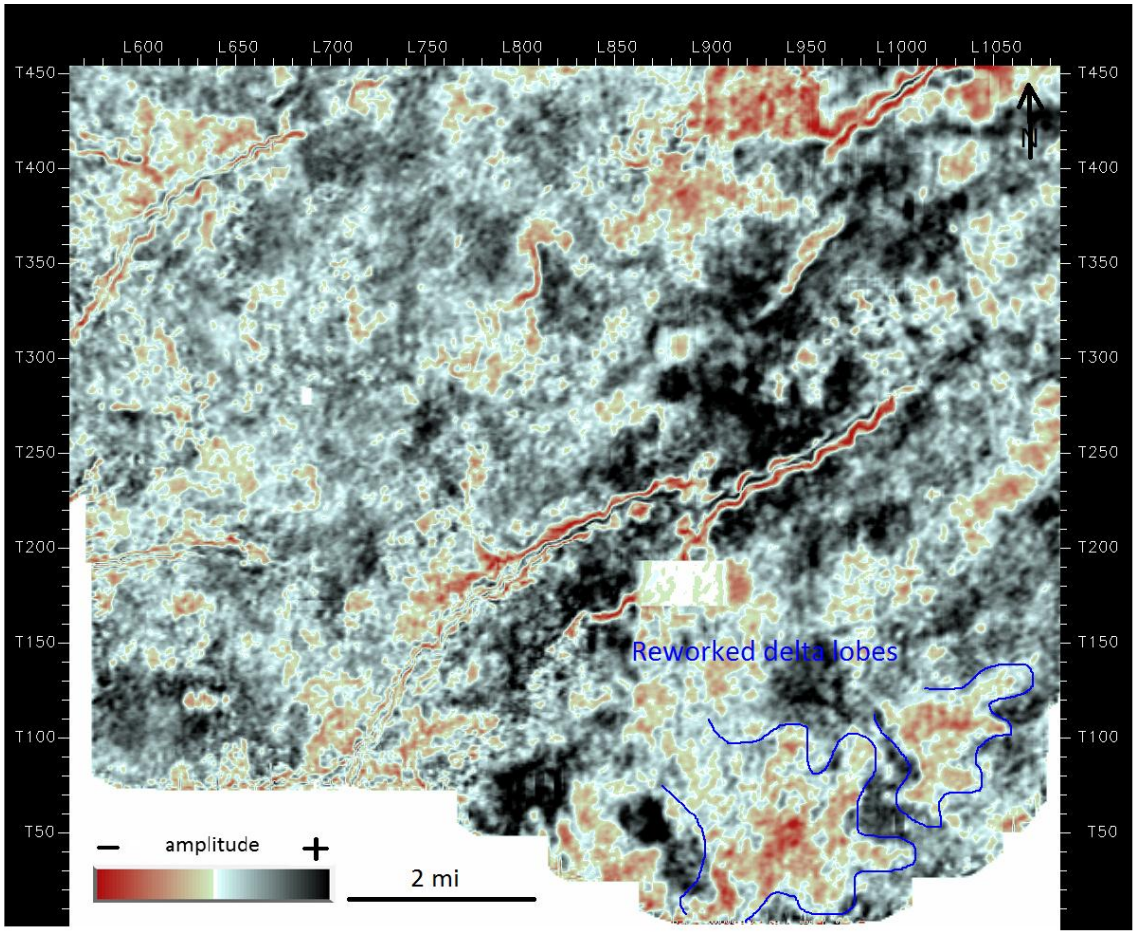

Figure: 4.21 Stratal slice D through TST2 deposits illustrating high amplitude features that have subtle lobate pattern interpreted to be reworked delta lobe during sea-level rise.

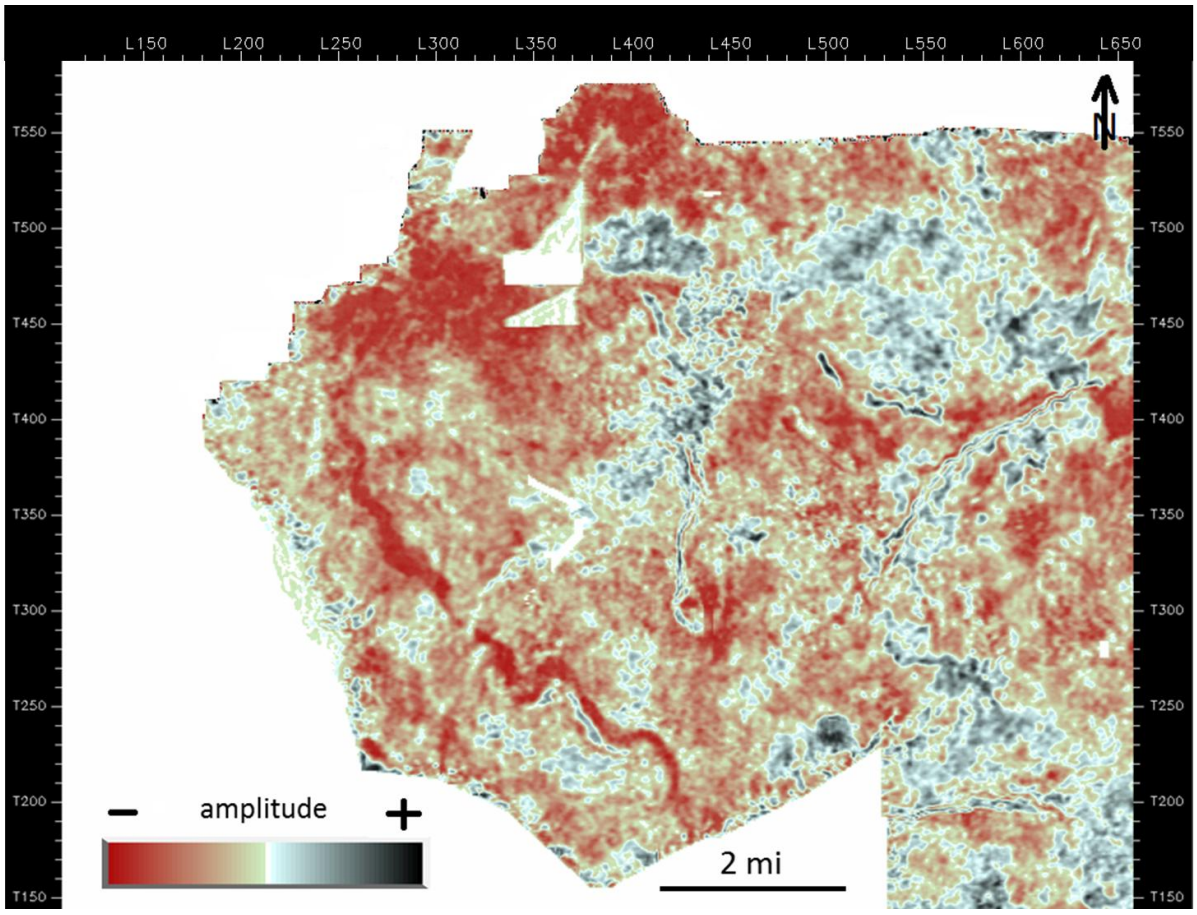

Figure: 4.22 Stratal slice E illustrating a sinuous fluvial channel associated with highstand conditions.

4.213 Lower Miocene Sequence 3

Sequence 3, the thickest sequence in the lower Miocene section in the study area, is 400-600 ft (122-183 m) thick. It locally contains LST that is a sharp-based sandstone superimposed on HST2, although this stratal relationship is not clearly evident in some wells. The LST is relatively sandstone-poor compared to the other two sequences. However, it shows variation in erosional relief along strike from 15-100 ft (5-30 m) and therefore is interpreted to be an incised-valley system filled with muddy sediments.

The TST is well preserved in sequence 3 with thickness of 40 ft up to 150 ft. Based on log profiles, it exhibits retrogradational stacking pattern and contains some sandy strata encased in muddy sediments which locally exhibit abnormally high gamma ray and high resistivity values understood to be coal beds (Fig.4.8 and 4.10). The depositional environments are interpreted to be lagoon-embayment and reworked delta lobes from stepping backward well log patterns on Dip A and B lines and strata slice F (Fig. 4.23).

The HST exhibits an aggradational trend above the MFS and grades upward into a more progradational profile. A set of upward-coarsening, funnel shape well log patterns suggests a deltaic system of which well log pattern shows cleaner and less heterogeneous lithology that might be a result of a wave reworking process. Stratal slice G (Fig 4.24) reveals high negative amplitude, dip-elongate features in the northwestern area (landward) interpreted to be a fluvial system on the coastal plain. The smaller but higher-amplitude features within the large dip-elongate feature are interpreted to be fluvial channels and the bending curved line next to the channels is potentially an abandoned meander loop.

4.214 Lower Miocene Sequence 4

Sequence 4 ranges in thickness from 200-300 ft (60-100 m). The LST of sequence 4 is either absent or cannot be adequately inferred from log data. The sequence boundary is recognized by erosional evidence on the top of the previous highstand deposits. An erosional relief of 20-40 ft (6-12 m) can be observed from well log correlations. The TST above HST3 is a thin (20-50 ft, 6-15 m) upward-fining interval. The depositional environments associated with this transgressive event are not well resolved but possibly include estuarine facies.

HST4 is the thickest and most sandstone-rich among the other HSTs. The HST4 exhibits a progradational pattern above the MFS, inferred from its upward-coarsening log response. Most sandstone bodies interpreted from well logs have upward-coarsening to massive or tabular responses which are more uniform along strike. Moreover, GR responses indicate that these sandstones are sandstone-rich, thereby suggesting shorezone/strandplain environment. The massive sandstone above the MFS, for example in Figure 4.10, could possibly indicate rapid progradation following transgression; however these thick massive sandstones above the MFS occur locally, not continuously along strike. The HST4 is bounded above by the sequence boundary that has the approximate age of 18.7 Ma which also marks the top of the lower Miocence Oakville Formation.

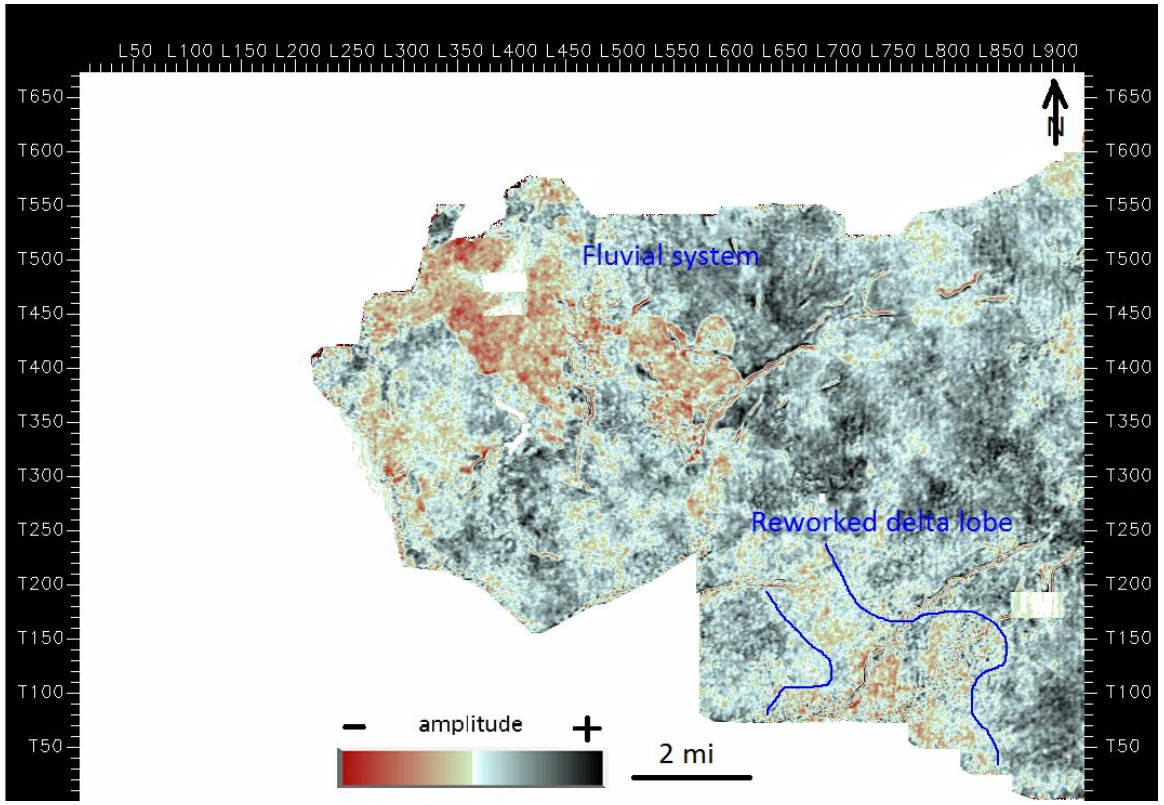

Figure: 4.23 Stratal slice F exhibiting a scattered high amplitude feature inferred reworked delta lobe during transgressive event, TST3.

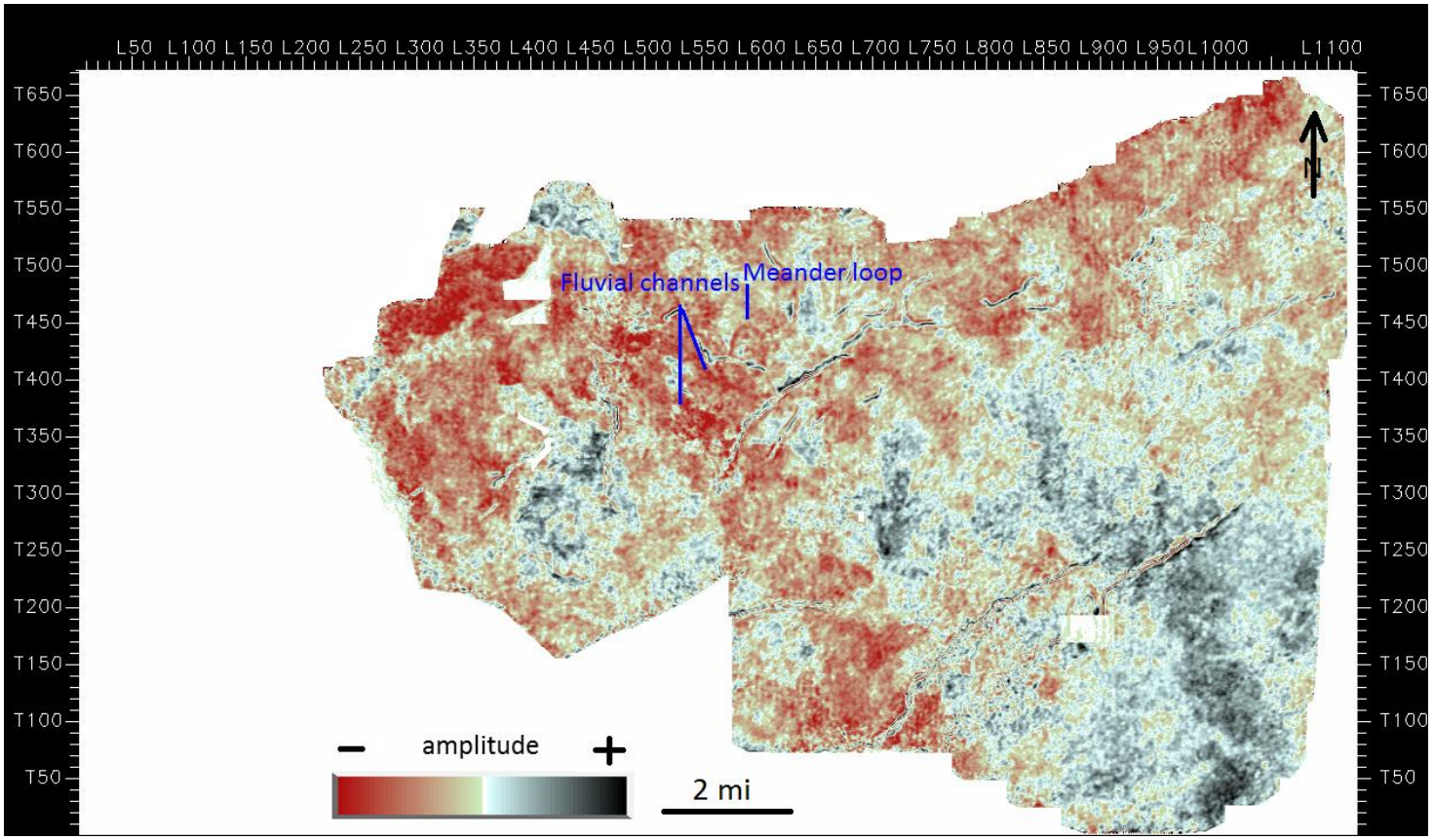

Figure: 4.24 Stratal slice G above the MFS of sequence 3 displaying high-amplitude dip elongate features in the northwestern area suggesting a fluvial system that deliver sediments to the deltaic system basinward. Curved-strong amplitude patterns might represent fluvial channel whereas the bend feature might be an abandoned meander loop.

4.215 Lower Miocene Sequence 5

Sequence 5 is approximately 200-250 ft (60-76 m) thick. The bottom of LST5 is a tabular sandstone body (15-25 ft or 5-8 m-thick) defined by R curves abruptly reflecting to low values. In addition, SP and GR curves show abrupt changes to cleaner lithology. Based on these log curves, the deposits are inferred to be coarse-grained at the bottom then interbeded with muddy interval and grade to coarse-grained bed with sharp top representing a flooding event. The characteristics of LST5 suggest incised-valley fill facies, however this interpretation will be assured from sandstone geometry on a net sandstone map. The TST is approximately 30-100 ft (10-30 m) thick in sequence 5. It exhibits a prominent retrogradational pattern on log curves. The sediments are thought to be deposited in an estuarine environment.

HST5 is similar to the HST4 in terms of progradational tabular sand bodies deposited in a strandplain environment but the deposits have less interbedded shale or mudstone, which might suggest increase in coarse grained sediment supply or higher degree of sandstone body amalgamation. The HST5 is bound at its top by a third-order sequence boundary that from the Carancahua S^5 benchmark chart has an age at approximately 16.2 Ma.

4.216 High-frequency sequence

Mitchum et al. (1991) explain that high-frequency sequences are the result of Milankovitch cycles. The Milankovitch cycles were introduced by Heys et al. (1976) as changes in orbital parameters controlling global climate and glacioeustatic fluctuations, which have different cycle frequencies including: precession (approximately 19-23 kyr), obliquity (approximately 42 kyr) and eccentricity (approximately 100 kyr). High-frequency cycles range from 0.1-0.2 Ma (fourth-order) to 0.01-0.02 Ma (fifth-order). They have similar components to those of third order sequences but are at smaller scales. For example, fourth-order sequences of the Miocene Gulf of Mexico are typically 30 to 100 ft (10-30 m) thick (Zeng et al., 2007). Accordingly, high-frequency sequences are recognizable in outcrop or well log data. Moreover, the strata slicing method has been demonstrated to efficiently resolve high-frequency sequences from 3D seismic data (Zeng and Hentz, 2004 and Zeng et al., 2007).

Relative sea-level fall that results from interplay between tectonic subsidence and rate of eustatic fall is a factor controlling development of high-frequency sequences. They are recognizable in depocenters where sedimentation rates were relatively very high, whereas tectonic subsidence rates were relatively low (Mitchum et al., 1991). The lower Miocene Gulf of Mexico is an example of high sedimentation rates and low tectonic subsidence (Galloway et al., 1986 and Galloway, 1989).

Fourth-order sequences are important in petroleum exploration because their thickness roughly approximates thicknesses of reservoirs and seal. Consequently, analysis of fourth-order sequences can lead to better understanding and resolving reservoir complexity (Mitchum et al., 1991).

At least 17 (fourth-order) high-frequency sequences are recognized in the lower Miocene interval in this study. Given the premise that high-frequency sequences control the fundamental sand dispersal patterns at the reservoir level, I produced net sand maps of the HSTs of three high-frequency sequences within the Lower Miocene Sequence 1. These high-frequency sequences are termed HST-HF1, HST-HF2 and, HST-HF3 (Fig. 4.25) to illustrate distribution of depocenters through time (Fig. 4.26-4.28).

Sand dispersal patterns in HST-HF1 exhibit a strike-elongate trend crosscut by a muddy area. HST-HF2 contains lobate sand body patterns, although a strike-parallel trend is present in the southern part of the map area. HST-HF3 exhibits a lobate sand body trend in one depocenter. I interpreted an evolution of the dispersal patterns as changing depositional environments from a barrier-lagoon or tidal inlet during the time of HST-HF1 deposition to a deltaic system with an adjacent strandplain in HST-HF2. Eventually, the area is dominated by a deltaic system in the time of HST-HF3. In addition, the depositional environment of the HST-HF1 is interpreted to be a barrier-bar and tidal-inlet system that represents deposition during sea-level rise, based on the stratigraphic position of HST-HF1 within the third-order TST1.

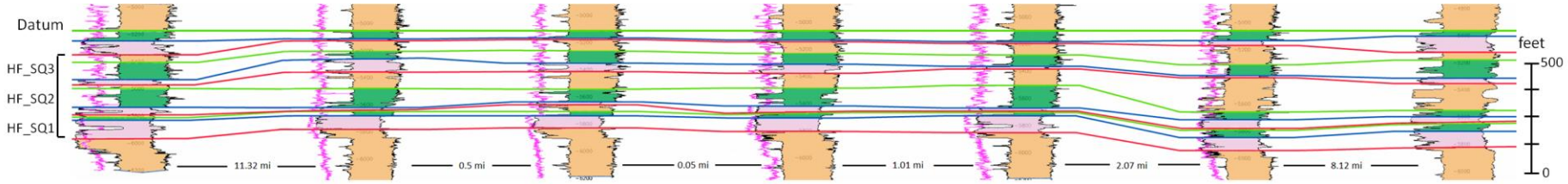

Figure: 4.25 Strike section B showing three high-frequency sequences (fourth-order) in third-order Lower Miocene Sequence 1. HF_SQ stands for high-frequency sequence.

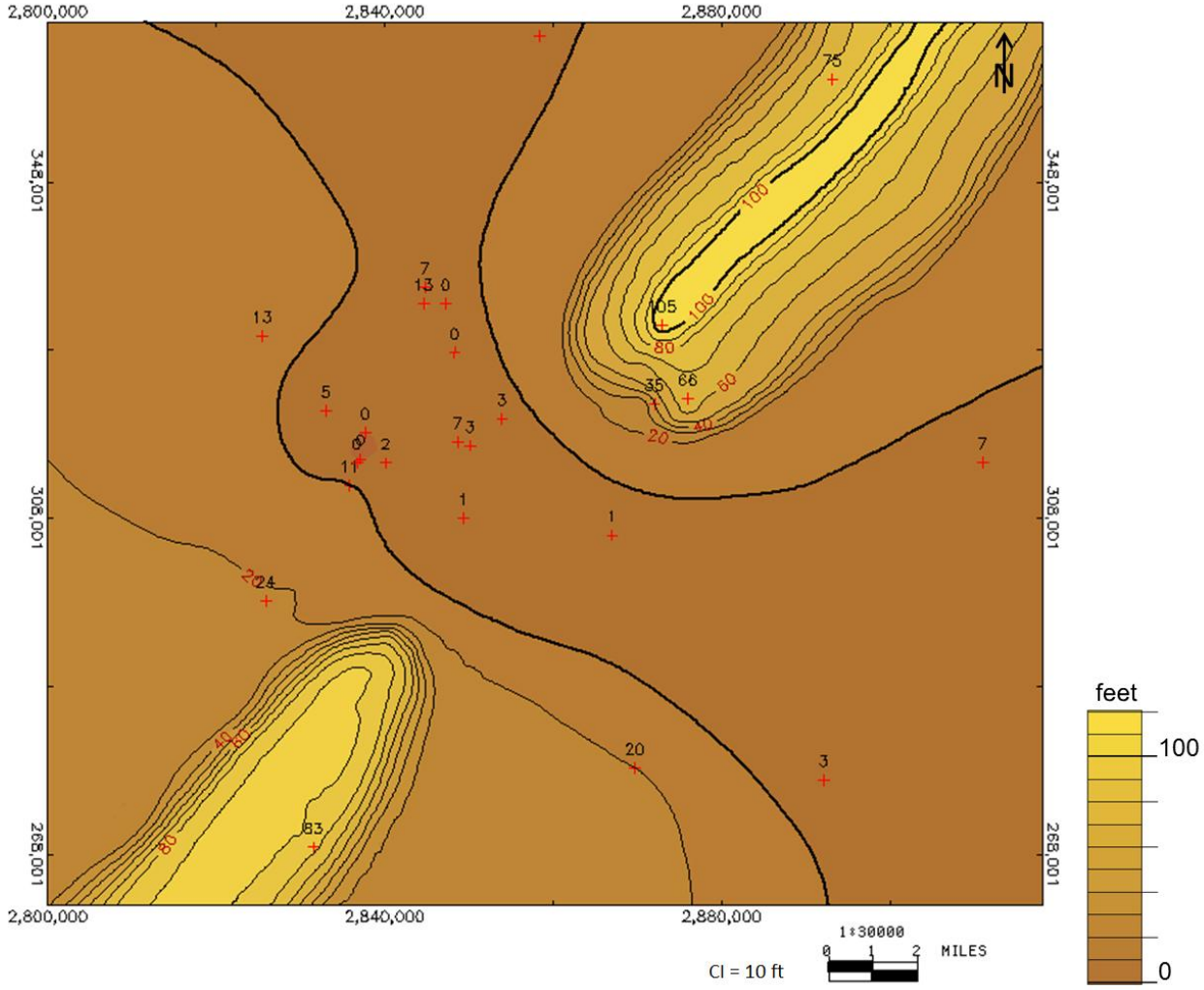

Figure: 4.26 Net sandstone map of the highstand systems tract of the high-frequency 1 (HST_HF1).

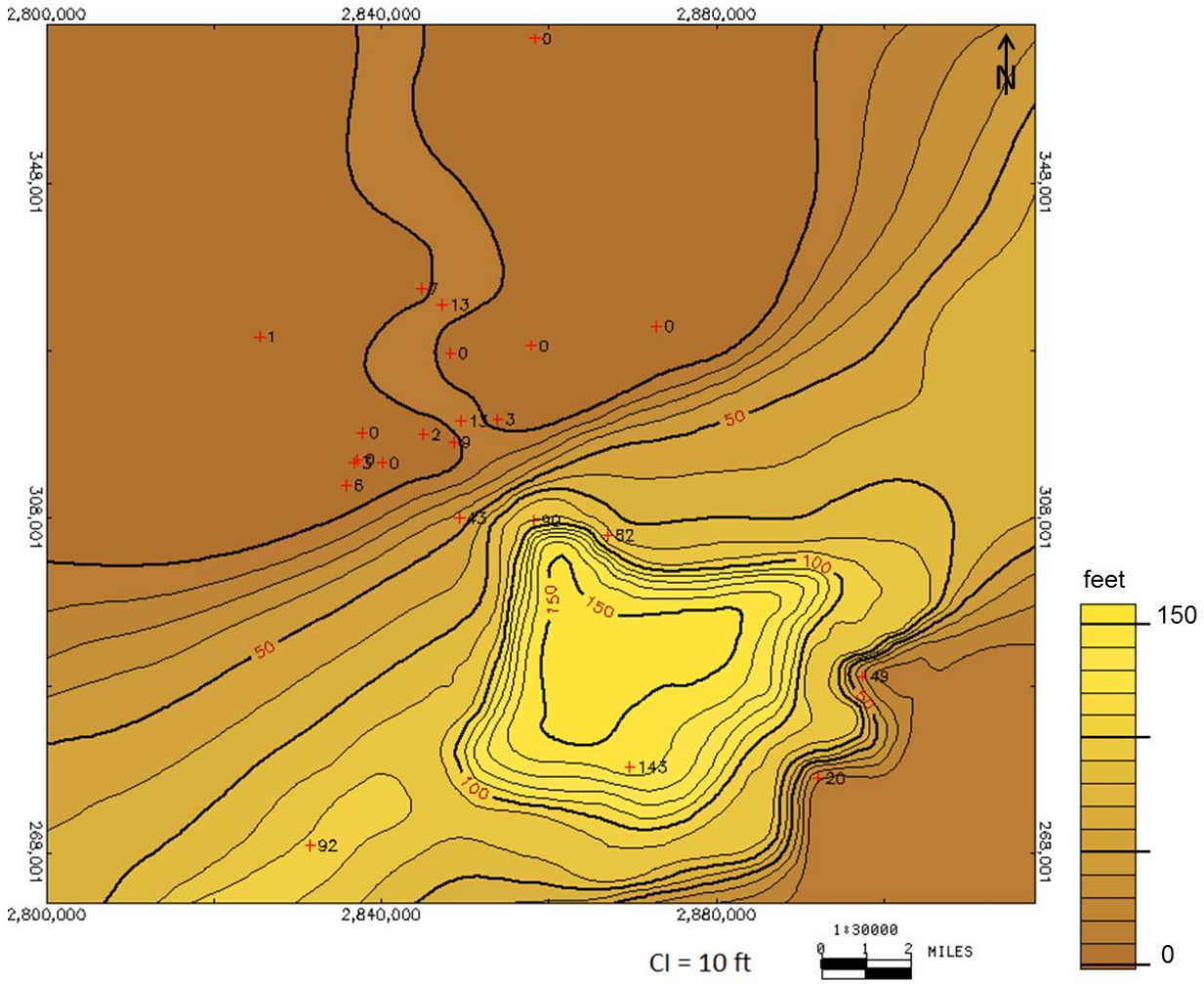

Figure: 4.27 Net sandstone map of the highstand systems tract of the high-frequency 2 (HST_HF2).

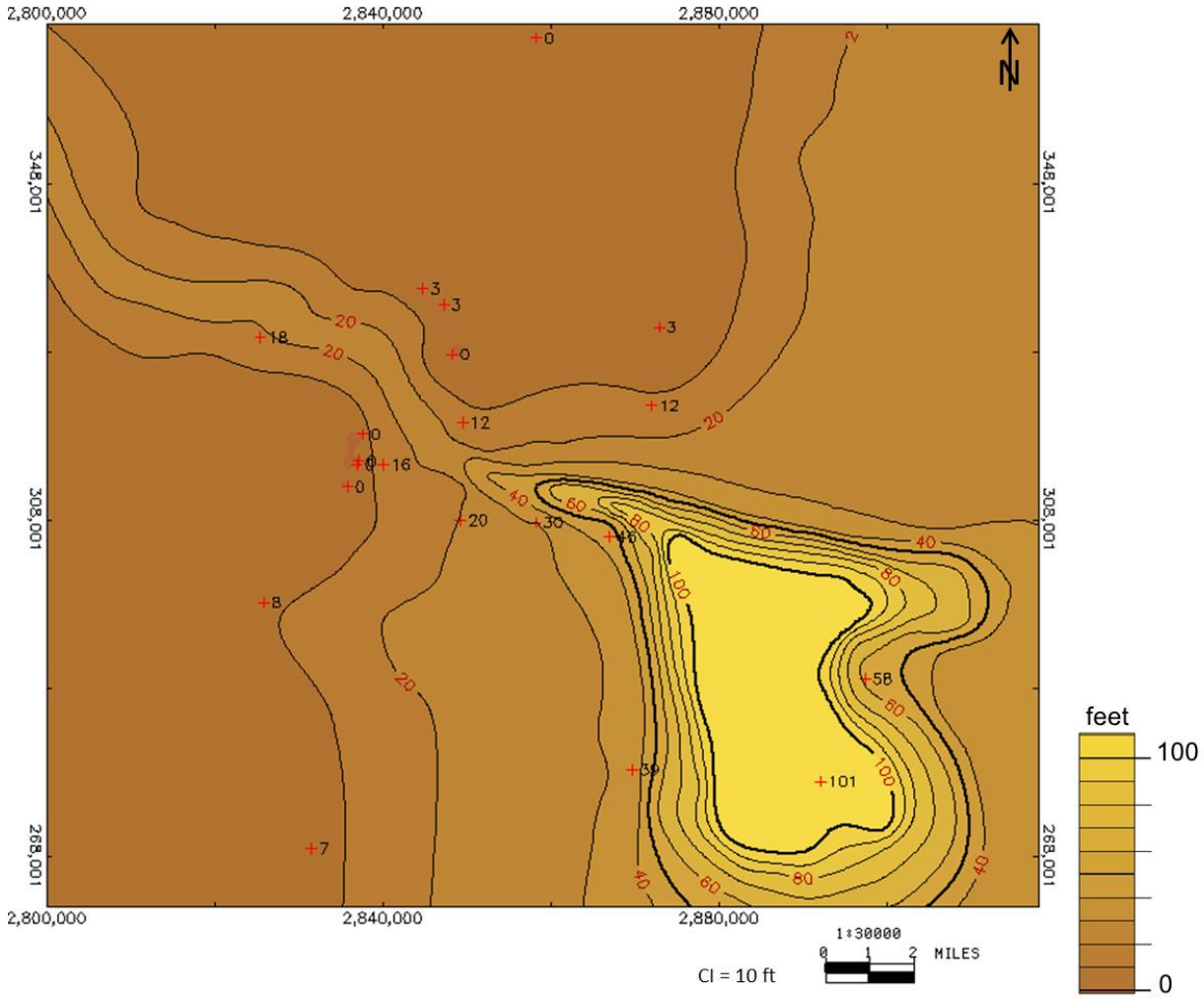

Figure: 4.28 Net sandstone map of the highstand systems tract of the high-frequency 3 (HST_HF3).

4.22 T-R sequences

Net sandstone content of four regressive systems tracts were mapped from bottom to top within the study interval: regressive units (R-Unit) 1 to 4 (Fig. 4.29 to 4.32). R-Unit1 has a distinctive sand dispersal pattern which is dip-elongated whereas the others show both dip (point source) and strike trends. Net sandstone maps of five units share a common trend, which is thin and dip-elongate landward (northwest or west of the study area). Sandstone thickness values abruptly increase across an arbitrary hinge line where accommodation space is inferred to change. The hinge line is interpreted to have been a result of flexure loading associated with rapid/high sedimentation rate and depocenter progradation, a dominant subsidence mechanism of the Cenozoic of the Gulf of Mexico (Winker, 1982). Furthermore, this hinge line represents a depositional shoreline which is a boundary between a lower delta plain and delta front according to Bhattacharya (2006).

R-Unit 1 (Fig. 4.29) shows major dip-oriented sand dispersal patterns. However, these sandstone bodies have a minor degree of continuity along a strike. This is consistent with a progradational shoreline punctuated by fluvial sediment delivery. R-Unit2 (Fig. 4.30), although displaying a dip-elongate depositional trend (north to northwest), has the thickest net sandstone content along strike, implying wave reworking by longshore currents. In R-Unit3 (Fig. 4.31), the thickest accumulation of sandstone occurs westward of the R-Unit2. The sandstone bodies have a dip-elongate trend landward, grading basinward into lobate patterns. This sandstone lobe has one side extending along the shoreline to the east, reflecting the wave processes that reworked and transported sediments downdrift. The amount of sandy sediments deposited during this period significantly decreases from an approximate maximum thickness of 520 ft (156 m) to 200 ft (60 m). R-Unit4 (Fig. 4.32) has similar sand dispersal pattern to R-Unit3 but the strike-

parallel sand body is slightly thicker (210 ft, 63 m), more uniform and widespread both in strike and dip directions.

The regressive unit net sandstone maps associated with well log patterns illustrate an evolution from fluvial and fluvial dominated deltaic systems in R-Unit1 to a wave-dominated deltaic system in time of R-Unit2 deposition. R-Unit3 also suggests a wave-dominated deltaic system but the depocenter had shifted westward from the previous episode, reflecting delta lobe switching. R-Unit4 could represent the highest wave influence on sandstone deposition among the other units because the sediments have been reworked into strike-elongate bodies of likely strandplain origin.

Assuming that the shoreline or the flexural line divides a source or bypass zone from a depocenter, the changing position of the line could represent depocenter switching. Figure 4.33 shows the relative positions of shorelines of all regressive units. At reference locations A and B the depocenter steps back from the time of R-Unit 1 to R-Unit2. A transition from R-Unit2 and R-Unit3 shows a progadational trend at location A but no basinward movement at location A which suggests more aggradational stacking pattern. The deposits exhibit a retrogradational pattern from R-Unit3 to R-Unit4 but it occurs more at location B whereas at location A stable or aggradational stacking pattern tends to be more prominent. Progradation of the shorelines occur more at location B than location A which could be implied that depocenters have overall trend of shifting toward northeast direction through time.

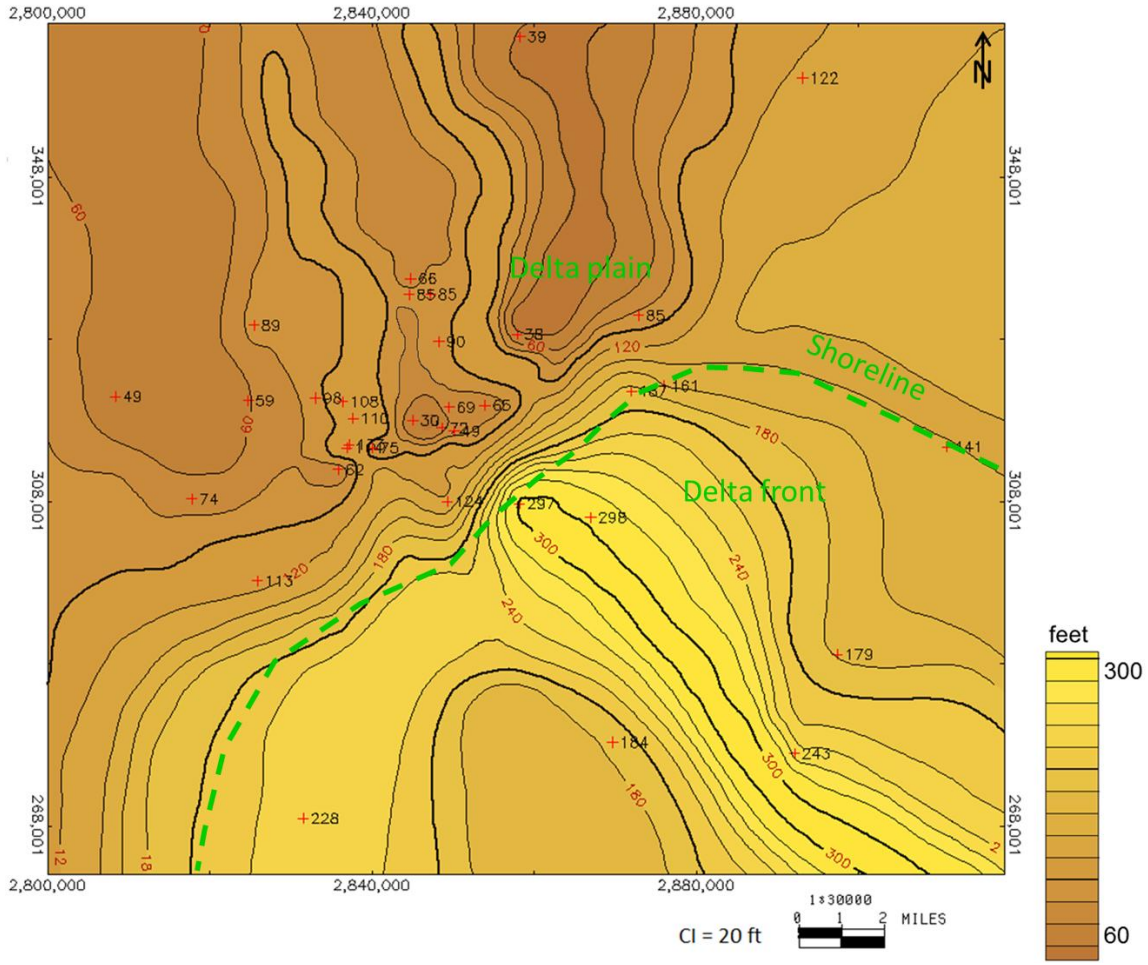

Figure: 4.29 R-Unit1 net sandstone map showing dip-elongate sandstone bodies.

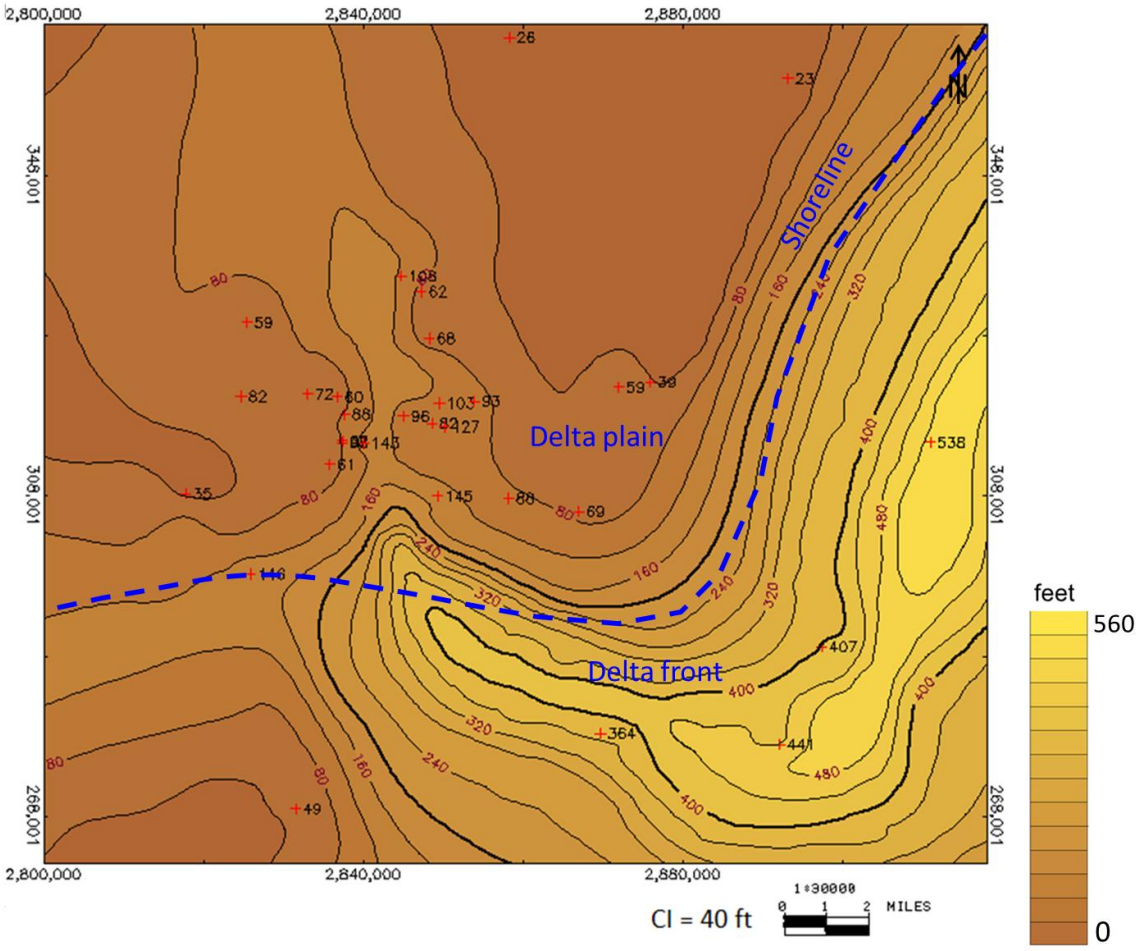

Figure: 4.30 R-Unit2 net sandstone map containing the highest sandstone content in the regressive unit.

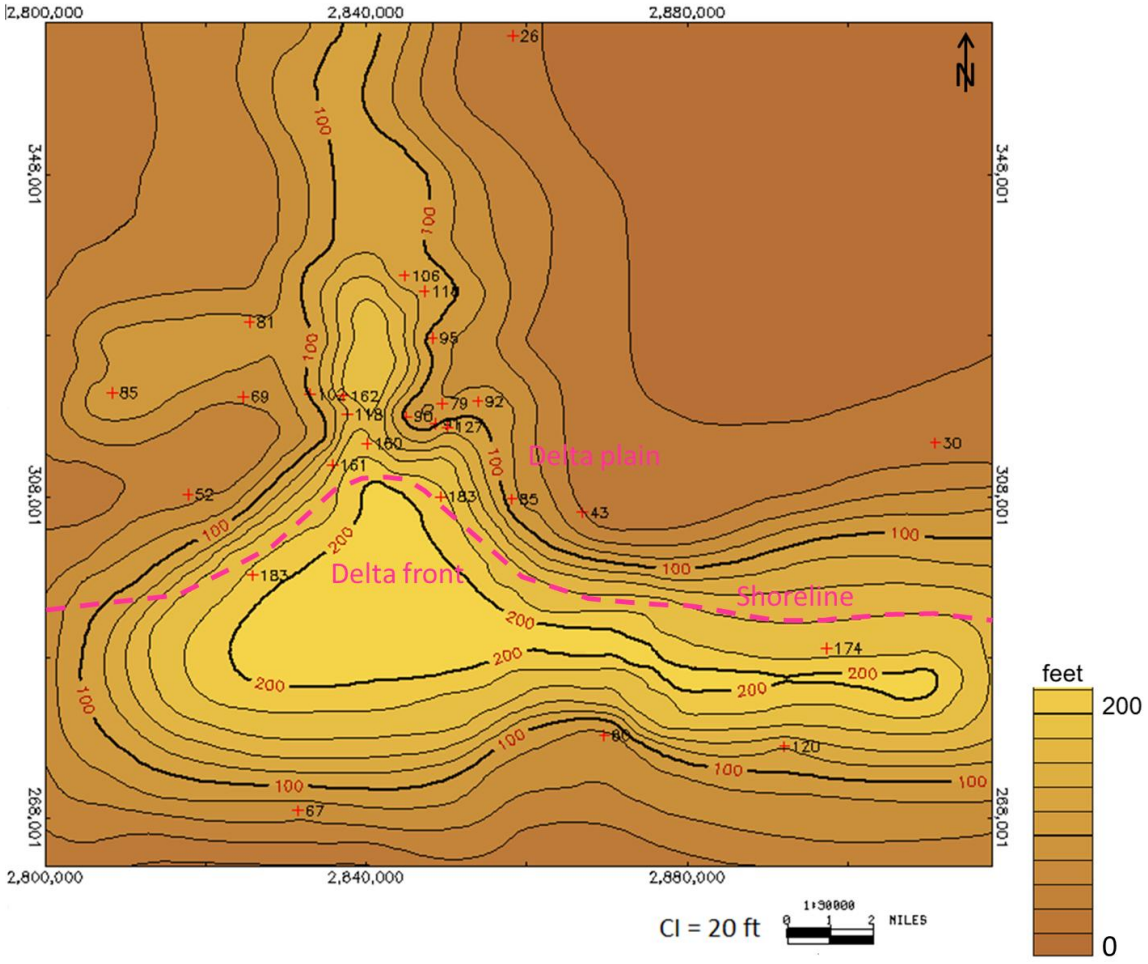

Figure: 4.31 R-Unit3 net sandstone map suggesting a delta lobe reworked by wave processes.

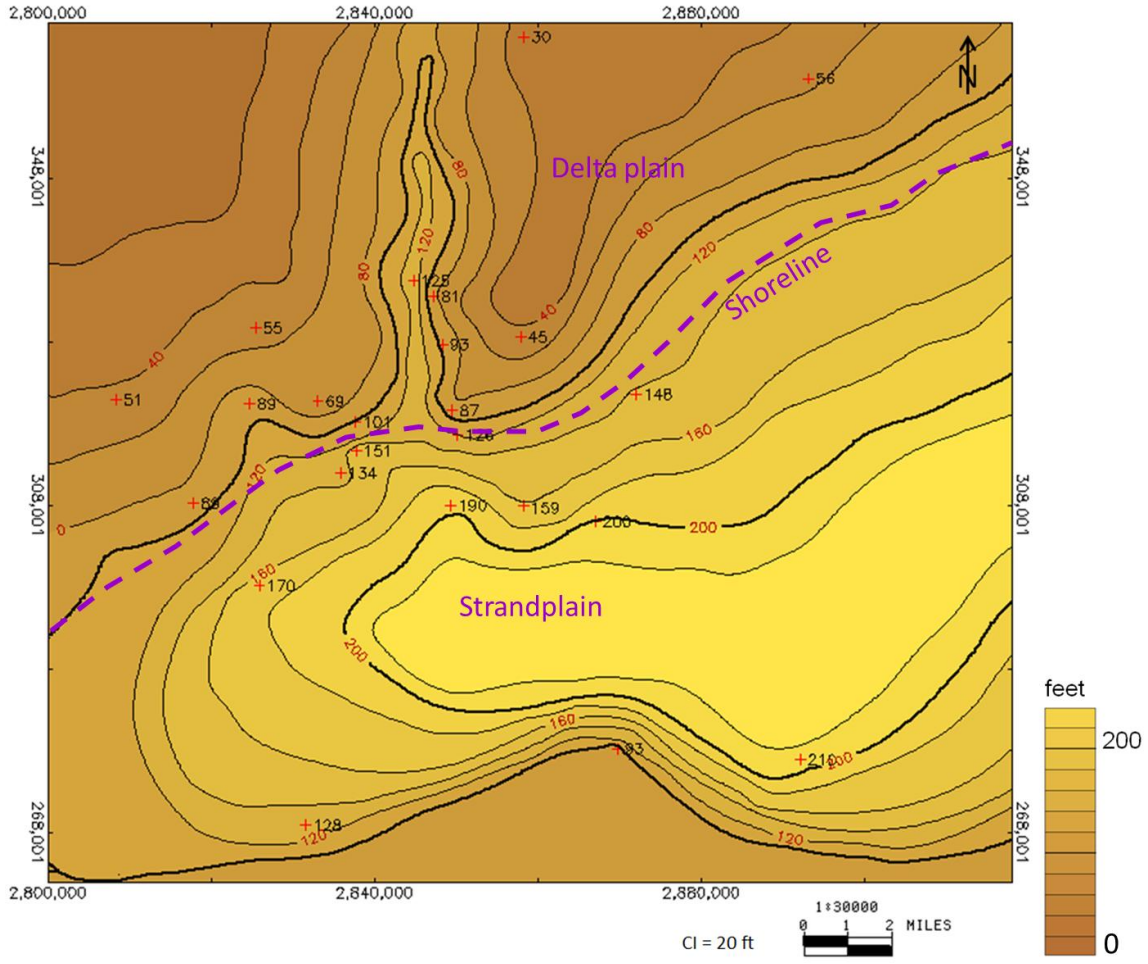

Figure: 4.32 R-Unit4 net sandstone map which illustrates prominent sand dispersal patterns along strike.

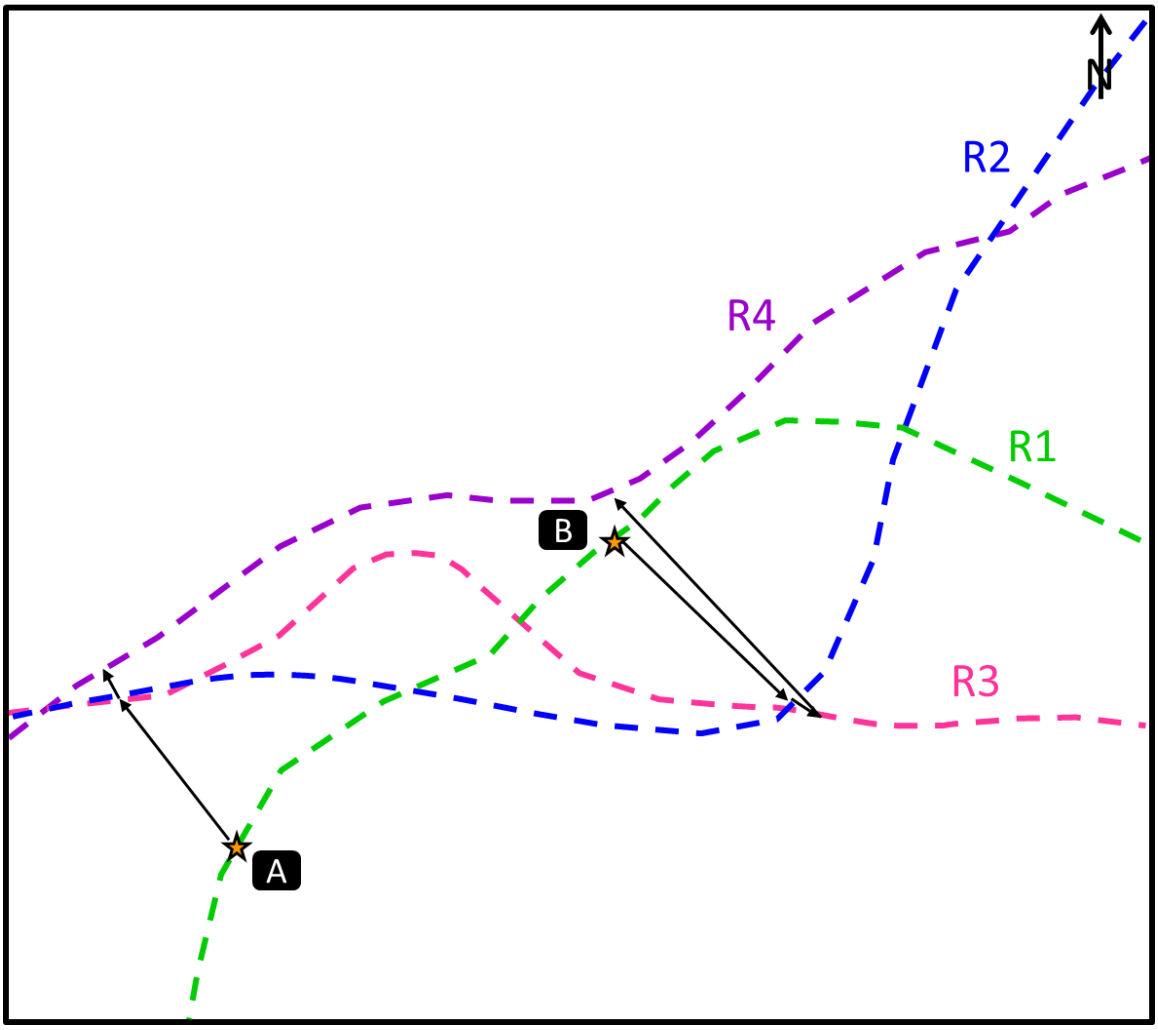

Figure: 4.33 Relative locations of the shorelines of all R-Units to analyze the net migration of depocenters through time.

Chapter5: Discussion and Conclusion

DISCUSSION

Using the S5 (Site-specific sequence-stratigraphic section) benchmark chart as a reference, the estimated approximate ages of sequence boundaries from the oldest to the youngest (sequence 1 to 5) are 23.6, 22.8, 22.2, 19.5, 18.7 and 16.2 Ma, respectively. The positions of sequence boundaries on the sea-level curve (O^{18} isotope record) mark the onset of base-level fall (Fig. 5.1). Note that the approximate age of sequence boundaries of sequence 2 and 3 are close and occur on the same sea-level cycle. As previously described, sequence boundaries were picked from well logs based on recognition of sandstones with blocky GR and SP responses and not from age on base-level curve. Sandstones above the sequence boundary 2 exhibit such characteristics and therefore sequence boundaries were designated with this criterion. According to Galloway (2008), Basin and Range tectonism during early Miocene resulted in uplift of Cretaceous strata and movement along the Balcones fault system in Central Texas (Rio Grande Rift of Dickinson, 1981) that could have resulted in increased sediment/water discharge and fluvial erosion of the lower Texas coastal plain (Boyd et al., 2006). Consequently, despite potential control by glacioeustasy, sediment supply was possibly a short-term controlling factor for bypass processes and generating sequence boundaries.

Some previous studies of the lower Miocene succession in the study area do not mention incised-valley systems, as for example Galloway et al. (1986 and 2000), and instead simply focused on net sandstone mapping at the regional scale. These authors interpreted the depositional setting of the study area as an interdeltaic-shorezone or the Oakville shorezone. The reasons that incised valley systems were not recognized are (1) the regional scale of the study with widely spaced wells and (2), use of different stratigraphic marker beds as correlation surfaces, with consequent inclusion of blocky

sandstone bodies above sequence boundaries (early lowstand deposits), resulting in combining HST and LST sequence tracts in the same map.

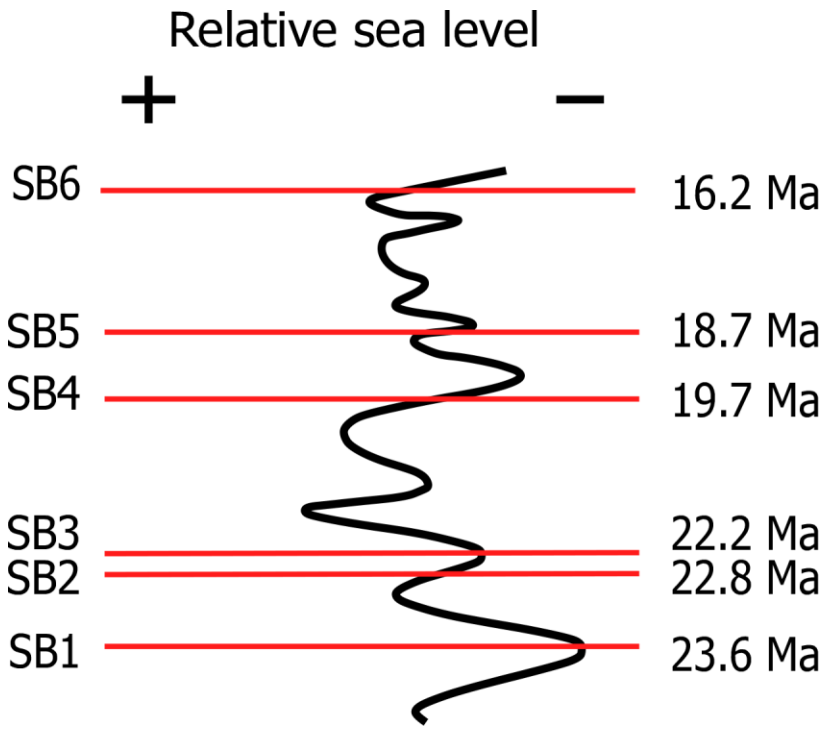

Figure: 5.1 Relative sea level curve from composite O^{18} isotope record (Abreu and Anderson, 1998) with the age of sequence boundaries indicated from the Carancahua S^5 benchmark chart)

An incised valley system represents a bypassing conduit of sediments to a downdip depocenter (Zaitlin et al., 1994). Hence, presence of incised-valley systems in the study area might be genetically linked to exploration targets such as submarine fans that commonly consist of coarse-grained deposits delivered to the basin by bypassing process during sea-level fall (Van Wagoner et al., 1990) (Fig. 5.2).

Lower Miocene sequence 1 and 2 LSTs are the most sandstone-rich system tracts followed byHST4 and HST1. The sandy LST deposits might represent amalgamation offluvial channels during the time of relatively lower accommodation space (slight

tectonic uplift from Rio Grande system), for example well log pattern in Figure 4.11 and stratal slice A in Figure 4.18. However, where present, the LST3 has high sandstone content as well. The more sandstone-rich HST4 than those of the lower sequences might indicate higher sediment supply during the period of high accommodation space which also resulted in uniform progradation along stike direction (Fig. 4.28).

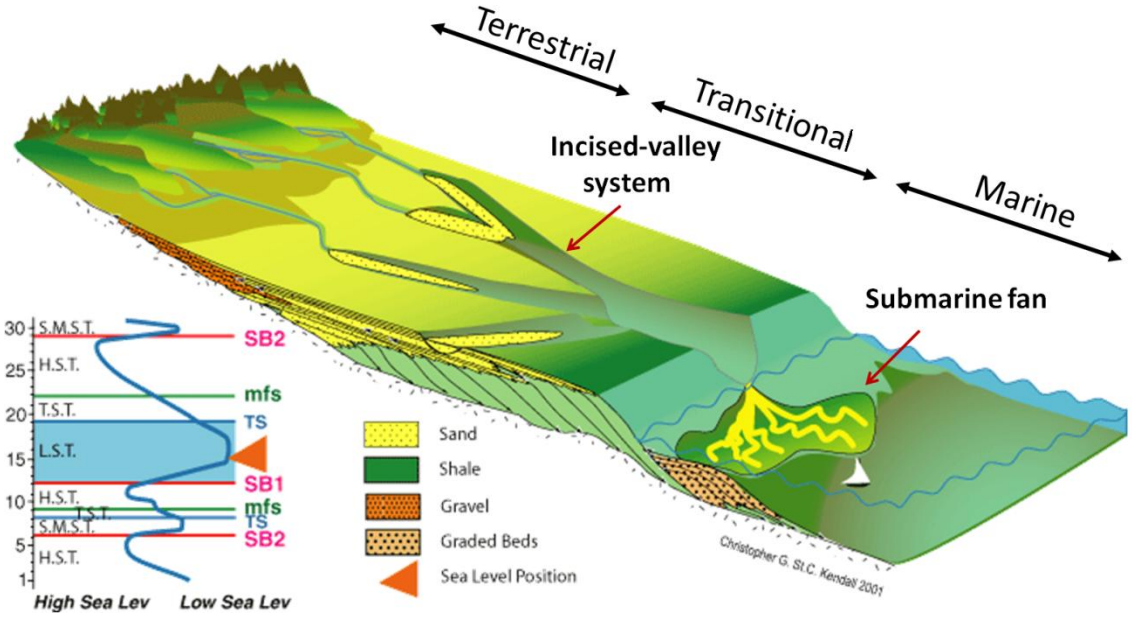

Figure: 5.2 Schematic block diagram illustrates a lowstand incied-valley system and associated submarine fan deposits (modified from Kendall, 2001).

From the systems tracts and R-Unit net sandstone maps the lower Miocene depocenters are located 10-20 miles basinward of the north or northwest corner of the study area. The net sandstone maps suggest that sediments were being delivered to the depocenters by fluvial systems that created dip-oriented sandstone bodies. Depocenters shifted positions between systems tracts and within the same systems tract. Net sandstone maps of sequence 1 (Fig.4.14-4.16) illustrate different depocenter distributions in LST, TST and HST. During sea level lowstands, sediments bypassed the coastal plain and

inner shelf via incised-valley systems, directly to the deepwater slope and eventually to the basin floor. In contrast, discrete depocenters are not evident during TSTs, possibly because of wave-reworking processes or most of the transgressive sediments were trapped in valleys, and the HST map infers that the depocenter is a deltaic system on shelf. The variation of depocenter distribution from one systems tract to another implies that accommodation space, possibly controlled by sea-level change, may have influenced sediment storage. R-Unit net sandstone maps display shifting of depocenters through time. For example, delta lobe shifting occurred from the time of R-Unit2 to R-Unit3, indicating autocyclic processes operating during deposition of the same regressive wedge.

CONCLUSION

1. The study interval that includes the lower Miocene Oakville Formation and the basal part of the middle Miocene Lagarto Formation was divided into five depositional sequences (1-5) that range in approximate duration from 0.5 to 2.5 My. Each sequence contains lowstand, transgressive, and highstand systems tracts except sequence 4, wherein the LST is absent in well logs and seismic data in the study area. A summary of each sequence is given in Table 5.1.

2. Sequence thickness increases upwards from sequence 1 to sequence 3 and then decreases from sequence 3 to sequence 5. Such trends imply that accommodation space was increasing during formation of sequence 1 to sequence 3 and decreasing from the time of sequence 4 toward the transition of lower Miocene to middle Miocene Epochs (sequence 5).

3. LSTs, defined at the base by sandstone bodies with blocky GR and SP responses, are inferred to have a sharp erosional base representing an erosional sequence boundary.

LST1 and LST2 are interpreted to be composed predominantly of incised-valley fill complexes on the basis of well log patterns, stratal slice maps, and/or net sandstone maps. LST3 and LST5, associated with 15-100 ft and 15-25 ft erosional reliefs respectively, exhibit similar characteristic to the LST1 and LST2 with the tabular sandstones above sequence boundaries from well logs suggesting fluvial deposits. However, additional evidence is required to validate the incised-valley interpretation. Presence of incised-valley systems implies sand bypass from the shelf and potential exploration targets downdip of the study area.

4. The TSTs exhibit upward-fining or retrogradational patterns on well logs. TST1 is interpreted to have been deposited in back-barrier lagoon and tidal inlet environments, on the basis of the TST1 net sandstone map and log facies distribution. TST2 and TST3 deposits are interpreted to contain thin reworked deltaic deposits based on well log patterns and stratal slices.

5. HSTs display aggradational to progradational stacking patterns. HST1, HST4 and HST5 are markedly sandstone-rich. From well log patterns, net sandstone maps and stratal slices HST1 deposits are interpreted to be deltaic in origin. HST2 and HST3 are interpreted in terms of a wave-modified deltaic setting. A system of longshore currents is inferred from net sandstone maps to have transported sediments in a downdrift pattern (toward E), but there is still evidence of a fluvial feeder. HST4 deposits have well log patterns and net sandstone map implying a strandplain/shorezone system without fluvial feeding in the immediate area.

6. Depocenter distribution and log pattern trends of the lower Miocene succession suggest that the main stratigraphic changes from one sequence to the next were allogenic responses to unsteady rates of the controlling supply, tectonic and sea-level variables. These responses were most certainly allogenic where the regionally erosive sequence

boundaries are most convincing. However, there are significant stratigraphic changes in the succession which may be autogenic responses, i.e., changes induced without rate changes in the main external variables; these include not only the repetition of parasequences (delta or shoreface lobe shifting) but can also include changes from regression to transgression in some of the sequences, via the now well-documented 'auto-retreat' autogenic response.

7. The different stratigraphic models used in this study, depositonal sequence of Van Wagoner (1990) and T-R sequence (Johnson and Murphy, 1984; Embry and Johannessen, 1992) contributed to the work in different ways. However, the net sand maps from both models do not lead to greatly different depositional environment interpretations. For example, R-Unit1 net sandstone map (Fig. 4.25), including HST1 and LST2, exhibits a combination of dip elongate and lobate sandstone body patterns and the systems tract net sandstone map of HST1 (Fig. 4.16) displays lobate sandstone body of the deltaic system. The regressive units of T-R sequences illustrate the development of the progradational shelf, as well as how sediments were distributed; also revealed the tendency for Lower Miocene depocenters to have shifted northeastward through time. The systems-tract net sandstone maps of depositional sequences illustrate distinct sandstone geometry and distribution of each depositional environment in relation to relative sea level.

Sequence	Sandstone dispersal pattern	Depositional environment	Facies	Potential exploration target
1	Dip elongate during LST and lobate during HST	Fluvial, incised valley, barrier/tidal inlet and delta	Channel fill, bayhead delta, berrier, inlet fill, delta plain and delta front	Downdip of the area (submarine fan), delta front
2	Dip elongate during LST and lobate during HST	Fluvial, incised valley, lagoon/ embayment, and delta	Channel fill, lagoon, delta plain, and delta front	Downdip of the area (submarine fan)
3	Possibly dip oriented during LST, lobate to arcuate	Fluvial, incised valley, and delta	Channel fill, crevasse splay, lagoon, delta plain, and delta front	Channel fills on alluvial plain and down dip area
4	Asymmetric lobate to strike elongate	Fluvial, estuarine and strandplain	Channel fill, estuary fill, and strandplain	Strandplain deposits
5	Possibly dip elongate during LST and strike elongate during HST	Fluvial, incised valley, esturine and strandplain	Channel fill, estuary fill, and strandplain	Downdip area, strandplain deposits

Table: 5.1 Summary of characteristics and potential exploration target of each sequence.

Appendix

Table: 1.1 Abbreviations and common well names

Well no.	Abbreviation	Common well name
1	Ap#1	Appling #1
2	Ba-B13	Bayou Bengal B-13 # 1
3	DS1	Damstrom #1
4	Dsc	Dan Schicke #1
5	EH-17	Elizabeth Hardie #17
6	EP	Ella Peterson De Bord #1
7	ES-1	ELLIOTT, SUSIE #1
8	EA-1	Ethel Abraham #1
9	Ap#B13	F.E. Appling #B13
10	GR1	Green Ranch #1
11	GD291	Gulf D ST 291 #1
12	HH1	Harold Hunt #1
13	HH	Harold N. Hunt #1
14	HM1	Harriman #1
15	HS1	Harrison #1
16	MR	Moody Ranch #B-4
17	OL.GU1	Oyster Lake Temp. GU #1
18	PCO	PIDCO
19	PCO1	PIDCO1
20	PO1	Planet Oil #1
21	RL-1	R. Loff #1
22	SW	SARTWELLE
23	SW-1	Sartwelle #1
24	SW-3	Sartwelle #3
25	SW-4	Sartwelle 4
26	SLR-1	Silver Lake Ranch #1
27	STa	ST 195 #1
28	STb	ST 205 #2
29	STc	ST 240 #1
30	STd	ST 254 #1
31	STe	ST 255 #1
32	STf	ST 257 #1
33	STg	ST 259 #1
34	STh	ST 259 #2

Well no.	Abbreviation	Common well name
35	St.A1	St. Andrews #1
37	St.G2	St. George GU #2
38	Sti	ST254 Brigham
39	StT109	STATE TRACT 109
40	StT110	STATE TRACT 110
41	TXGa	Texas Gulf Sulphur # 1(a)
42	TXG1	Texas Gulf Sulphur #1
43	T-B	TRULL 'B
44	TB	TRULL B
45	TB-1	Trull B #1

References

Abreu, V. S. and Anderson, J. B., 1998, Glacial eustasy during the Cenozoic; sequence stratigraphic implications: AAPG Bulletin, v. 82, No.7, p. 1385-1400.

Ambrose, W. A., Johnson, B. E., Hammes, U., and Johnstone, D., 2010, Sequence stratigraphic framework and depositional history of Oligocene Frio slope-fan, lowstand prograding wedge, and shallow-marine transgressive-regressive deposits in the Lavaca Bay area, Texas: Gulf Coast Association of Geological Societies Transactions, v. 60, p. 29–38.

Bhattacharya, J.P., 2006, Daltas. In: Posamentier, HW, and Walker, RG, eds, Facies Models Revisited: SEPM, Special Publication, v. 84, p. 237-292.

Bonnaffe, Florence, Hammes, U., Carr, D. L., and Brown, L. F., Jr., 2008, High-resolution sequence stratigraphic correlations of the Oligocene Frio Formation in south Texas. In: Gulf Coast Association of Geological Societies Transactions, v. 58, p. 125–142.

Boyd, R., Dalrymple, R.W., and Zaitlin, B.A., 2006, Estuary and incised valley facies models. In: Posamentier, H.W., and Walker, R.G., eds., Facies Models Revisited: SEPM, Special Publication, v. 84, p. 171-235.

Brown Jr., L.F., Fisher, W.L., 1977, Seismic stratigraphic interpretation of depositional systems: examples from Brazilian rift and pull apart basins. In: Payton, C.E., ed., Seismic Stratigraphy: Applications to Hydrocarbon Exploration: AAPG Memoir, v. 26, p. 213–248.

Brown Jr., L. F., and Loucks, R. G., 2009, Chronostratigraphy of Cenozoic depositional sequences and systems tracts: A wheeler chart of the northwest margin of the Gulf of Mexico Basin: University of Texas at Austin, Bureau of Economic Geology Report of Investigations 273, 28 p.

Brown Jr., L. F., Loucks, R. G., and Treviño, R. H., 2005, Site-specific sequence-stratigraphic section benchmark charts are key to regional chronostratigraphic systems tract analysis in growth-faulted basins: AAPG Bulletin, v. 89, no. 6, p. 715-724.

Brown Jr., L. F., Loucks, R. G., Trevino, R. H., and Hammes, U., 2004b, Understanding growth-faulted, intraslope subbasins by applying sequence-stratigraphic principles: Examples from the south Texas Oligocene Frio Formation: AAPG Bulletin, v. 88, p. 1501– 1522.

Cattaneo, A. and Steel R. J., 2002, Transgressive deposits: a review of their variability: Earth Science Reviews, v. 1277, p. 1-43.

Catuneanu, O., Abreu, V., Bhattacharya, J.P., Blum, M.D., Dalrymple, R.W., Eriksson, P.G., Fielding, C.R., Fisher, W.L., Galloway, W.E., Gibling, M.R., Giles, K.A., Holbrook, J.M., Jordan, R., Kendall, C.G.St.C., Macurda, B., Martinsen, O.J.,

Miall, A.D., Neal, J.E., Nummedal, D., Pomar, L., Posamentier, H.W., Pratt, B.R., Sarg, J.F., Shanley, K.W., Steel, R.J., Strasser, A., Tucker, M.E. and Winker, C. 2009, Towards the standardization of sequence stratigraphy: Earth-Science Reviews, v. 92, p 1-33.

Catuneanu, O., Bhattacharya, J.P., Blum, M.D., Dalrymple, R.W., Eriksson, P.G., Fielding, C.R., Fisher, W.L., Galloway, W.E., Gianolla, P., Gibling, M.R., Giles, K.A., Holbrook, J.M., Jordan, R., Kendall, Macurda, B., Martinsen, O.J., Miall, A.D., Nummedal, D., Posamentier, H.W., Pratt, B.R., Shanley, K.W., Steel, R.J., Strasser, A. and Tucker, M.E. 2010, Sequence Stratigraphy: common ground after three decades of development: First Break, v. 28, p. 21-34.

Clifton, H.E., 2006, A reexamination of facies models for clastic shorelines. In: Posamentier, HW, and Walker, RG, eds, Facies Models Revisited: SEPM, Special Publication, v. 84, p. 293–337.

Dalrymple, R.W., 2006, Incised valley in time and space: an introduction to the volume and an examination of the controls on valley forming and filling: In Dalrymple, R.W., Leckie, D. A., and Tillman, R. W., eds, Incised valleys in time and space: SEPM, Special Publication, v. 85, p. 5-12.

Dalrymple, R.W., Zaitlin, B.A., and Boyd, R., 1992, Estuarine facies models: Conceptual basis and stratigraphic implications: Journal of Sedimentary Petrology, v. 62, p. 1130–1146.

Diegel, F. A., Karlo, J. F., Schuster, D. C., Shoup, R. C., and Tauvers, P. R., 1995, Cenozoic structural evolution and tectono-stratigraphic framework of the northern Gulf coast continental margin. In: Jackson, M. P. A., Roberts, D. G., and Snelson, S. eds., Salt tectonics. A global perspective: AAPG, Tulsa, OK, p. 109–152.

Embry, A.F., 2009, Practical Sequence Stratigraphy: Canadian Society of Petroleum Geologists, 79 p.

Embry, A.F. and Johannessen, E.P., 1992, T-R sequence stratigraphy, facies analysis and reservoir distribution in the uppermost Triassic-Lower Jurassic succession, western Sverdrup Basin, Arctic Canada. In: Vorren, T.O., Bergsager, E., Dahl-Stamnes, O.A., Holter, E., Johansen, B., Lie, E. and Lund, T.B., eds., Arctic Geology and Petroleum Potential: Norwegian Petroleum Society, Special Publication, v. 2, p. 121-146.

Galloway, W.E. 1989, Genetic stratigraphic sequences in basin analysis, I. Architecture and genesis of flooding-surface bounded depositional units: AAPG Bulletin, v. 73, p. 125-142.

Galloway, W. E., 1989b, Genetic stratigraphic sequences in basin analysis II: application to northwest Gulf of Mexico Cenozoic basin: AAPG Bulletin, v. 73, p. 143–154.

Galloway, W. E., 2008, Depositional Evolution of the Gulf of Mexico Sedimentary Basin. In: K.J. Hs ü, ed: Sedimentary Basins of the World, v. 5, The Sedimentary Basins of the United States and Canada, Andrew D. Miall. The Netherlands: Elsevier, p. 505 – 549.

Galloway,W.E. and D. K. Hobday, 1983, Terrigenous clastic depositional systems. Applications to petroleum, coal and uranium exploration: Springer-Verlag,New York, NY, p.420.

Galloway, W. E., Hobday, D. K., and Magara, K., 1982b, Frio Formation of the Texas Gulf Coast basin—depositional systems, structural framework, and hydrocarbon origin, migration, distribution, and exploration potential: University of Texas at Austin, Bureau of Economic Geology Report of Investigations 122, 78 p.

Galloway, W. E., Ganey-Curry, P. E., Li, X., and Buffler, R. T., 2000, Cenozoic depositional history of the Gulf of Mexico basin: AAPG Bulletin, v. 84, p. 1743–1774.

Galloway, W. E., Jirik, L. A., Morton, R. A., and DuBar, J. R., 1986, Lower Miocene (Fleming) depositional episode of the Texas coastal plain and continental shelf: structural framework, facies, and hydrocarbon resources: University of Texas at Austin, Bureau of Economic Geology Report of Investigations 150, 50 p.

Hayes, M.O., 1976, Transitional-coastal depositional environments. In Hayes, M.O. and Kana, T.W., eds., Terrigenous Clastic Depositional Environments: AAPG Field Course, Univ. South Carolina, Columbia, Tech. Rept. No.11-CRD, Part I, p. 32-111.

Hays, J., Imbrie J., and Shackleton, N. 1976, Variations in the Earth's Orbit: Pacemaker of the Ice Ages: Science, v. 194. p. 1121-1132.

Johnson, J.G. and Murphy, M.A., 1984, Time-rock model for Siluro-Devonian continental shelf, western United States: Geological Society of America Bulletin, v. 95, p. 1349-1359.

McGowen, J. H. 1971. Gum Hollow fan delta, Nueces Bay, Texas: University of Texas at Austin, Bureau of Economic Geology Report of Investigations 69, 91 p.

Mitchum, R.J. 1977, Glossary of seismic stratigraphy. In: Payton, C.E. (Ed.) Seismic Stratigraphy – Applications to Hydrocarbon Exploration: AAPG Memoir 26, p. 205-212.

Mitchum, R.M., Jr. and Van Wagoner, J.C., 1991. High-frequency sequences and their stacking patterns: sequence-stratigraphic evidence of high-frequency eustatic cycles. In: Biddle, K.T. and Schlager, W., eds., The Record of Sea-Level Fluctuations: Sediment. Geol., v. 70, p. 131-160.

Moore, B. T., 2005, Sequence stratigraphic framework and systems tracts analysis of Lower Miocene shelfal clastic deposits: Redfish Bay area, Texas Gulf Coast: MS thesis, University of Texas at Austin, Austin, 86 p.

Morton, R. A., Jirik, L. A., and Galloway, W. E., 1988, Middle-upper Miocene depositional sequences of the Texas coastal plain and continental shelf: geologic framework, sedimentary facies, and hydrocarbon plays: University of Texas at Austin, Bureau of Economic Geology Report of Investigations 174, 40 p.

Muto, T. and Steel, R. J. 1998, Principles of regression and transgression: the nature of the interplay between accommodation and sediment supply. Journal Sedimentary Research, v. 67, p. 994-1000.

Muto, T., Steel, R. and Swenson, J., 2007, Autostratigraphy: a framework norm for genetic stratigraphy. J. Sedim, Research, v. 77, p. 2-12

Plint, A.G., 1988, Sharp-based shoreface sequences and "offshore bars" in the Cardium Formation of Alberta: their relationship to relative changes in sea level. In: Wilgus, C.K., Hastings, B.S., Kendall, C.G.St.G., Posamentier, H.W., Ross, C.A., and Van Wagoner, J.C., eds., Sea Level Changes: An Integrated Approach: SEPM, Special Publication 42, p. 357–370.

Porębski, S.J., and Steel, R.J., 2003, Shelf-margin deltas: their stratigraphic significance and relation to deepwater sands: Earth-Science Reviews, v. 62, p. 283–326.

Porębski, S.J., and Steel, R.J., 2006, Delta and sea-level change: Journal of Sedimentary Research, v. 76, p. 390–403.

Posamentier, H.W., Allen, G.P., James, D.P., and Tesson, M., 1992, Forced regressions in a sequence stratigraphic framework: concept, examples, and exploration significance: AAPG Bulletin, v. 76, p. 1687–1709.

Thomas, M.A. and Anderson, J.B., 1994, Sea-level controls on the facies architecture of the Trinity/Sabine incised-valley system, Texas continental shelf. In: Dalrymple R., Boyd, R. and Zaitlin, B.A. eds, Incised-Valley Systems: Origin and Sedimentary Sequence: SEPM Special Publication, v. 51, p. 63-82.

Torres-Verdín, T.C., 2010, Integrated geophysical-petrophysical interpretation of well logs: PEG385M, Advanced well logging and correlation class note, University of Texas at Austin, Austin, 72 p.

Van Wagoner, J.C., Mitchum, R.M., Campion, K.M., and Rahmanian, V.D. 1990, Siliciclastic Sequence Stratigraphy in Well Logs, Cores, and Outcrops: AAPG, Tulsa, 55 p.

Winker, C. D., 1982, Cenozoic shelf margins, northwestern Gulf of Mexico: Gulf Coast Association of Geological Societies Transactions, v. 32, p. 427–448.

Ye Q., Galloway W. E., and Matthews R. K., 1995, High-Frequency Glacioeustatic Cyclicity of the Miocene in Central Texas and Western Louisiana and its Application in Hydrocarbon Exploration: Gulf of Mexico: Gulf Coast Association of Geological Societies Transactions, v. 45, p. 587-594.

Zaitlin, B.A., Dalrymple, R.W., and Boyd, R., 1994, The stratigraphic organization of incised-valley systems associated with relative sea level change. In: Dalrymple, R.W., Boyd, R., and Zaitlin, B.A., eds., Incised-Valley Systems: Origin and Sedimentary Sequences: SEPM, Special Publication, v. 51, p. 45–60.

Zeng, H., and Hentz, T. F., 2004, High-frequency sequence stratigraphy from seismic sedimentology: Applied to Miocene, Vermilion/Block 50-Tiger Shoal area, offshore Louisiana: AAPG Bulletin, v. 88, no. 2, p. 153–174.

Zeng, H., Brown, L. F. Jr., and Loucks R. G., 2007, Mapping sediment-dispersal patterns and associated systems tracts in fourth- and fifth-order sequences using seismic sedimentology: Example from Corpus Christi Bay, Texas: AAPG Bulletin, v. 91, no. 7, p. 981-1003.

Vita

Rattanaporn Fong-Ngern was born in Chiang Mai, the city with the highest mountain peak of Thailand. She went to a secondary and high school that offered a magnificent view of the mountain and this is what sparked her interest in geology.

During high school she discovered that she was good at biology, chemistry, and physics but did not want to go deeper in any specific fields. In fact she loves the integration of pure sciences and thus geology is a perfect world for her.

After graduating with a bachelor's degree in 2008, she won a scholarship from the Royal Thai Government to study and to complete a doctoral program abroad. She plans to continue her education in PhD program at the Jackson School of Geosciences, University of Texas at Austin. She believes it was a kind of destiny that brought her here to one of the best schools for geology. Her major goal is to gain an expertise in the fields of sequence startigraphy and basin analysis and then to return home to teach in a university and play a role in the petroleum industry in Thailand.

Email address: RattanapornF@maill.utexas.edu

This thesis was typed by the author.